This is to certify that the
dissertation entitled

DYNAMICS OF FLUORESCENT BIOLOGICAL PROBES IN SOLUTION PHASE PROCESSES

presented by

Lee Kelepouris

has been accepted towards fulfillment
of the requirements for the

Ph. D. degree in Chemistry

Major Professor's Signature

October 4, 2002
Date

# DYNAMICS OF FLUORESCENT BIOLOGICAL PROBES IN SOLUTION PHASE PROCESSES

By

Lee Kelepouris

A DISSERTATION

Submitted to
Michigan State University
in partial fulfillment of the requirements
for the degree of

DOCTOR OF PHILOSOPHY

Department of Chemistry

2002

## Abstract

# DYNAMICS OF FLUORESCENT BIOLOGICAL PROBES IN SOLUTION PHASE PROCESSES

By

Lee Kelepouris

In the past decade the use of fluorescence based methods has flourished in many areas of science. Fluorescence is relevant to chemical, physical, and biological sciences as a tool of investigation, analysis, control and diagnosis. The recent advances in light sources, detectors, and compact fast electronics has prompted the advent of new technology in these areas. Great advances in time-resolved spectroscopy have been made in fluorescence lifetime imaging microscopy and fluorescence correlation spectroscopy. Also, increased detection sensitivity allows single molecule detection in the restricted field of a confocal microscope making possible studies of phenomena at the molecular level. These numerous applicatons are possible due to the sensitivity of the emission properties of organic chromophores to their molecular environment. Chromophore emission may be affected the pH, polarity, dielectric constant, viscosity, quenchers and many other factors.

The development and characterization of new fluorescent probes is needed. The ability to tailor probes for specific environments is important. Many potential *in vivo* applications exist with the introduction of fluorescent residues amenable to protein incorporation and biological systems.

This thesis is a study of fluorescent molecules in heterogeneous environments. The study focuses on understanding the factors that determine a fluorescent probes ability

to interact with and report on its molecular environment. The probes are derivatives of the naturally occurring amino acid tryptophan and its non-natural analog 7-azatryptophan. We began by studying 7-azaindole and 7-azatryptophan in saturated solutions of aqueous adipic acid in an effort to detect the onset of crystallization. 7-Azatryptophan has a carboxylic functionality in common the adipic acid and may act as a site for aggregation enabling it to detect self-assembly of solutes preceding crystallization. We monitor the steady state and time resolved emission and rotational dynamics of the chromophores as a function adipic acid concentration to determine the ability of the probe to sense solute events. The comparison of concentration-dependent results reveal the probes unique interactions with solutes arising from their structural differences.

We use the information gained on the properties of the 7-azaindole chromophore in the adipic acid system and extend its use to the biological realm for the study of small peptides. 7-Azatryptophan was attached covalently to a series of valine oligomers and studied in water and in several aqueous micelle solutions to provide well defined heterogeneous environments. This study establishes that a balance exists between ionic and dispersion forces and mediates interactions with micelles. The study of probe micelle interactions was continued using several tryptophan and 7-azatryptophan derivatives. This work elucidated structural criteria for interaction with micelles and revealed that the subtle differences in the indole and 7-azaindole chromophores lead to measurably different interactions in these heterogeneous environments. The work in this thesis provides a knowledge base to aid in the application and interpretation of tryptophan and azatryptophan derivatives as probes of heterogeneous systems and peptide environments.

Το Σλίας Κελεπούρις

# Acknowledgements

My Graduate school experience has been a pleasant one. This was due, in large part, to the people I will acknowledge in the following paragraphs. Among these persons are those I was fortunate enough to work with, those I developed friendships with, and loved ones who encouraged and supported me throughout my academic career.

Of the people I must thank, my advisor, Gary Blanchard is at the forefront. Gary has dutifully served as my research advisor. Of this, I am greatly appreciative. On many occasions during my time in the group we have said Gary is "The Best". Some of the things earn him this description as an advisor and boss are his knowledge, patience, generosity, humor, and the true interest he has in helping his students succeed as well as others. Gary has not only taught me how to become a better scientist but I have learned much about management, politics, and the scientific community in general through his willingness to share his own experiences and endeavors.

I would also like to thank my committee members, John McCracken, Rob Maleczka, and Simon Garrett. Simon deserves special mention for graciously stepping in as my second reader on short notice.

I was lucky to have joined Gary's group at a time when comradery was at a high. During this time, I have made several very good friends. Joe Tulock showed me the ropes of graduate school and the laser lab. Joining the group a mere half hour before me Steve Bakiamoh was on a parallel course and was my partner though many graduate school hurdles. Thanks Steve, it was nice to have someone to suffer with. You could always count on Punit Kohli to be in the lab and ready for science or fun. These are the

gro

frie

futu

rec

not

scie

sup

perf

who

you

group members with whom I was closest. We have had the opportunity to prove our friendship many times over the years and I am sure we will continue to do so in the future.

There are other group members both past and present I consider friends and could recognize. I wish them the best, among them, the well deserving, Jaycoda Major. While not a group member, I must thank Todd Bryden, for his friendship and for discussing science in a manner that challenged and encouraged me.

I am indebted to my sister Nina and brother in-law Rob for providing tremendous support and stability at just the right time during my undergraduate studies helping me to perform at my potential. I likely would not have attended graduate school without them.

These people were all part of my successful graduate school career but the one who helped most to make graduate school a pleasant journey is Carina, thank you for your love, caring, and patience.

# TABLE OF CONTENTS

# LIST OF TABLES

Fig

Fig

Fig

Figu

Figu

Figur

Figur

Figure

Figure

# LIST OF FIGURES

Fig

Figu

Figu

Figu

Figu

Figu

of res

could

better

phase

neat s

fluores

dynam

fluores

yieldin

spontar

crystall

and foc

understa

commu

problem

that con

solution

# Chapter 1

## Introduction

Understanding the dynamics of solution phase interactions has been an active area of research for several decades. A greater understanding of intermolecular interactions could lead to the ability to predict and control chemical reactions and separations and to better understand biological phenomena. A primary tool for the investigation of solution phase events has been through transient and steady state spectroscopy of chromophores in neat solvents. Many models have been used for the interpretation of such data and fluorescence spectroscopy has proven to be a powerful method for understanding the dynamics of chromophores, peptides, and proteins in solution. The time scale of fluorescence decay and depolarization make it ideally suited to study these events, yielding information on picosecond to nanosecond time scales.[1]

A detailed understanding of the intermolecular interactions that lead to the spontaneous self-assembly of solutes from solution could greatly benefit the process of crystallization. Crystallization is an important technique in chemical, pharmaceutical, and food industries for the separation and purification of many materials. A greater understanding of crystallization would not only benefit these industries, but the scientific community in general. A scientist investigating crystallization is faced with several problems that must be solved in order to develop a general theory of crystallization so that control and monitoring of the process may be implemented.

Many techniques have been used to study the structure of supersaturated solutions. Attempts to correlate supersaturation with changes in physical properties as a

function

discontin

solubilit

glucose

vibratio

water m

is hinde

to the

suggest

probe n

by stu

sensitiv

molecu

microe

in solv

to calc

quanti

molec

Their

solute

work

exami

function of concentration have been made. These bulk physical properties rarely show discontinuities with concentration at the equilibrium saturation point, especially in low solubility systems.[2] Mathlouthi *et al.*[3-5] used vibrational spectroscopies to study aqueous glucose solutions. Measurements were made of concentration dependent changes in vibrational frequencies of both solvent and solute. Their data showed that some of the water molecules are coordinated in a tetrahedral manner and that H-O-H bending motion is hindered in concentrated solutions. It was not clear what specific interactions gave rise to the observed motional hindrance, but their investigations did provide evidence to suggest some level of solute organization in supersaturated solutions.

There is precedent in the literature for studying crystallization with fluorescent probe molecules. Berglund *et al.*[6,7] used fluorescent probes to understand crystallization by studying the behavior of solvent molecules in crystallizing systems. A solvent sensitive probe, pyranine, was used to study changes in the environment of water molecules in sugar solutions. The authors reported that water experiences two microenvironments in sugar solutions. In one environment water molecules are involved in solvating sugar molecules and in the other they are not. The authors found it possible to calculate the peak intensity ratio (PIR) from the steady state emission spectra of trace quantities of pyranine in the sugar solutions. This ratio reflects the number of water molecules in each environment and this PIR is sensitive to the degree of supersaturation. Their results, while informative, were not sensitive to and did not provide a description of solute organization.

Rasimas *et al.*[8,9] performed investigations of aqueous systems of glucose. In this work the fluorescent probes carminic acid and glycosylated resorufin were used to examine solute environments. Both probes possess a pendant glucose moiety to allow for

incorpo

of the n

time-re

rotation

concent

rotation

contain

several

carmini

glucose

resoruf

of the

glycosy

study:

dynam

proton

theoret

deproto

The sl

charge

reorien

viscosi

glycosy

incorporation into aggregates of glucose molecules in solution. To gain an understanding of the nature of the incorporation of carminic acid at the molecular level, steady state and time-resolved spectroscopies were used. Measurements of fluorescence lifetimes and rotational diffusion dynamics showed carminic acid to be sensitive to changes in glucose concentration. This sensitivity was displayed in discontinuities of the lifetime and rotational diffusion measurements near and at glucose saturation. These measurements contained a wealth of information but were complicated due to the contributions of several protonated forms of carminic acid. However, these findings indicated that carminic acid could serve as a tool for understanding crystallization from solution in the glucose system.

The glucose system was further studied by Rasimas *et al.* using glycosylated resorufin as the probe. Glycosylated resorufin was chosen to study the effect the identity of the probe molecule can have on the experimental results. Unlike carminic acid, glycosylated resorufin has no labile protons. Three forms of the probe were used in this study: glycosylated, protonated, and deprotonated resorufin. Rotational diffusion dynamics were again utilized as a key means to understand crystallization. The protonated species exhibited rotational diffusion dynamics that agreed well with theoretical predictions due to bulk properties of the solutions studied, but the deprotonated form exhibited slower rotational diffusion times than predicted from theory. The slower rotational times of the deprotonated form highlighted the importance of charge in describing the interactions of molecules in solution. Most importantly, the reorientation times of glycosylated resorufin were shown to be independent of solution viscosity at glucose concentrations near saturation. This was said to be evidence that the glycosylated probe must reside in an environment that renders it insensitive to changes in

bulk solu

probes w

environm

T

trace amo

fluoresce

the solut

response

Fluoresc

molecula

informat

distance

T

by the

crystalli

focuses

study du

It is use

It is esti

most co

solubili

work w

solubili

bulk solution viscosity near saturation. The authors concluded the non-glycosylated probes were not involved in solute aggregation and that they sensed an aqueous environment not associated with solution structuring.

This work by the Blanchard and Berglund demonstrated the effectiveness of using trace amounts of fluorescent probes with a lock-and-key approach. This method uses a fluorescent probe molecule that incorporates selectively into pre-crystalline aggregates of the solute system via functionality in common with the crystallizing species. The optical response of the probe is then monitored as a function of solution composition. Fluorescence measurements are sensitive and rich in information about the immediate molecular environment of the probe molecule. Fluorescent probe molecules may report information on their immediate surroundings regarding concentration, pH, polarity, distance, possible complexing, and electric field based on their optical response.[10]

The work reported in chapter 2 is a continuation of earlier experiments performed by the Blanchard and Berglund groups to gain a mesoscopic understanding of crystallization. While early experiments studied the crystallization of glucose, this work focuses on the crystallization of dicarboxylic acids. In particular, adipic acid is under study due to its economic importance and simplicity. Adipic acid has a variety of uses. It is used in the manufacture of resins, plastics, urethane foams, and as a food additive[11] It is estimated that the annual global demand for adipic acid exceeds $1.9 \times 10^9$ kg with the most common use being the production of nylon-6,6.[12] Adipic acid has a relatively low solubility in water (1.9 g per 100 g water at 20° C).[2] This serves in contrast to earlier work with glucose where solubility is high (90 g per 100 g water at 20° C).[2] In low solubility systems, solution properties such as viscosity, density, and refractive index will

not be a

traditior

behavio

(7AT) (

betweer

(7AI).

concent

fluoresc

aggrega

chromo

reorient

that are

with aq

biophys

intermo

tryptoph

includin

biologic

as a bio

cell mer

physiolo

not be altered to a great extent, and therefore the ability to monitor solution saturation by traditional means is difficult.

We employ this lock-and-key approach to study the pre-crystalline aggregation behavior of adipic acid using the chromophores 7-azaindole (7AI) and 7-azatryptophan (7AT) (fig. 2.1) as probes. The use of these two probes allows direct comparison between a probe expected be included (7AT) in aggregation events and one that is not (7AI). The steady state response of these probes was found to be sensitive to adipic acid concentration due to a labile proton on the chromophore ring at position $N_7$. Although fluorescence lifetime measurements did not reveal direct information indicating solute aggregation, opposite trends in lifetimes were evident revealing that the two chromophores undergo very different interactions with adipic acid. The experimental reorientation data showed evidence that adipic acid does form weak complexes with 7AT that are not present with 7AI.

In chapter 3 we utilize 7AT incorporated into peptides to probe their interactions with aqueous micelles. Protein fluorescence spectroscopy has proven to be a valuable biophysical technique in the study of protein function, structure, dynamics and intermolecular interactions in solution.[1,13] 7AT has been used as an alternative to tryptophan for peptide dynamics. Several factors render 7AT a useful biological probe including that it is amenable to protein synthesis[14-16] and has been shown to retain biological activity when incorporated into proteins. In addition to proteins, 7AT is useful as a biological probe of peptides. The study of interactions between small peptides and cell membranes is an advancing area of research. These interactions are important to physiological functions like hormonal response and neurotransmission.[17] We covalently

attach 7

size affe

were ini

because

consists

charged

surfactar

equilibri

well-stu

provide

interacti

between

is model

charge a

Because

affords

probes i

measure

interacti

reorienta

for analo

attach 7AT to a series of peptide oligomers though a peptide bond and study how peptide size affects their ability to associate with micellar structures.

Micellar environments have been studied extensively for decades. These studies were initially fueled by interest over the nature of the intramicellar microenvironment[18] because they could serve as membrane mimetic systems. The simple model of a micelle consists of a roughly spherical entity with hydrocarbon like core surrounded by a highly charged layer (Stern layer) which contains the ionic headgroups of the individual surfactant molecules, counterions, and water.[19,20] This assembly is in dynamic equilibrium with monomeric surfactant molecules in solution. Aqueous micelles are well-studied organized molecular aggregates and we employ ionic and neutral micelles to provide known and different heterogeneous environments in which to examine the interactions of the 7AT tagged oligomers. The reorientation data point to a balance between ionic and dispersion interactions of the peptides with micelles and this behavior is modeled as a hindered rotor.

In chapter 4 we use several 7AT and tryptophan derivatives to study the role of charge and substituent structure on the dynamics of these probes in micelle solutions. Because 7AT is considered a biological probe, as an alternative to tryptophan, this study affords us the opportunity to investigate the nature in which these structurally similar probes interact with their surroundings. The steady state and fluorescence lifetime measurements indicate partitioning of probes into micelles is highly dependent on ionic interactions and governed by structural features in common with the micelles. The reorientation data give evidence of subtle differences between interactions with micelles for analogous 7AT and tryptophan derivatives.

polymer

fluoresc

examine

associat

molecul

environ

the respo

Chapter 5 summarizes the findings in chapters 2-4 and proposes the use of polymerized micelle assemblies as a medium in which to study the factors dictating fluorescent probes interactions with their environment. These molecular micelles can be examined with covalently attached intramolecular probes and non-bound freely associating probes. These molecular micelles may serve a role in tailoring site-specific molecular probes. These studies could provide a wealth of information regarding the environment of polymerized micelles and could be useful systems in which to compare to the response of probes in potentially larger and more highly ordered dendrimers.

## 1.1 Lit


1. Lak

   Pub

2. Mu

3. Mat

4. Mat

5. Mat

   *81*,

6. Cha

7. Pan

8. Ras

9. Ras

10. Tea

11. *The*

12. Dra

13. Bee

14. Rich

    *Pho*

15. Stev

    Cha

16. Neg

    *Am*

## 1.1 Literature Cited


1. Lakowicz, J. R. *Principles of Fluorescence Spectroscopy*; second ed.; Plenum Publishers: New York, 1999.
2. Mullin, J. W. *Crystallization*; Butterworth-Heinimann: Oxford, 1993.
3. Mathlouthi, M.; Luu, D. V. *Carbohydrate Res.* **1980**, *78*, 225.
4. Mathlouthi, M.; Luu, D. V. *Carbohydrate Res.* **1980**, *78*, 203.
5. Mathlouthi, M.; Luu, C.; Meffrov-Biget, M.; Luu, D. V. *Carbohydrate Res.* **1980**, *81*, 213.
6. Chakraborty, R.; Berglund, K. A. *J. Cryst. Growth* **1992**, *125*, 81.
7. Pan, B.; Chakraborty, R.; Berglund, K. A. *J. Cryst. Growth* **1993**, *130*, 587.
8. Rasimas, J. P.; Blanchard, G. J. *J. Phys. Chem.* **1995**, *99*, 11333.
9. Rasimas, J. P.; Berglund, K. A.; Blanchard, G. J. *J. Phys. Chem.* **1996**, *100*, 7220.
10. Teale, F. W.; Constable, D. *Fluorescent Probes*; Academic Press: New York, 1981.
11. *The Merck Index*; Merck & Co. Inc.: Rahway, 1989.
12. Draths, K. M.; Frost, J. W. *J. Am. Chem. Soc.* **1994**, *116*, 399.
13. Beechem, J. M.; Brand, L. M. *Ann. Rev. Biochem.* **1985**, *54*, 43.
14. Rich, R. L.; Negrerie, M.; Li, J.; Elliott, S.; Thronburg, R. W.; Petrich, J. W. *Photochem. Photobiol.* **1993**, *58*, 28-30.
15. Steward, L. E.; Collins, C. S.; Gilmore, M. A.; Carlson, J. E.; Ross, J. B. A.; Chamberlin, A. R. *J. Am. Chem. Soc.* **1997**, *119*, 6-11.
16. Negrerie, M.; Bellefeuille, S. M.; Whitham, S.; Petrich, J. W.; Thornburg, R. W. *J. Am. Chem. Soc.* **1990**, *112*, 7419-7421.

17. Sa

18. Fe

19. Ta

20. *Ca*

17. Sargent, D. F.; Bean, J. W.; Schwyzer, R. *Biophys. Chem.* **1988**, *31*, 183.

18. Fendler, E. J.; Fendler, J. H. *Adv. Phys. Org. Chem.* **1970**, *8*, 271.

19. Tanford, C. *J. Phys. Chem.* **1972**, *76*, 3020.

20. *Cationic Surfactants*; Marcel Dekker, Inc: New York, 1991; Vol. 37.

L
Aza
F

(7AT)
have s
water
These
acid si
them s
buffer
concen
heteroc
near an
7AT ar
time of
reorient

# Chapter 2

## Lifetime and Reorientation Measurements of 7-Azaindole and 7-Azatryptophan in Aqueous Adipic Acid Solutions. The Significance of Pendant Functionalities in Solution Phase Association Processes

## Summary

In this chapter we report on the ability of the chromophores 7-azatryptophan (7AT) and 7-azaindole (7AI) to sense aggregation of adipic acid in aqueous solution. We have studied the fluorescence lifetime and reorientation dynamics of 7AT and 7AI in water and aqueous adipic acid solutions from subsaturation through supersaturation. These probe molecules, differing by the presence (7AT) or absence (7AI) of an amino acid side group, each possess a labile proton on the chromophore ring system that renders them sensitive to changes in pH, and both chromophores are quenched collisionally in buffer solution. The dependence of the 7AI fluorescence lifetime on adipic acid concentration differs fundamentally from that of 7AT, indicating complexation of the 7AI heterocyclic nitrogen(s) with adipic acid. 7AT exhibits an increase in reorientation time near and above adipic acid saturation concentration and this trend is absent for 7AI. The 7AT amino acid side group interacts with adipic acid with a characteristic persistence time of $< 50$ ps. For 7AI, the interaction with adipic acid is too short-lived to be seen by reorientation measurements.

## 2.1 Int

many i

purifica

crystall

the resu

molecul

crystalli

can and

associat

crystalli

influenc

crystalli

matter b

intermol

intermol

solution

criteria.

molecul

the inve

## 2.1 Introduction

The process of crystallization from solution is of vital economic importance to many industrial processes. Crystallization is the method of choice for separation and purification in the chemical, pharmaceutical, and food industries. Controlling crystallization from solution has a direct effect on the physical properties and purity of the resulting product. To control the crystallization process, we must first understand the molecular interactions between solution constituents that can ultimately lead to crystallization. The goal of this work is to understand the role of probe molecules, which can and do act as impurities, in mediating liquid phase self-assembly.

Crystallization from solution is a complex, dynamic process. The problems associated with studies of crystallization include determining the structure of pre-crystalline aggregates in supersaturated solutions, the nature of crystal nuclei, the influence of impurities, and the relationship between the capture of impurities and the crystallization conditions. The incorporation of impurities is perhaps the most significant matter because of the consequences and the dependence of this process on the details of intermolecular interactions in solution. For this reason we have focused on the intermolecular interactions between (fluorescent) impurity molecules and species in solution capable of crystallization.

The choice of the fluorescent probe molecules for this work is based on two criteria. First, we are interested in working with biologically benign and relevant molecules in aqueous environments because of the potential utility of such molecules to the investigation of protein and peptide structure. Second, using probe molecules with

well-be

data. I

amino a

of trypt

due to

Unfortu

behavio

understo

**Figure 2**
(7AT), a

synthet

7-azain

well-behaved photophysical properties allows for easier interpretation of spectroscopic data. For these reasons, tryptophan is one obvious choice. Tryptophan is an essential amino acid with a well-characterized fluorescence response. The fluorescence properties of tryptophan along with its chromophore moiety, indole, have been studied extensively due to its use as a standard optical probe of protein structure and dynamics.[1-3] Unfortunately, tryptophan is characterized by non-exponential fluorescence relaxation behavior and, without the excited state properties of the chromophore being well understood, interpreting transient fluorescence data in complex systems is problematic.[4-6]

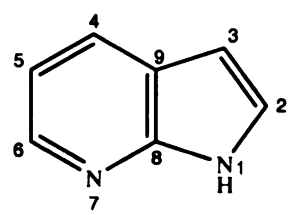


7-azaindole

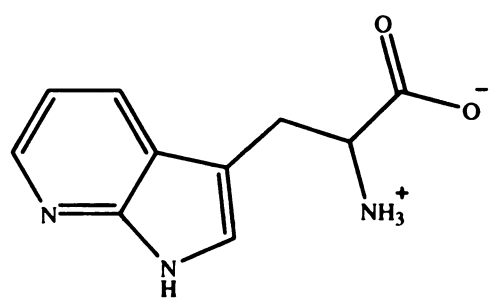


7-azatryptophan

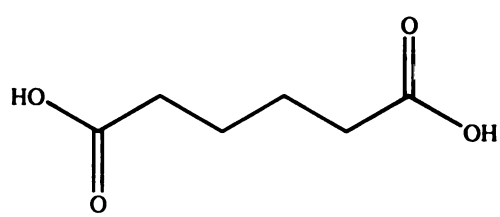


adipic acid

**Figure 2.1** Structures of the chromophores, 7-azaindole (7AI) and 7-azatryptophan (7AT), and solute, adipic acid.

One consequence of this spectroscopic complication is the development of the synthetic amino acid 7-azatryptophan (7AT) and its corresponding chromophore moiety 7-azaindole (7AI) as biological probes (Fig. 2.1).[7-10] 7AT has been used as an alternative

to tryptophan in the study of protein structure and dynamics[8,11,12] because of its well-behaved, single exponential fluorescence decay over a wide pH range.[8,11] The 7AI chromophore is a prototypical model for excited state proton transfer, a fundamental reaction in many chemical and biochemical processes. The dimer of the 7AI chromophore is structurally similar to hydrogen-bonded DNA base-pairs and is regarded as a model for the study of photoinduced mutagenesis.[13-15]

We use these two chromophores to study the pre-crystalline aggregation behavior of aqueous adipic acid. This method is, in effect, a direct examination of impurity incorporation because it uses trace amounts of a chromophore either with (7AT) or without (7AI) a functionality in common with the crystallizing matrix. The time- and frequency-domain optical responses of the probe are monitored as a function of solution composition and these data reveal the details of the intermolecular interactions at work in these systems. The adipic acid system has been studied previously using the optical probes pyrene and pyrene carboxylic acid.[16] Based on the results of that work, we expect 7AT to incorporate into adipic acid pre-crystalline aggregates through its carboxylic acid functionality. In contrast, we expect 7AI to provide the complementary, non-incorporated response. Comparing the results we report here to those for the pyrene-based probes in adipic acid solutions provides information not only on the role of different probes but also allows comparison of amino acids to carboxylic acids for their action as impurities in the crystallization of carboxylic acids.

## 2.2 E

Sigma

obtain

dipotas

Produc

Solutio

concen

maintai

with a

spectro

4500 o

using 2

the spe

and 7A

with a

are gen

100 ps

nm pu

Doubli

with ar

## 2.2 Experimental Section

*Chemicals.* 7-Azaindole (99+%) and D,L-7-azatryptophan were obtained from Sigma Chemical Company and used without further purification. Adipic acid was obtained from Aldrich (99%) and used as received. The buffer solutions were made from dipotassium hydrogen phosphate and citric acid purchased from Spectrum Quality Products, Inc. All solutions were prepared with HPLC grade water from Aldrich. Solutions used for lifetime and reorientation measurements were 5 μM in chromophore concentration. The sample cuvette was temperature-controlled with a brass block holder maintained at 20.0 ±0.1 °C (Neslab RTE-221).

*Steady-State Absorption and Emission Spectra.* Absorption spectra were acquired with a 2 nm band pass using an ATI-Unicam double beam UV-visible absorption spectrometer. Emission spectra were recorded with one of two fluorimeters: a Hitachi F-4500 operating with 5 nm excitation and emission bandpass or a Spex 1681 Fluorolog using 2 nm bandpass for excitation and emission.

*Time-Correlated Single Photon Counting (TCSPC) Spectrometer.* A schematic of the spectrometer used for fluorescence lifetime and reorientation measurements of 7AI and 7AT is shown in figure 2.2 The light pulses used to excite the sample are produced with a cavity-dumped, synchronously pumped dye laser (Coherent 702-2). Light pulses are generated by a CW mode locked Nd:YAG laser (Quantronix 416) producing pulses of 100 ps duration FWHM at 1064 nm with ~9 watts average power at 80 MHz. The 1064 nm pulse train is frequency doubled with Quantronix SHG assembly model 324. Doubling is achieved by angle tuning a type II KTP crystal yielding pulses at 532 nm with an average power of ~800 mW. The 532 nm light pulses are directed for excitation

of a cav

cavity d

of dye

pulses v

pulses r

observe

with 90

creating

delay b

focused

introdu

filtering

harmon

Laser (

88mm

≤ 1 m

light w

(G-T)

pseudo

(Amer

detail

Hama

and o

chann

of a cavity dumped synchronously pumped dye laser (Coherent 702-2). The dye laser is cavity dumped and its output can be tuned from ~550-1000 nm depending on the choice of dye and optics used. For these experiments, the cavity was dumped at 4 MHz and pulses were generated at 580 nm using Rhodamine 6G (Eastman Kodak) dye. The output pulses in this configuration are ~90 mW average power with pulses of 5 ps FWHM as observed by autocorrelation. The output of the dye laser is divided by a beam splitter with 90% of the output being sent for excitation of the sample and 10% of the output creating a reference pulse that is sent into a fiber optic delay line allowing for temporal delay between signal and reference. The portion of the beam sent for excitation is focused into an angle tuned 1 cm KDP crystal to produce 290 nm light. The KTP crystal introduces and astigmatism that is compensated by a plano-convex lens followed by filtering through a colored glass filter to remove the fundamental from the second harmonic light. The polarization is then rotated by a fused silica half-wave rhomb (CVI Laser Corporation) to 0° (vertical). The polarized UV is focused into the sample with an 88mm focal length bi-convex fused silica lens resulting in average power at the sample of $\leq$ 1 mW. For all experiments emission is collected at 90° with respect to the incident light with a reflecting microscope objective (Ealing x36/0.5) followed by a Glan-Taylor (G-T) prism for selection of polarization. The selected polarization is then sent thought a pseudo polarization scrambler and focused into a subtractive double monochromator (American Holographic DB10-S). The detection electronics have been described in detail elsewhere,[17] and we review the salient features briefly here. For detection, a Hamamatzu (R3809U-50) cooled dual stage microchannelplate photomultiplier is used and operated at a bias of 3.1 kV. The signal produced from the detector is sent to one channel of a four channel constant fraction discriminator (CFD, Tennelec TC455) for

process
the TA
start. T
delay
termina
whose
referen
channe
helps t
range.
(Tektro
(MCA,
maxim
Fluores
respect
instrur
to ~1
reorie
Analy
times
non-

processing prior to input to the time-to-amplitude converter (TAC, TC864). We operate the TAC in "reverse mode", as such the input signal from the MCP-PMT serves as the start. The stop signal originates from the portion of laser pulse split into the fiber optic delay line. This custom made optical delay consists of varying lengths of fiber terminating in detection by an avalanche photodiode detector (PD, Hamamatsu S2381) whose signal is routed into a second channel of the CFD. The output of the CFD reference signal is electronically delayed (Tennelec TC412A) and sent to the TAC stop channel. This configuration of start and stop channels is termed "reverse mode" and helps to eliminates pulse pile-up and ensure operation of the TAC in a linear conversion range. The valid conversions of the TAC are output and displayed on an oscilloscope (Tektronix 2230) and rate meter (Tennelec TC525) and sent to a multichannel analyzer (MCA, Tennelec PCA-II) for collection. Emission was monitored at the fluorescence maxima of the chromophores using a 20 nm bandpass on the collection monochromator. Fluorescence intensity decays were collected at polarizations of 0°, 54.7° and 90° with respect to the (vertical) polarization of the incident excitation pulse. The typical instrument response function is 35 ps and the chromophore lifetimes range from ~400 ps to ~1 ns. No deconvolution of the response function from the data was required. For the reorientation data, where $\tau_{OR}$ ~ 30-50 ps, deconvolution may be thought to be important. Analysis of the experimental data, however, show deconvolution to produce reorientation times that are the same to within the experimental uncertainty as those extracted from non-deconvoluted data.

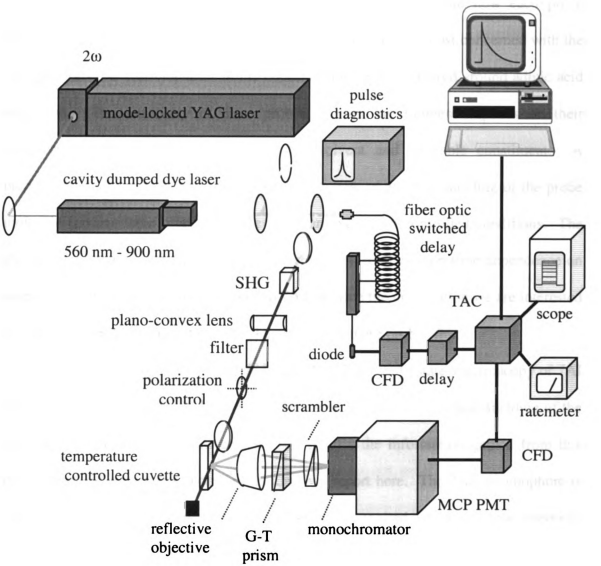


**Figure 2.2** Schematic of the time correlated single photon counter used to measure fluorescence lifetimes and rotational diffusion dynamics.

## 2.3 Results and Discussion

The objective of the work we report here is to understand how each probe molecule interacts with adipic acid in aqueous solution. We are most concerned with the influence of these chromophores in the concentration region centered around adipic acid saturation. The sensitivity of these probes to their environment depends on their chemical structures and the identity of the solvent and saturable constituent. A prerequisite to these measurements is the development of an understanding of the probe molecule spectroscopic properties under comparatively well-controlled conditions. The steady state linear response, fluorescence lifetime and reorientation time dependence on adipic acid concentration for both 7AI and 7AT provide the information we are interested in. We consider the steady-state optical properties of these probes first.

*Steady-State Spectroscopy of 7AI and 7AT.* The steady state spectroscopy of 7AI and 7AT has been investigated previously and there is a substantial understanding of the electronic structure of these molecules. [7-12] We use the information gained from this literature to aid our understanding of the data we report here. The 7AI chromophore is characterized by the presence of several electronic excited states in close energetic proximity, with the energetic spacing and transition strengths depending on the protonation condition of the heterocyclic nitrogens. At chromophore concentrations well above those we use in this work, there is some spectroscopic evidence for the formation of H-bonded oligomers.[18] For the experiments we report here, we do not see evidence for H-bonded dimers that can lead to $H^+$-exchange.

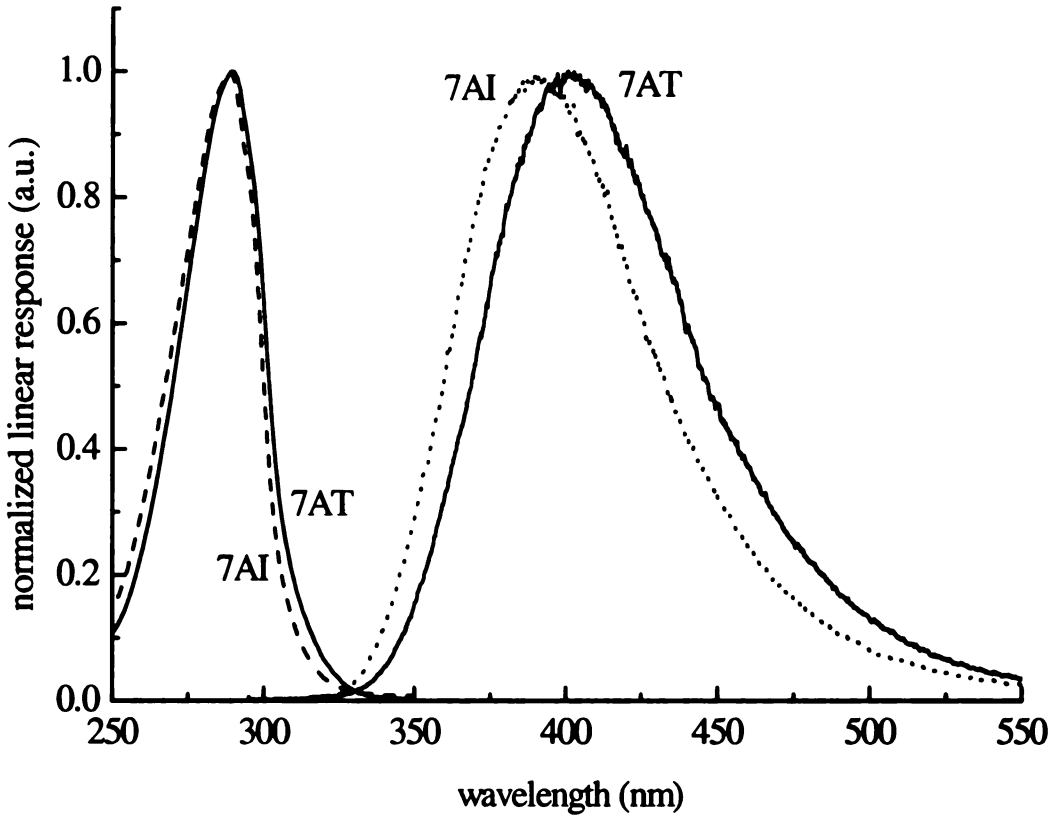


**Figure 2.3** Linear absorption and emission spectra for the probes 7AI (dotted trace) and 7AT (solid line) in aqueous solution. Intensities of the bands have been normalized for presentation.

Linear response data provide information on the nature of the local environment sensed by the probes. Steady state absorption and emission measurements were obtained for 7AI and 7AT in aqueous adipic acid solutions. The absorption and emission maxima of aqueous 7AI are 288 nm and 389 nm, respectively (Fig. 2.3). In adipic acid solutions, absorption band shifts to the red by ~2 nm, and for adipic acid concentrations higher than 10% of saturation, the fluorescence maximum of 7AI shifts to 441 nm (Fig. 2.4a). This significant emission red shift is nearly complete by 5% of saturation and is thought to arise from protonation of the azaindole chromophore at position $N_7$. The ground state $pK_a$ of 7AI is 4.5[19] and the pH for the solutions of adipic acid we use are in the range of

pH 3.80 at 1% of saturation to 2.68 at 110% of saturation. A species distribution plot for 7AI (Fig. 2.5a) indicates that the dominant species interrogated spectroscopically is the protonated form.

The sensitivity of 7AT to its local environment is similar, but more complex than that of 7AI. The presence of the amino acid side group on 7AT gives rise to a wider variety of (likely stronger) interactions with adipic acid than those seen for 7AI. The amino acid side chain of 7AT can exist in cationic, zwitterionic, and anionic forms along with the labile proton of the chromophore at $N_7$. Potentiometric titrations of 7AT show that the ground state $pK_a$ values for $CO_2H$, $N_7$, and $NH_3^+$ are 2.70, 3.85 and 9.35, respectively.[20] With these $pK_a$ values, we calculated a species distribution plot of 7AT as a function of pH (Fig 2.5b). Three species coexist in the pH range of the adipic acid solutions used here. The experimental absorption maxima of 7AT aqueous and adipic acid solutions were 290 nm and 292 nm, respectively, showing the same behavior as we see for 7AI. The fluorescence maximum of aqueous 7AT is at 399 nm (Fig. 2.3) and in adipic acid solutions greater than 20% of the saturation concentration, the fluorescence maximum shifts to 450 nm (Fig. 2.4b). As with 7AI, the fluorescence spectral shift with decreasing pH is the result of protonation of the azaindole chromophore at the $N_7$ position. The emission spectral shift is more gradual for 7AT than it is for 7AI because of the lower $N_7$ $pK_a$ of 7AT (3.85) compared to that for 7AI (4.5). Because of this difference, solutions of higher adipic acid concentration are required to reach the pH values where the emission spectrum is dominated by the $N_7$-H protonated species. For 7AT, there is also a change in the protonation of the carboxylic acid side chain in this pH range. Because the amino acid side group is not conjugated with the azaindole

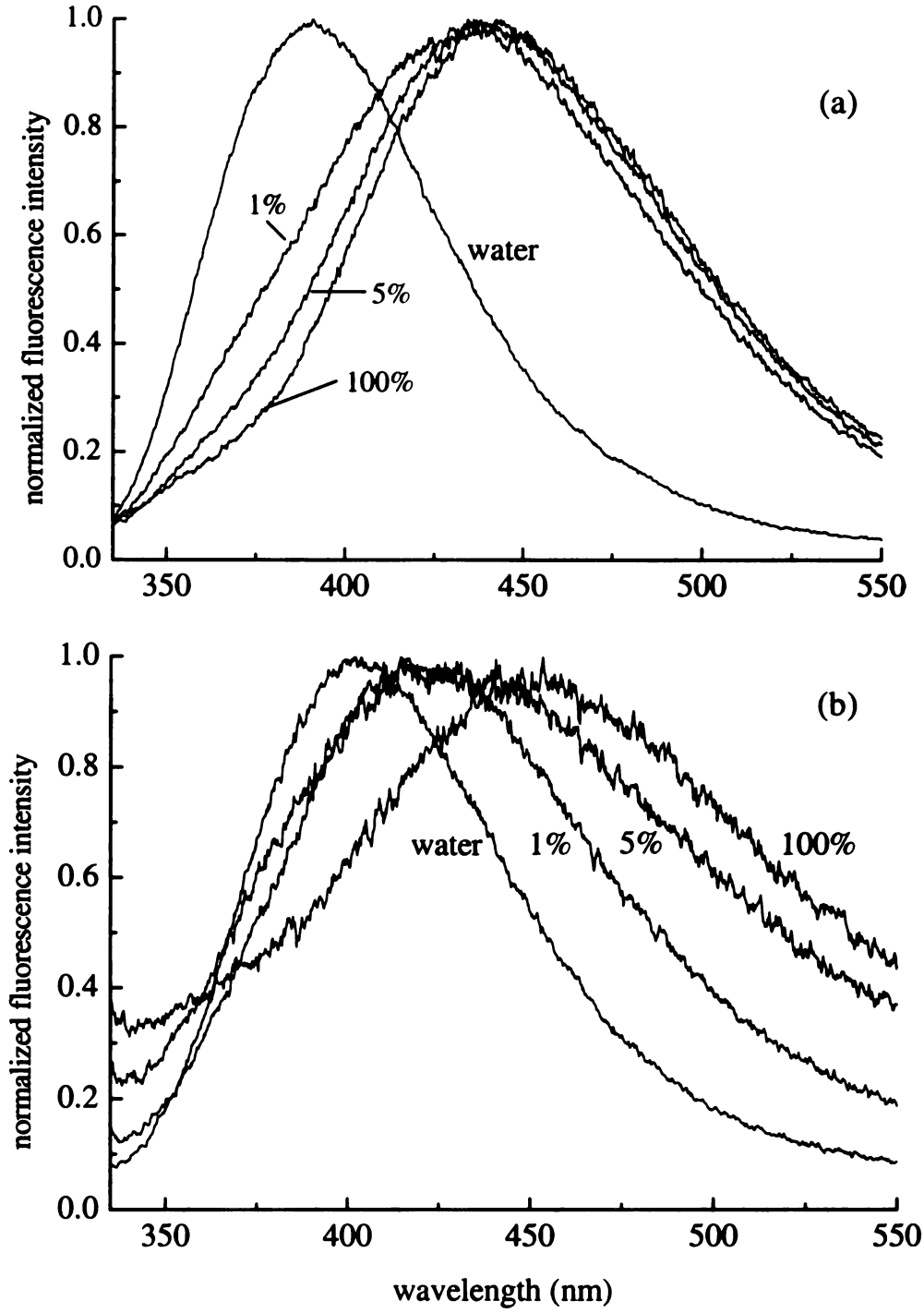


**Figure 2.4** Normalized emission spectra for (a) 7AI and (b) 7AT as a function of adipic acid concentration. Chromophore concentrations are 5 μM for all solutions. The emission spectra shift progressively to the red with increasing adipic acid concentrations. Shown are spectra in water, 1%, 5%, and 100% of saturation adipic acid solutions.

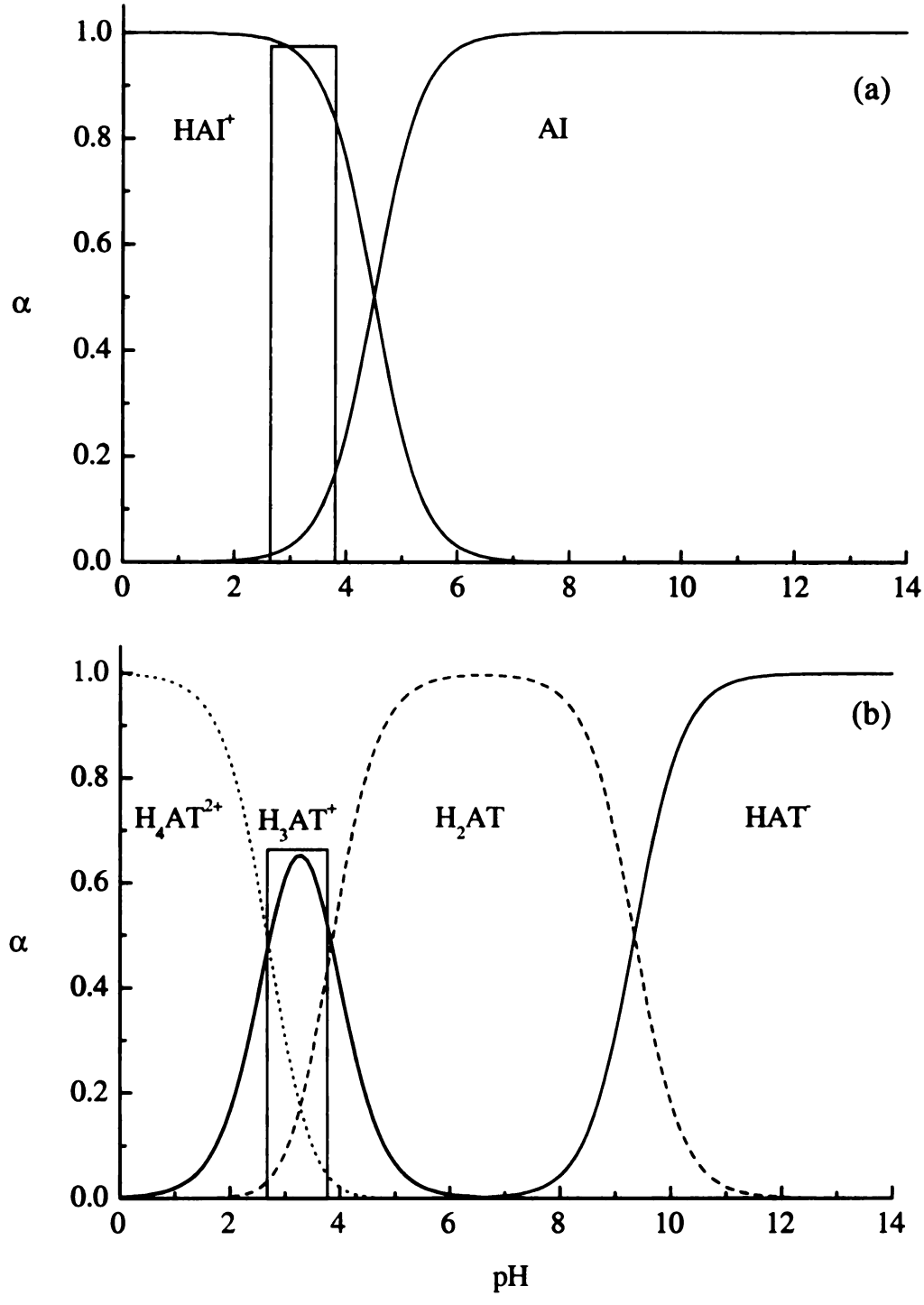


**Figure 2.5** Calculated α-fractions for (a) 7AI and (b) 7AT. The pH range of adipic acid solutions (2.7 - 3.8) is boxed. The calculations were made using ground state $pK_a$ values for each chromophore. For 7AI, pK = 4.5 and for 7AT, $pK_1 = 2.70$, $pK_2 = 3.85$ and $pK_3 = 9.35$.

chrom

functi

inform

Due t

excite

local

organ

intera

terms

For 7

the N

surrou

this in

fluore

be as

possi

the c

availa

nonra

modu

chromophore, we do not expect the protonation status of the amino acid carboxylic acid functionality to have a pronounced effect on the spectroscopic response of the probe.

*Fluorescence Lifetimes of 7AI and 7AT.* Lifetime measurements yield information on solution composition and may be sensitive to solute local organization. Due to the number of intermolecular and intramolecular factors that can influence the excited state lifetime of a given chromophore, the dependence of fluorescence lifetime on local environment remains in the realm of phenomenology for most systems. For many organic molecules, the excited state lifetime depends on site-specific intermolecular interactions, such as H-bonding or complexation, and this effect can be understood in terms of the influence of the interaction on the electronic structure of the chromophore. For 7AI, the most likely locations for site-specific intermolecular interactions to occur are the $N_1$-H and $N_7$ functionalities.[18] The 7AI $N_1$-H moiety will interact with its surroundings through hydrogen bonding and there is some evidence that the strength of this interaction is related to the chromophore fluorescence lifetime.[18] The relatively short fluorescence lifetime ($\tau_{fl}$) of ~ 900 ps for 7AI in water at room temperature is thought to be associated with internal conversion mediated by the $N_1$-H stretching mode or, possibly, dissociation of the N-H bond.[19,21]

Because of the labile and environmentally sensitive nature of the N-H bond(s) in the chromophore, 7AI and 7AT are relatively sensitive to the proton content and availability of their immediate surroundings. The impact of the $N_1$-H functionality on nonradiative decay channels is illustrated by methylation of $N_1$. When $N_1$ is methylated, modulation of the nonradiative pathways accessed by specific interactions at the $N_1$ site is

blocked, resulting in a longer radiative lifetime. Specifically, the fluorescence lifetime of 7AT is 800 ps and that of 1-methyl-7AT is 21 ns.[19]

Lifetimes for 7AI were measured in aqueous adipic acid solutions over the concentration range of 0 to 110% of saturation of adipic acid. The lifetime of 7AI in aqueous solution is 912 ± 3 ps and it increases in adipic acid solutions to ~ 1150 ps (Fig. 2.6a). The rise in lifetime follows the adipic acid concentration-dependence of the fluorescence spectral shift; it is nearly complete at 1 % saturation and remains constant at higher adipic acid concentrations. In principle, this lifetime change can be the result of either protonation of the chromophore at the $N_7$ position or complexation with adipic acid. We will return to a discussion of this point below. Under careful examination, the fluorescence lifetime of 7AI decreases slightly at higher adipic acid concentrations. This change is seen below saturation and continues though saturation. There is no indication that the fluorescence lifetime of 7AI is sensitive to any changes in local environment near saturation.

The single exponential fluorescence lifetime of 7AT, $\tau_{fl}$, is 796 ± 3 ps in water and, in contrast to the behavior seen for 7AI, the addition of adipic acid reduces the lifetime of 7AT (Fig. 2.6b). The change in lifetime of 7AT could also be the result of protonation of the azaindole chromophore because it follows the concentration-dependence of the steady state fluorescence spectral shift, or it could arise from some other effect. The lifetime remains constant through saturation of adipic acid. The fact that the lifetime decreases for 7AT in adipic acid solution while that of 7AI increases under the same conditions is a clear indication that the nature of their interactions with adipic acid are different.

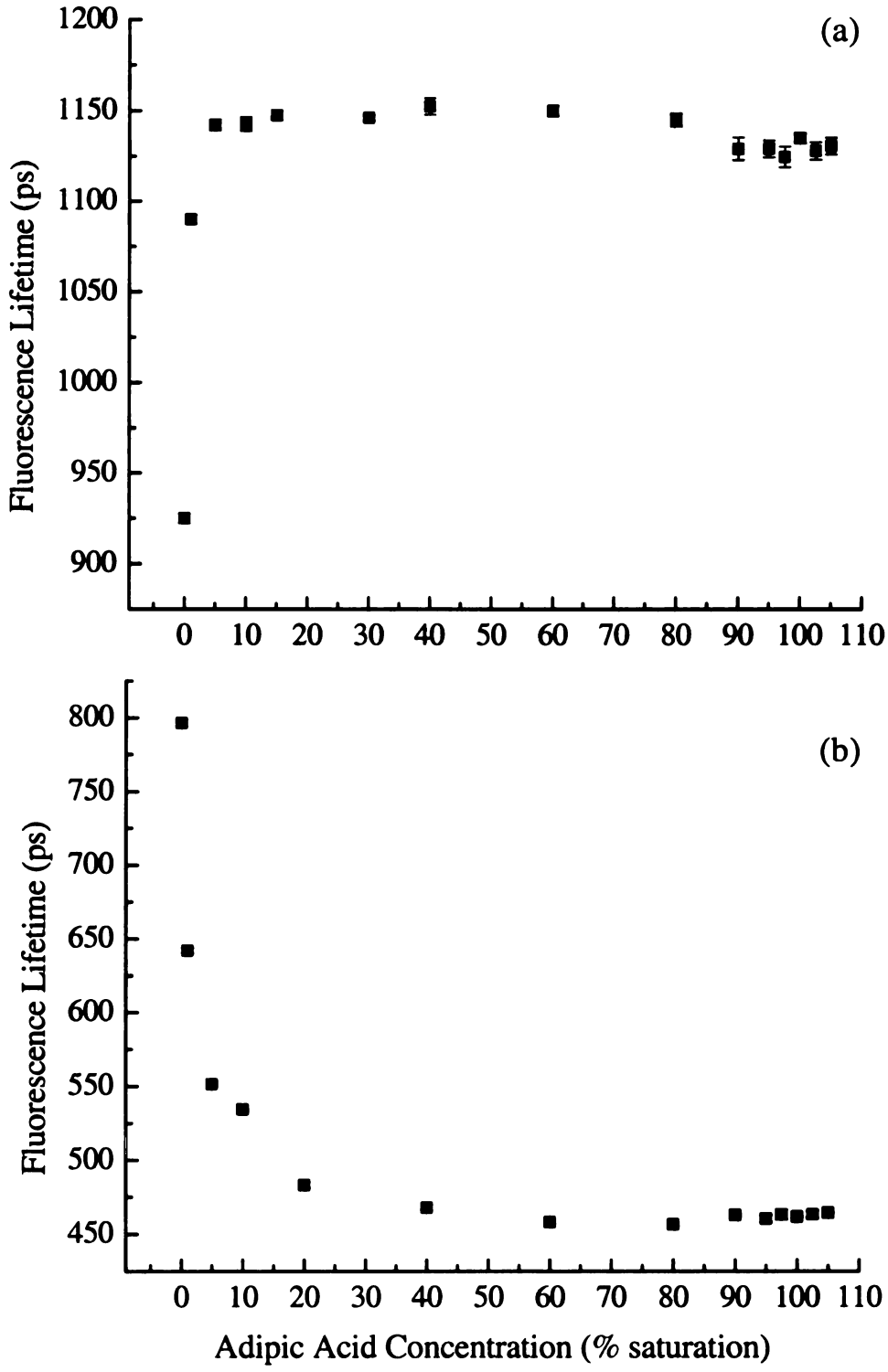


Figure 2.6 Fluorescence lifetimes of (a) 7AI and (b) 7AT as a function of adipic acid concentration. Where error bars are not visible, the uncertainty lies within the vertical dimension of the symbol.

In an effort to elucidate the specific role of adipic acid in these measurements, we have also measured the lifetimes of 7AI and 7AT in buffer solutions. It is important to separate the adipic acid and $H^+$ contributions to the lifetime dependence because we are interested in determining the role of adipic acid interactions with the chromophores. The buffer solutions spanned the same pH range as the adipic acid solutions. We used McIlvaine's buffer,[22] a system comprised of citric acid and dipotassium hydrogen phosphate such that the sum of the constituent analytical concentrations is 0.1 M. The 7AI lifetime data are plotted for both the adipic acid the buffer solutions as a function of pH in Fig. 2.7a. A striking feature of these data is the difference in the trends they exhibit and the large differences between lifetimes for 7AI in buffer and adipic acid solutions. For 7AT, the data, shown in Fig. 2.7b, exhibit similar behavior for both solutions, but with an offset in lifetime at lower pH. We understand these data as follows.

The differences we observe for 7AI in buffer and adipic acid solutions cannot be based solely on pH. The direct interaction or complexation of adipic acid with 7AI must be responsible for the data shown in Fig. 2.6a. The dependence of the 7AI lifetime on protonation at the $N_7$ position is manifested in the buffered solutions. The buffered solutions exhibit the same absorption and emission spectra as the adipic acid solutions at corresponding pH values, so the existence of a strong complex between adipic acid and the chromophore heterocyclic nitrogens is not evident. Thus, the formation of a weak, or short-lived complex between adipic acid and 7AI based on H-bonding interactions is likely responsible for the form of the data shown in Fig. 2.6a. This conclusion is consistent with the reorientation data for 7AI, which we consider below.

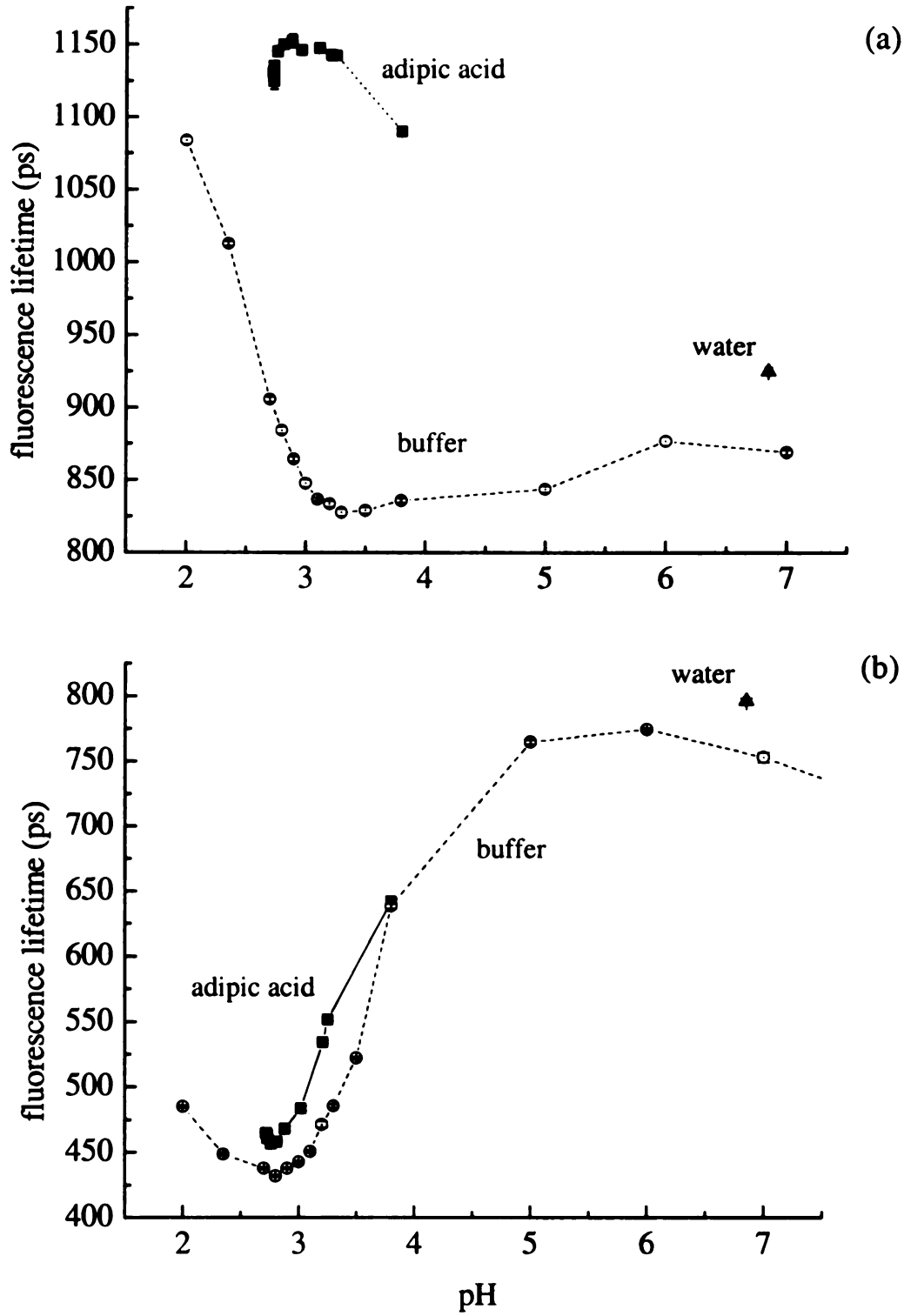


**Figure 2.7** Fluorescence lifetimes measured for aqueous solutions containing (a) 5 μM 7AI and (b) 5 μM 7AT in adipic acid (■), buffered (o), and un-buffered (▲), aqueous solutions as a function of pH.

For 7AT, the adipic acid-lifetime dependence and buffer solution pH-dependence mirror one another, and these data show that the lifetime of this chromophore is determined largely by protonation at the $N_7$ position. If there is an interaction with adipic acid for this chromophore, it is with the amino acid side chain and not at the chromophore heterocyclic nitrogens. Again, this is an issue that can be addressed through reorientation measurements (*vide infra*). The buffer solution pH-dependent lifetime data for 7AI and 7AT also mirror one another but are offset in pH (Figs. 2.7). We understand this offset as resulting from the different $N_7$ $pK_a$s for these molecules. The data in Fig. 2.7b show a systematic offset in lifetime between the adipic acid and buffer solutions for 7AT. This offset is the result of collisional quenching interactions in the buffer solution.

There are two possible mechanisms for quenching in these systems. The first is so-called static quenching because it is mediated by the formation of a ground state complex, where only the noncomplexed species exhibits a radiative response. This type of quenching is manifested by a decrease in fluorescence intensity but with no change in fluorescence lifetime of the radiatively active chromophores. Our experimental data are not consistent with this quenching mechanism. It has been shown previously that 7AI and 7AT are quenched by KI and acrylamide,[23] and our buffer system is seen to alter the fluorescence lifetime of the chromophores. The key question here is to what extent the pH-dependent changes in lifetimes are due to $[H^+]$ and to what extent the data can be understood in terms of collisional quenching at a constant pH? We can address this issue by measuring the chromophore lifetimes as a function of buffer concentration at a constant pH.

The fluorescence lifetime of a chromophore in the presence of a collisional quencher is expected to behave according to the Stern-Volmer relationship,[24] given by Eq. 2.1.

$$\tau_0/\tau = 1 + K_{sv}[Q] = 1 + k_q\tau_0[Q] \qquad (2.1)$$

where $\tau_0$ is the lifetime of the chromophore in the absence of quencher, $\tau$ is the observed lifetime in the presence quencher, $K_{sv}$ is the Stern-Volmer constant, and $k_q$ is the bimolecular quenching rate constant. Stern-Volmer plots for 7AI and 7AT in buffer solutions are shown in Figs. 2.7. For these measurements, the total buffer concentration was varied and the pH held constant at 3.2. The Stern-Volmer plot for 7AI gives a linear fit with the slope and intercept yielding the bimolecular collision rate constant and the intrinsic fluorescence lifetime, respectively. These values, $k_q$ = (2.5±0.1) x $10^9$ $\underline{M}^{-1}$ $s^{-1}$ and $\tau_0$ = 1053 ±20 ps result in a calculated value of $K_{sv}$ = 2.63 $\underline{M}^{-1}$. The Stern-Volmer plot for 7AT yields a linear fit with $k_q$ = (2.3±0.1) x $10^9$ $\underline{M}^{-1}$ $s^{-1}$, $\tau_0$ = 512 ±6 ps and $K_{sv}$ = 1.164 $\underline{M}^{-1}$. The extrapolated values for $\tau_0$ are in good agreement with experiment for 7AI and are approached closely for 7AT in adipic acid at pH 3.2, where $\tau_{fl}$ ~ 1150 ps. The ~10% difference between the Stern-Volmer $\tau_0$ value and the experimental $\tau_{fl}$ value in adipic acid solution is likely due to the difference in dielectric response sensed by the chromophore in the adipic acid and buffer solutions.

The Stern-Volmer plots indicate that the two probes are quenched collisionally with similar efficiency in the citric acid/dipotassium hydrogen phosphate buffer system, at least at pH 3.2. While the physics of the quenching process may be the same over the pH range of interest here, there is more than one species present for each probe at this pH, and it is possible that one form of each chromophore may be more susceptible to

$\tau^{-1}$ (ps$^{-1}$)

**Figu**
citri
and

quer

and

mul

whi

issu

quer

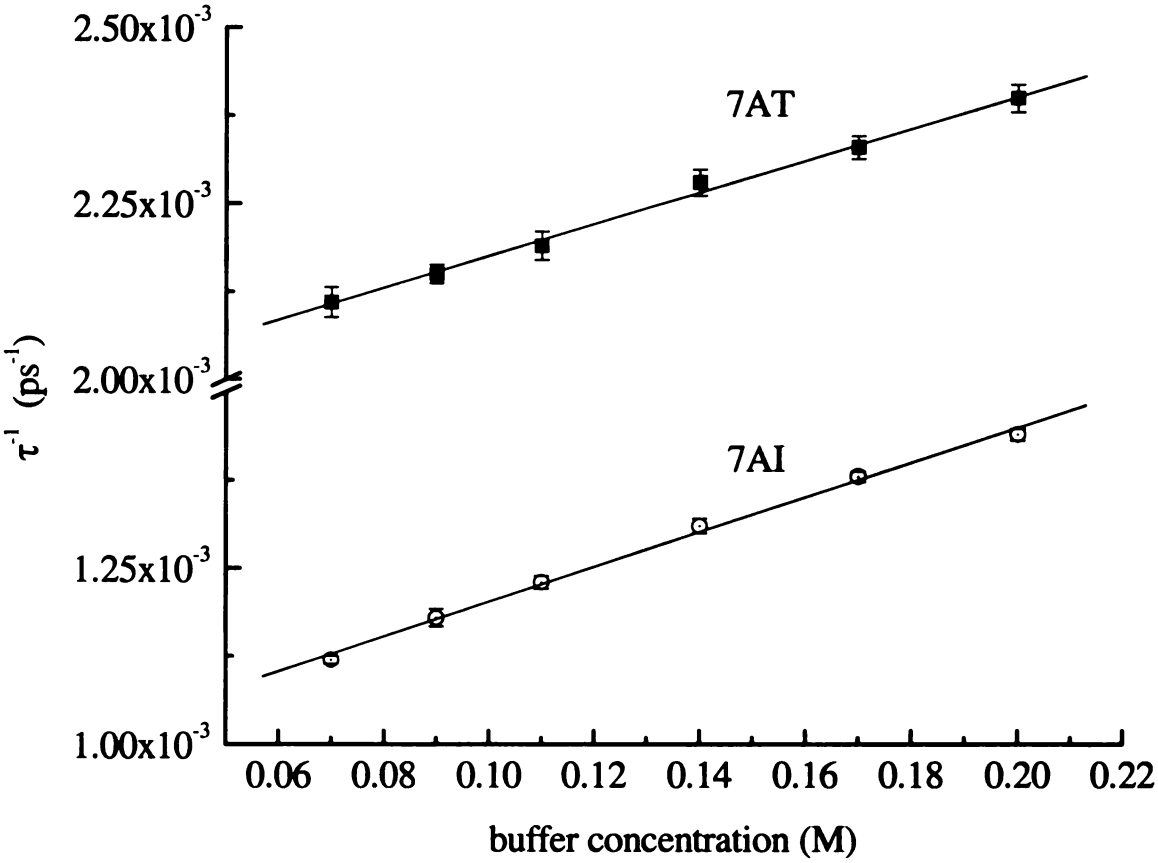


**Figure 2.8** Stern-Volmer plots for 7AI (o, bottom trace) and 7AT (■, top trace) in citric acid/dipotassium hydrogen phosphate buffer. For 7AI $k_q$=(2.5±0.1) x $10^9$ $\underline{M}^{-1}$ $s^{-1}$ and for 7AT $k_q$= (2.3±0.1) x $10^9$ $\underline{M}^{-1}$ $s^{-1}$.

quenching than another. 7AI at pH 3.2 exists primarily (~95%) in its protonated form and 7AT is ~80% protonated at the chromophore $N_7$ site. In addition to the issue of multiple probe molecule species being present, it is not clear from the data we report here which of the buffer constituents is responsible for the quenching. Regardless of these issues, recovery of the same value of $k_q$ for each chromophore suggests the same quenching mechanism for each.

*Reorientation of 7AI and 7AT.* The steady state and fluorescence lifetime measurements provide important information regarding the local environment of the probe molecules. These data are useful but cannot, by themselves, provide a complete picture of adipic acid interactions with 7AI and 7AT in solution. To better understand the nature of the local organization present in aqueous adipic acid solutions, we have examined the rotational diffusion dynamics of 7AI and 7AT in those systems. Rotational diffusion measurements can provide information about intermolecular interactions over the length scales comparable to and greater than the dimensions of the probe molecule.[25,26] Comparing the reorientation behavior of 7AI with that of 7AT provides direct insight into the existence and time scale of intermolecular interactions between the probe molecules and adipic acid in solution.

The theoretical framework for the interpretation of rotational diffusion data is well established,[26,27] and both neat and binary solvent systems have been modeled effectively. Reorientation measurements sense solvent-solute interactions over a time scale in which a large number of molecular collisions occur, and the information extracted from the data is relevant to the average environment experienced by the reorienting moiety. For many binary systems, such as those reported in this work, the molecular-scale interactions responsible for the motional behavior of the probes are not modeled accurately using only the bulk solution properties and, in many cases, the results are consistent with site-specific intermolecular interactions. For polar systems, dielectric friction,[28] dipolar interactions,[29] and the formation of solvent-solute complexes[30] can all contribute to the reorientation behavior of a given probe molecule. We consider the reorientation behavior of 7AI and 7AT and the role that such interactions play in determining the motional properties of these probe molecules.

To obtain reorientation data, we use our TCSPC system to excite the samples with a vertically polarized light pulse and collect the time-resolved emission response at polarizations parallel ($I_{\parallel}(t)$) and perpendicular ($I_{\perp}(t)$) to that of the excitation pulse. The combination of these time-domain data according to Eq. 2.2 yields the induced orientational anisotropy function, R(t).

$$R(t) = \frac{I_{\parallel}(t) - I_{\perp}(t)}{I_{\parallel}(t) + 2I_{\perp}(t)} \tag{2.2}$$

The form of the experimental R(t) function is modeled to infer information on the chromophore local environment. The form of R(t) depends on the optical properties of the probe and its interactions with its local environment. In principle, R(t) can contain up to five exponential decays, depending on the angle between the excited and emitting transition dipole moments and the effective rotor shape of the probe.[31] It is unusual to observe more than two decays in R(t) and the most common case is to recover a single exponential decay

$$R(t) = R(0)\exp(t/\tau_{OR}) \tag{2.3}$$

where $\tau_{OR}$ is the orientational relaxation time, related to the Cartesian components of the rotational diffusion constant, and R(0) is the zero time anisotropy, related to the intrinsic spectroscopic properties of the chromophore. For the reorientation measurements we report here, R(t) decays as a single exponential, as indicated in Eq. 2.3.

Extracting chemical information from reorientation data relies on relating $\tau_{OR}$ to the molecular properties of the system. The modified Debye-Stokes-Einstein (DSE) equation (Eq. 2.4) is the starting point for the extraction of chemical information from the decay of R(t).[32-34]

$$\tau_{OR} = \frac{\eta V f}{k_B T S} \tag{2.4}$$

The term $\eta$ is the bulk viscosity of the medium, V is the hydrodynamic volume of the probe molecule, $k_B$ is the Boltzmann constant, T is temperature, $S$ is a shape factor to account for the non-spherical shape of the probe, and $f$ is a friction coefficient. The bulk viscosity can be measured directly, and the quantities $S$ [33] and $V$ [35] are determined by models and are based on the molecular structure of the probe. The term $f$ is, effectively, the solvent-solute frictional coefficient and is estimated based on the shape of the probe.[34] In the stick limit, $f = 1$, and this quantity can vary from 0 to 1 in the slipping boundary condition. The values of $\tau_{OR}$ predicted by the DSE equation can be compared to those obtained experimentally as a means to gauge the strength of interaction between the probe molecule and its immediate surroundings. It is important to note, however, that there is substantial uncertainty in the determination of probe or system properties with the DSE equation. Specifically, estimation of the hydrodynamic volume, V, solute shape, S, and solvent-solute frictional term, $f$, all rest on model parameterizations, and the relationship between bulk and local solvent viscosity remains an open issue. Despite these limitations, comparison of experimental data to the predictions of the DSE model can provide some insight into the nature of intermolecular interactions.

Despite the simplicity of this model and the intrinsic complexity of the phenomena under consideration, the modified DSE equation provides a useful, qualitative prediction of the reorientation behavior of small molecules in polar solvents. Based on the experimental observation of a single exponential anisotropy decay and the assumption that the dominant electronic transition is long-axis polarized,[36] we model 7AI as a prolate rotor. For 7AI we calculate V = 109 $Å^3$ using the method of van der Waals increments.[35]

To approximate the non-spherical shape of 7AI in the context of a prolate rotor, the long-axis and short-axis molecular dimensions of the optimized geometry in the plane of the ring were used. The axial ratio was held constant and dimensions were scaled to give the calculated hydrodynamic volume. Perrin's equation[33] gives a shape factor S = 0.82 for a prolate ellipsoid with a major axis of 8 Å and a minor axis of 5 Å. Using these parameters and assuming a sticking limit boundary condition ($f$ = 1), appropriate for polar solvents and solutes, we calculate a reorientation time of 32 ps for 7AI in water. This value agrees well with the experimental data for 7AI water and in aqueous adipic acid solutions (Fig. 2.9). The reorientation time for 7AI is constant to within experimental uncertainty for all adipic acid solutions. From our previous work we know that the bulk solution viscosity change over this range of adipic acid concentration is negligible.[16] We also know from that work that, near saturation concentration, there are oligomeric adipic acid species present in solution. The reorientation data for 7AI suggest that this probe molecule does not associate strongly with the adipic acid. We do, however, know that there is a detectable interaction between 7AI and adipic acid as seen in the lifetime data (Fig. 2.6a). The fact that we do not see any adipic acid concentration-dependence to the reorientation data (Fig. 2.9) shows that the lifetime of the 7AI-adipic acid interaction is much less than the reorientation time of 30 ps.

We present our reorientation data for 7AT in Fig. 2.9. The results for this probe molecule are qualitatively different than those we recover for 7AI. Modeling the shape of 7AT is not as straightforward as it is for 7AI. As for 7AI, the anisotropy decay is observed experimentally to be single exponential and because of the similarity of the chromophore portion of 7AI and 7AT, we model 7AT as a prolate rotor with a van der Waals volume of 179 $Å^3$.[35] The effective rotor shape of 7AT will not necessarily

$\tau_{vv}$ (ps)

**Figu**
adip

be a

The

leng

dim

prol

with

solu

time

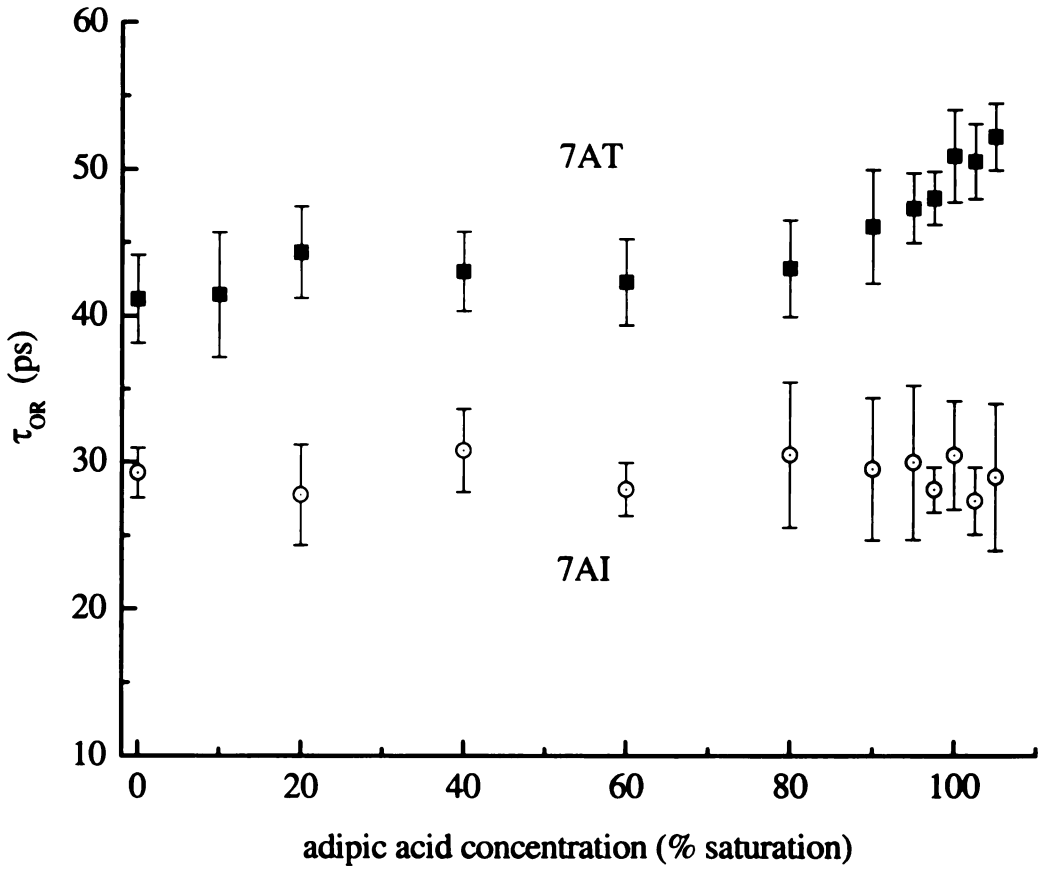


**Figure 2.9** Reorientation data for 7AT (■, top) and 7AI (o, bottom) in aqueous adipic acid solutions.

be approximated well by its optimized geometry due to the labile nature of its side chain. The one dimension that will not change is the long axis of the chromophore. We use the length of 8 Å for this axis. The hydrodynamic volume of 7AT dictates a second axis dimension of 6.5 Å. With these values, the shape factor *S* is 0.94 and modeling 7AT as a prolate rotor in the stick limit yields $\tau_{OR}$ = 47 ps. This calculated time constant falls within the range of experimental reorientation times for 7AT in aqueous adipic acid solutions (Fig. 2.9). The adipic acid-concentration dependence of the 7AT reorientation times possesses a form that is discernibly different than that seen for 7AI. The

reori

= 52

conc

envi

we r

led t

are k

to fo

obse

ascri

rang

$pK_a$

data

for

inter

betw

that

com

reor

corr

with

that

reorientation time increases from $\tau_{OR}$ = 43 ± 3 ps at 80% of adipic acid saturation to $\tau_{OR}$ = 52 ± 2 ps at 105% of saturation. This increase in reorientation time with adipic acid concentration near saturation demonstrates that 7AT senses changes in its molecular environment that are not reflected by the bulk solution. Comparing these results to those we reported previously for a different complexing system is instructive.

Previous reorientation studies of 1-pyrenecarboxylic acid in adipic acid solution led to the conclusion that adipic acid oligomers formed in solution.[16] Carboxylic acids are known to form ring-bound dimers by hydrogen bonding.[37] For this type of complex to form, both carboxylic acid moieties must be protonated. The fact that we do not observe the same behavior for 7AT as was seen for 1-pyrenecarboxylic acid can be ascribed to the fact that the 7AT amino acid side group is largely deprotonated in the pH range we work in here. The $pK_a$ of 1-pyrenecarboxylic acid is 4.0[38] in comparison to a $pK_a$ of 2.70 for the carboxylic acid functionality of 7AT. The experimental reorientation data do not exhibit a step-wise increase in reorientation time near saturation, as was seen for pyrenecarboxylic acid. We conclude from this finding that the details of the intermolecular interactions between 7AT and adipic acid are different than those seen between 1-pyrenecarboxylic acid and adipic acid.

The continuous trend in the reorientation time of 7AT near saturation suggests that the 7AT-adipic acid system does indeed form complexes but the lifetime of these complexes is short relative to the reorientation time of the molecule. If we use the reorientation time of 50 ps as an estimate, at room temperature this upper bound corresponds to a complexation energy of ~ 3-5 kcal/mol, an energy entirely consistent with hydrogen bonding. Because this effect is seen for 7AT and not for 7AI, we infer that the interaction responsible for the behavior we observe is with the 7AT side group.

There can be a number of H-bonding interactions between adipic acid and the zwitterionic amino acid group, and our experimental data do not allow resolution of this matter.

It is also possible that, near saturation, the fraction of 7AT molecules that are fully protonated increases and such a condition could lead to stronger solvent-solute interactions, accounting for the reorientation data. The ground state $\alpha$-fraction plot, shown in Fig. 2.5b would seem to be consistent with this possibility, but there are two factors that serve to make it unlikely. The first is that the excited state $pK_a$ values, which are relevant to the measurements we report here, are not known but are almost certainly quite different than those for the ground state of 7AT. The second factor that makes a change in species distribution unable to account for these data is that, in the adipic acid concentration range around saturation, there is very little change in the steady state emission spectrum, suggesting no substantial variation in species distribution over the range where the reorientation times of 7AT vary.

## 2.4 Conclusions

We have examined the steady state and time-resolved responses of 7AI and 7AT in adipic acid solutions over the subsaturation to supersaturation concentration range. Our lifetime data indicate the existence of a weak complex between 7AI and adipic acid. For 7AT, the change in lifetime with adipic acid concentration can be accounted for in terms of protonation at the $N_7$ position. The reorientation data for 7AT reveal interactions with adipic acid that have a characteristic persistence time somewhat less than 50 ps. The interactions seen in the 7AI lifetime data are too short-lived to be detected with reorientation measurements. The 7AT amino acid side group interacts with adipic acid in solution more strongly than do the chromophore heterocyclic nitrogens. The choice of the probe molecule for studies involving association with short-lived species can be made with reasonable certainty based on the chemical structures and properties. This work also underscores the importance of probe molecule identity and functionality when examining multicomponent, heterogeneous systems. When this work is viewed in the context of impurity incorporation in crystallizing systems, it is clear that the chemical identity of the impurity is of central importance, consistent with the well-known structural selectivity of the crystallization process. With knowledge of the relationship between chemical structure and role in mediating crystallization, judicious choice of impurity could, in principle, be used to control crystal properties such as habit and growth rate.

2.5

1

2.

3.

4.

5.

6.

7.

8.

9.

10.

11.

12.

13.

## 2.5 Literature Cited


1 Alexander, J.; Ross, B.; Rousslang, K. W.; Brand, L. *Photochem. Photobiol.* **1981**, *20*, 4361.

2. Chen, L. X. Q.; Petrich, J. W.; Fleming, G. R. *Chem. Phys. Lett.* **1987**, *20*, 55.

3. Cockle, S. A.; Szabo, A. G. *Photochem. Photobiol.* **1981**, *34*, 23-27.

4. Petrich, J. W.; Chang, M. C.; McDonald, D. B.; Fleming, G. R. *J. Am. Chem. Soc.* **1983**, *105*, 3824-3832.

5. Szabo, A. G.; Rayner, D. M. *J. Am. Chem. Soc.* **1980**, *102*, 554-563.

6. Robbins, R. J.; Fleming, G. R.; Bedded, G. S.; Robinson, G. W.; Thistlethwaite, P. J.; Woolfe, G. J. *J. Am. Chem. Soc.* **1980**, *102*, 6271-6279.

7. Negrerie, M.; Bellefeuille, S. M.; Whitham, S.; Petrich, J. W.; Thornburg, R. W. *J. Am. Chem. Soc.* **1990**, *112*, 7419-7421.

8. Rich, R. L.; Negrerie, M.; Li, J.; Elliott, S.; Thronburg, R. W.; Petrich, J. W. *Photochem. Photobiol.* **1993**, *58*, 28-30.

9. Rich, R. L.; Smirnov, A. V.; Schwabacher, A. W.; Petrich, J. W. *J. Am. Chem. Soc.* **1995**, *117*, 11850-11853.

10. Rich, R. L.; Chen, Y.; Neven, D.; Negrerie, M.; Gai, F.; Petrich, J. W. *J. Phys. Chem.* **1993**, *97*, 1781-1788.

11. Hogue, C. W.; Szabo, A. G. *Biophys. Chem.* **1993**, *48*, 159-169.

12. Brennan, J. D.; Clark, I. D.; Hogue, C. W. V.; Ito, A. S.; Juliano, L.; Paiva, A. C. M.; Rajendran, B.; Szablo, A. G. *Appl. Spectrosc.* **1995**, *49*, 51-59.

13. Guallar, G.; Batista, V.; Miller, W. *J. Phys. Chem.* **1999**, *110*, 9922.

14. Taylor, C. A.; El-Bayoumi, M. A.; Kasha, M. *Proc. Natl. Acad. Sci. U.S.A.* **1969**, *63*, 253.

15. Fiebig, T.; Chachisvilis, M.; Manger, M.; Zewail, A. H.; Douhal, A.; Garcia-Ochoa, I.; de La Hoz Ayuso, A. *J. Phys. Chem. A* **1999**, *103*, 7419-7431.

16. Tulock, J. J.; Blanchard, G. J. *J. Phys. Chem. B* **1998**, *102*, 7148-7155.

17. DeWitt, L.; Blanchard, G. J.; LeGoff, E.; Benz, M. E.; Liao, J. H.; Kanatzidis, M. G. *J. Am. Chem. Soc.* **1993**, *115*, 12158-12164.

18. Bulska, H.; Grabowska, A.; Pakula, B.; Sepiol, J.; Waluk, J.; Wild, U. P. *J. Lumin.* **1984**, *29*, 65-81.

19. Chen, Y.; Rich, R. L.; Gai, F.; Petrich, J. W. *J. Phys. Chem.* **1993**, *97*, 1770-1780.

20. Chen, Y.; Gai, F.; Petrich, J. W. *J. Phys. Chem.* **1994**, *98*, 2203-2209.

21. Chon, P. T.; Martines, M. L.; Cooper, W. C.; Collins, S. T.; McMorrow, D. P.; Kasha, M. *J. Phys. Chem.* **1992**, *96*, 5203.

22. Day, R. A., Jr.; Underwood, A. L. *Quantitative Analysis*, 6th ed.; Prentice Hall: Englewood Cliffs, NJ, 1991.

23. Petrich, J. W.; Rich, R. L.; English, D. S. *Photochem. Photobiol.* **1998**, *67*, 76.

24. Ingle, J. D.; Crouch, S. R. *Spectrochemical Analysis,* Englewood Cliffs: NJ, 1988.

25. Jiang, Y.; Blanchard, G. J. *J. Phys. Chem.* **1994**, *98*, 9411-9416.

26. Jiang, Y.; Blanchard, G. J. *J. Phys. Chem.* **1995**, *99*, 7904-7912.

27. Gudgin-Templeton, E. F. K.-W., G. A. *J. Phys. Chem.* **1986**, 2896.

28. Kivelson, D.; Spears, K. G. *J. Phys. Chem.* **1985**, *89*, 1999-2001.

29. Blanchard, G. J. *J. of Phys. Chem.* **1989**, *93*, 4315-4319.

30. Blanchard, G. J. *Ana.l. Chem.* **1989**, *61*, 2394-2398.

31. Chuang, T. J.; Eisenthal, K. B. *J. Chem. Phys.* **1972**, *57*, 5094-5097.

32. Debye, P. *Polar Molecules* New York, 1929.

33. Perrin, F. *J. Phys. Radium* **1934**, *4*, 497.

34. Hu, C.-M.; Zwanzig, R. *J. Chem. Phys.* **1974**, *60*, 4354-4357.

35. Edward, J. T. *J. Chem. Ed.* **1970**, *47*, 261.

36. Ilich, P. *J. of Molec. Struc.* **1995**, *354*, 37-47.

37. Pauling, L.; Brockway, L. O. *Proc. Natl. Acad. Sci. U.S.A.* **1934**, *20*, 336.

38. Donckt, E.; Dramaix, J.; Nasielski, J.; Vogels, C. *Trans. Faraday Soc.* **1969**, *65*, 3258.

# Chapter 3

## Dynamics of 7-Azatryptophan Derivatives in Micellar Media. Elucidating the Interactions Between Peptide Oligomers and Micelles

## Summary

We have investigated the motional and population relaxation dynamics of the non-natural amino acid 7-azatryptophan (7AT) in free (zwitterionic) form and bonded to polyvaline oligomers in aqueous micelles. We have studied the oligomers in solutions of anionic, cationic, and neutral surfactants above their critical micelle concentrations. The use of these peptide oligomers enables the study of charge and structure on interactions with aqueous micelles. The 7AT fluorescence population decay and reorientation dynamics were monitored in aqueous and micellar solutions as a function of micellar head group charge and oligopeptide chain length. The lifetime data on 7AT are discussed in terms of its local environment, and the data point to partitioning of probes into micelles mediated by ionic and dispersion interactions with the micelles. The reorientation dynamics are indicative of persistent 7AT-micelle interactions and can be understood in the context of the hindered rotor model.

3.

to

So

nu

wi

int

org

(ph

wo

atta

Our

pep

obt

dep

nan

qua

pro

and

cor

Ex

suc

## 3.1 Introduction

Understanding the dynamics of intermolecular interactions in solution has proven to be a substantial challenge to the chemistry community over the past several decades. Solution phase interactions are important because of their central role in mediating a number of phenomena, ranging from organic synthesis to chemical separations and a wide range of biologically important processes. We are interested in understanding the interactions of selected chromophores with entities that exhibit some level of self-organization in solution. [1-5] Such systems include species undergoing crystallization (phase separation), liquid crystalline materials, and micelles, which are the focus of this work. To interrogate these micelles we have synthesized polyvaline oligomers and have attached the non-natural amino acid 7-azatryptophan (7AT) for use as a chromophore. Our intent is to understand a simplistic mimic of a biomembrane and the interactions a peptide oligomer will have with such a system. We use fluorescence spectroscopy to obtain information on 7AT-tagged peptide oligomers in solution. Fluorescence depolarization gives information on restricted rotational motions that proceed on nanosecond and picosecond time scales in these systems.[6]

Tryptophan is a fluorescent amino acid that possesses a significant fluorescence quantum yield and a strong absorbance near 280 nm.[7,8] Tryptophan is not an ideal optical probe, however. It is characterized by a non-exponential fluorescence population decay and, for many systems, the presence of multiple tryptophan residues can serve to complicate the site-specificity of the information garnered from such experiments. Extrinsic fluorescent probes such as dansyl have been used in the study of proteins but such probes often attach in a non-specific manner and disrupt native structure. Site-

directed mutagenesis can help overcome these limitations by selective removal of tryptophan residues and or replacement by a single fluorescent chromophore whose spectral properties are distinguishable from all other intrinsic species.[9] In recent years, an effort has been made to develop and characterize the non-natural amino acid 7AT for use as a biological probe.[10-13] This chromophore has been used to study protein structure and dynamics[14-16] because its spectral response is shifted relative to that of tryptophan, its $S_1$ population decay is characterized by a single exponential over a wide pH range, and the time constant of the decay is sensitive to the immediate environment of the chromophore.[10,16]

A large amount of research has gone into understanding the structure and dynamics of micelles because these labile structures serve as model systems for biological membranes, as a medium in which chemical reactions and excitation transfer studies can be performed and, due to their ability to solubilize proteins and other organic compounds, micelles have found use in chemical separations. Many investigations of micellar systems utilize the fluorescence of (presumably incorporated) dye molecules to provide information on micellization. We report here on our study of the dynamics of small peptide fragments composed of the fluorescent non-natural amino acid 7AT linked via peptide bond to valine oligomers (Figure 3.1) in aqueous micelles formed by anionic, cationic and neutral surfactants (Figure 3.2). Our experimental data suggest that the polyvaline oligomer interacts significantly with the hydrophobic portion of the micelle, that the 7AT chromophore protrudes from the micellar structure and its motional dynamics are mediated by the identity and charge of the micelle constituent polar head group. We interpret these results in the context of the hindered rotor model.

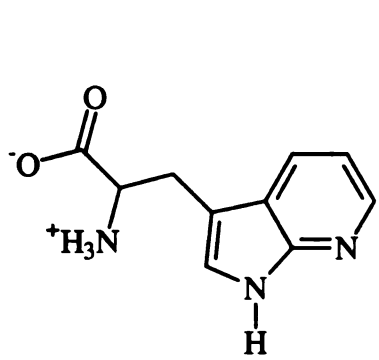

7-azatryptophan (7AT)

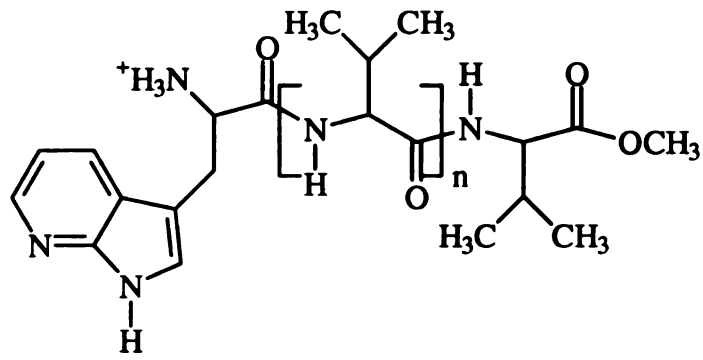

7-azatryptophan-valine methyl ester AT-$(Val)_n$

**Figure 3.1** Structures of 7-azatryptophan (7AT) and 7-azatryptophan-valine methyl ester (7AT-$Val_n$), n = 1-5.

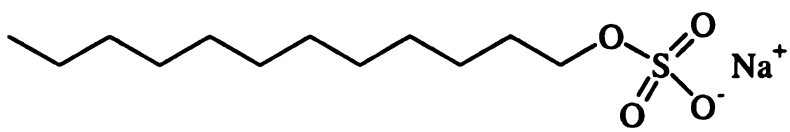

sodium dodecyl sulfate (SDS)

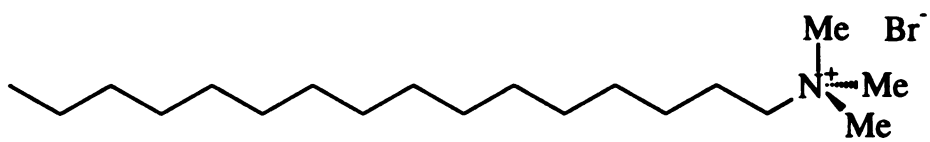

cetyltrimethylammonium bromide (CTAB)

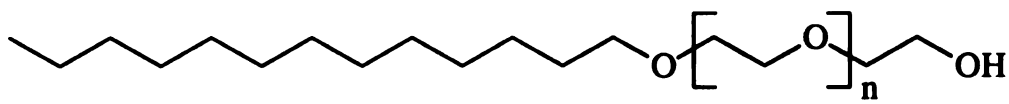

polyethylene glycol 400 dodecyl ether (Thesit)

**Figure 3.2** Structure of surfactants used in this work. Top: anionic SDS; center; cationic CTAB; bottom neutral Thesit®.

## 3.2 Experimental

All reagents were obtained from Sigma-Aldrich, Inc. and used as received. *N-t*-boc-7-azatryptophan was prepared by the procedure described by Petrich[13] using D,L-7-azatryptophan hydrate, BOC-ON [2-(*tert*-butoxycarbonyloxyimino)-2-phenylacetonitrile], and triethylamine in water/dioxane solvent.

*Synthesis of N-7-azatryptophan-(1-5) valine methyl ester peptides (7AT-Val$_1$ - 7AT-Val$_5$).* A series of five peptides containing one 7AT and multiple valine (Val) residues was synthesized. In the final form, these peptides all had a free amine *N*-terminus and a methyl ester *C*-terminus. All amino acid couplings were performed using the water soluble carbodiimide, 1-[3-(Dimethylamino)propyl]-3-ethylcarbodiimide, hydrochloride (EDCI)[17,18] along with the coupling catalyst hydroxybenzotriazole (HOBt). Throughout the peptide couplings *t*-boc α-amino protection/deprotection chemistry was used.[19] Peptides were prepared by sequential condensations of *N-t*-boc-Valine with L-Valine methyl ester, followed by addition of *N-t*-boc-7-azatryptophan to deprotected and isolated valine peptides. A description of the coupling and deprotection procedure is as follows: EDCI (1.92 g, 10 mmol) and triethylamine (TEA) (1.4 mL, 10 mmol) was added to a stirred solution of *N-t*-boc-Valine (2.17 g, 10 mmol) in 20 mL N,N-dimethylformamide (DMF) at 0° C. The solution was stirred for five minutes and HOBt (1.35 g, 10 mmol) was added and stirred for an additional 30 minutes. In a separate flask L-Valine methyl ester hydrochloride (1.67 g, 10 mmol) and TEA (1.4 mL, 8 mmol) was added to 10 mL of DMF and stirred for five minutes, then filtered to remove triethylamine hydrochloride salt. The filtrate was added to the *N-t*-boc-Valine vessel and stirred for 1 hour at 0° C, then at room temperature until completion of the reaction as

determined by thin layer chromatography (TLC). The reaction was acidified with aqueous 5% citric acid and a white precipitate formed. Enough ethyl acetate was added to dissolve and extract the reaction product. The ethyl acetate fraction was washed with citric acid solution, saturated NaCl, saturated $NaHCO_3$, and again with saturated NaCl solutions, then dried over anhydrous $Na_2SO_4$. Solvent was removed under reduced pressure to yield product *N-t*-boc-Valine-Valine methyl ester (3.09 g, 66%).

*Deprotection of t-boc-modified peptides.* 2.5 g *N-t*-boc-valine-valine methyl ester was added to a stirred mixture of 10 mL trifluoroacetic acid (TFA) and 10 mL of dry dichloromethane (DCM). Thioanisole was added as a scavenger when deprotecting peptides containing 7AT to protect the aromatic ring from attack by liberated carbocations. The progress of the reaction was followed by TLC in $CHCl_3$:MeOH (9:1 v/v). DCM was removed *in vacuo* and dry ether added to precipitate the trifluoroacetate salt. The salt was collected by filtration and washed several times with dry ether. The product was dried over $P_2O_5$/KOH.

*Micelle Preparation.* Sodium dodecyl sulfate (SDS), cetyltrimethylammonium bromide (CTAB) (99%+), and Thesit®, (polyethylene glycol 400 dodecyl ether) were obtained from Sigma-Aldrich, Inc., checked for fluorescent impurities, and used as received.

*Methods.* All aqueous solutions were prepared with water from a Milli-Q water filtration system. All solutions used for dynamical measurements were ~5 μM in 7AT. Upon preparation, surfactant solutions were sonicated for five minutes, stored overnight and measured the next day. The sample cuvette was temperature-controlled with a brass block holder maintained at 20.0 ±0.1 °C (Neslab).

To ensure micelle formation, the concentrations of surfactants in this study were several times their critical micelle concentration (CMC). Certain physical parameters and solution properties of the surfactants and micelle solutions must be known for proper interpretation of the data and to ensure that changes in the optical response of the probes are not due to changes in bulk solution properties. The physical parameters of the surfactant solutions used are given in Table 3.1. One of the relevant physical parameters needed for interpretation of the data is the hydrodynamic radius ($r_h$) of the micelles. For ionic surfactants this value is the sum of the micelle core radius, the head group radius, and two layers of water.[20,21] For ionic surfactants this method of determining $r_h$ has been found to match values found from light scattering experiments. The structure of the non-ionic surfactant Thesit® micelle is not as well ordered as CTAB and SDS. The hydrophilic portion of Thesit® is made up of a polyethyleneglycol chain and not a bulky head group. This structural condition produces a hydrated mantle resulting in a less well defined surface aqueous region and $r_h$ is estimated at 35 Å.

**Table 3.1** Solution and physical parameters of micelles used in this work.

| Surfactant[a] | Charge | Viscosity (cP) | pH | Concentration (mM)/number of CMC | $r_h$ (Å) | $\tau_M$ (ns) |
|---|---|---|---|---|---|---|
| CTAB | + | 1.00 ± .01 | 6.2 | 2.5 / 0.92 | 25.7 | 17.6 |
| SDS | - | 1.03 ± .01 | 6.6 | 25.0 / 8.3 | 20.7 | 9.2 |
| Thesit® | neutral | 0.99 ± .01 | 7.1 | 1.0 / 0.1 | 35 | 44.4 |

[a] CTAB = Cetyltrimethylammonium bromide; SDS = sodium dodecyl sulfate; Thesit® = poly(ethylene glycol) 400 dodecyl ether.

The azaindole chromophore is sensitive to solution pH because it can be protonated at the $N_1$ position. This sensitivity is manifested as a significant emission red shift and decreased excited state lifetime below pH ~5.[22] Thus the position of the 7AT emission spectrum and the fluorescence lifetime are both sensitive to local environment. Rotational diffusion time constant(s) are related to "viscosity" according to the Debye-Stokes-Einstein equation and its modifications.[23-25] The viscosities of surfactant solutions were determined by bulk measurements using a viscometer and the pH was determined using a pH meter, with all measurements being controlled at 20°C. The small changes in bulk solution properties associated with the formation of the micelles will not affect the optical response of the chromophores substantially. The viscosity changes associated with the addition of amphiphiles to form micelles are negligible and the pH changes do not occur in a range that affects the protonation of the chromophore or the polyvaline peptides.

*Steady-State Absorption and Emission Spectra.* Absorption spectra were acquired using Cary Model 300 double beam UV-visible absorption spectrometer. Absorption data were collected with 2 nm resolution. Emission spectra were recorded with a Spex Fluorolog 3 spectrometer, with a 5 nm bandpass for excitation and a 2 nm bandpass for emission collection.

*Time-Correlated Single Photon Counting (TCSPC) Spectrometer.* The spectrometer we used for the lifetime and dynamical measurements in this work was described in detail in chapter 2. The light pulses used to excite the sample are produced with a synchronously pumped, cavity-dumped dye laser (Coherent 702-2). The dye laser is excited by the second harmonic of the output of a continuous wave (CW) mode-locked

Nd:YAG laser (Quantronix 416). Samples were excited with 290 nm light (Rhodamine 6G dye, Kodak, KDP Type I SHG). Emission was monitored at the florescence maximum of 7AT in the solution of interest using a 20 nm collection bandpass. Fluorescence was collected at 0°, 54.7°, and 90° with respect to the polarization of the incident pulse. The instrument response function for this system is typically 35 ps FWHM and lifetimes measured range from ~600 ps to ~1.2 ns. We did not need to deconvolute the instrument response function from the experimental data. The shortest reorientation times we measure are on the order of 50 ps, and because we can recover the entire anisotropy decay, some loss of the initial portion does not affect the accuracy of our determinations. Because of the size of the chromophores used (*vide infra*), it is not realistic to expect any anisotropy components with time constants less than ~ 50 ps.

## 3.3 Results and Discussion

The objectives of these experiments are to understand the optical response of a chromophore incorporated into a peptide fragment as a function of chain length and determine how these peptides interact with aqueous micelles. The peptide chromophore senses and reports on changes in its local environment. In this study changes of environment are dictated by intramolecular interactions of 7AT with associated valine residues and by specific interactions of the peptide oligomers with surfactant molecules and micellar structures. The optical response of these probes will be used as a means to detect and understand factors that lead to partitioning and surfactant association of probes in micellar environments. We consider the steady state and time-resolved spectroscopic data separately.

*Steady-State Spectroscopy of 7-azatryptophan and 7AT-$(Val)_{1-5}$ methyl ester.* The absorbance spectrum of 7AT in aqueous solution is centered at 290 nm and the emission maximum is 399 nm in both pure water and in surfactant solutions (Figure 3.3). When 7AT is linked covalently though its carboxyl functionality by formation of a peptide bond with valine, the absorbance spectrum remains unchanged. The emission maxima of the 7AT-$(Val)_{1-5}$ methyl ester series exhibit a small blue shift of 2 – 3 nm in pure water as a function of number of valine residues (Figure 3.4). 7AT is known to be sensitive to its immediate environment which, in this case, is the primary and secondary structure of the peptide to which it is bound. The incorporation of 7AT into peptide fragments is known to cause emission red-shifts; the 7AT emission band is centered at 414 nm in Nac-Pro-7AT-Asn-$NH_2$, [11] 402 nm for Lys-D-7AT-Lys and 399 nm for Lys-L-7AT-Lys[14] in the

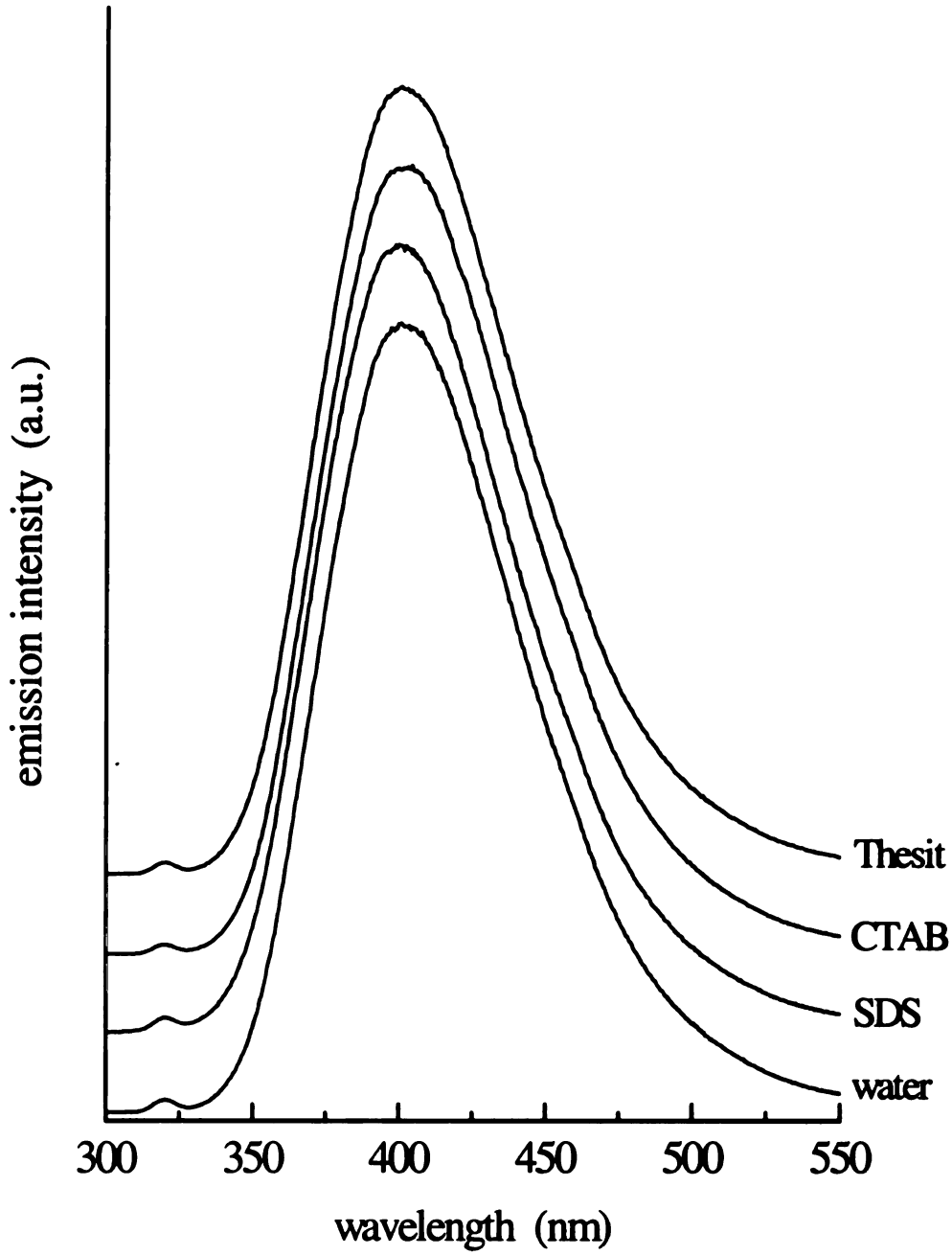


**Figure 3.3** Fluorescence spectra of 7AT in water and surfactant solutions. Spectra have been normalized and are offset for clarity of presentation.

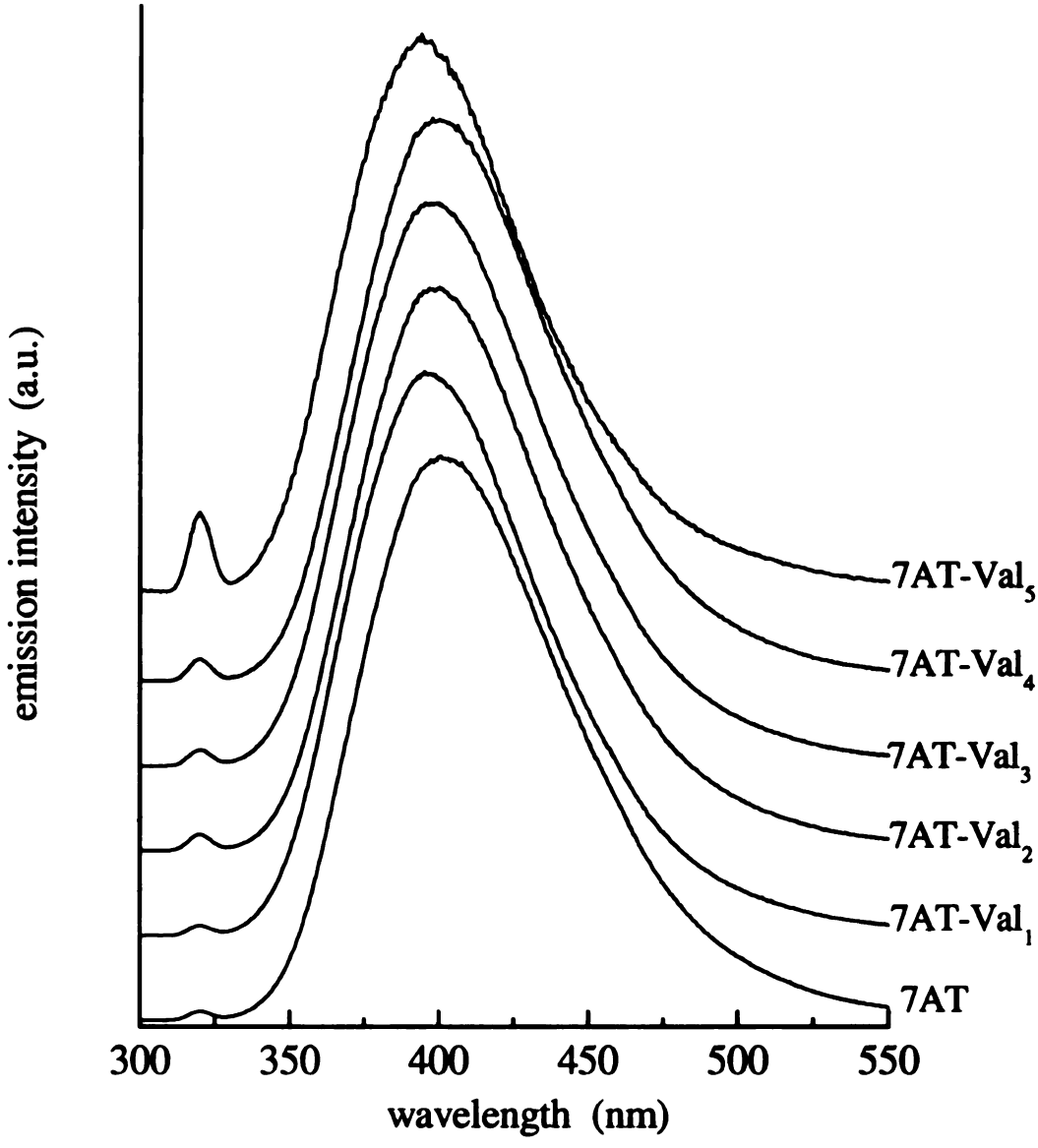


**Figure 3.4** Fluorescence spectra of 7AT and 7AT-$val_n$ oligopeptides in water. Spectra have been normalized and offset for clarity of presentation.

pH range of ~5 – 8, where the azaindole chromophore is not protonated. From these studies and the information we report here, it is clear that the primary structure of a peptide can have a substantial effect on the 7AT emission response and that different enantiomeric forms of a single peptide can cause small shifts in the 7AT emission spectrum. It is not surprising that the 7AT-$(Val)_n$ peptides differing only in the number of valine residues exhibit small spectral shifts despite the fact that the chromophore is adjacent to the same residue in all cases. The emission spectra for the peptide series in the cationic surfactant CTAB solution and the neutral surfactant Thesit® solution are identical to those in water. We see modest spectral shifts for 7AT in (anionic) SDS solution, but in SDS the 7AT-$(Val)_{1\text{-}5}$ oligomers show a larger blue shift of ~13 nm. Emission shifts in organic dye molecules in surfactant solutions are common and are attributed typically to the dye partitioning into micelles. For example, spectral blue shifts of various indoles have been attributed to incorporation into the micellar core of Brij-35 at concentrations far above the CMC. [27] The steady state absorption spectra are thus consistent with our expectations and provide some level of insight into 7AT-micelle interactions.

*Fluorescence Lifetimes of 7-azatryptophan and 7AT-$(Val)_{1\text{-}5}$ methyl ester.* Excited state lifetime measurements can provide information on solution composition and may also contain information on the location of probe relative to the micelle. The fluorescence lifetime of 7AT is sensitive to local environment. 7AT is zwitterionic at pH 7 and its emission decays as a single exponential with a time constant of ~800 ps. As noted above, 7AT has been incorporated into peptide fragments and oligomers and

generally decays as a single exponential in a nominally uniform environment, with the exception of the octapeptide as reported by Petrich. [28]

In pure water and in micellar solutions, the emission intensity decays of 7AT and all of the AT-$Val_n$ oligomers are best fit to single exponentials and these decays time

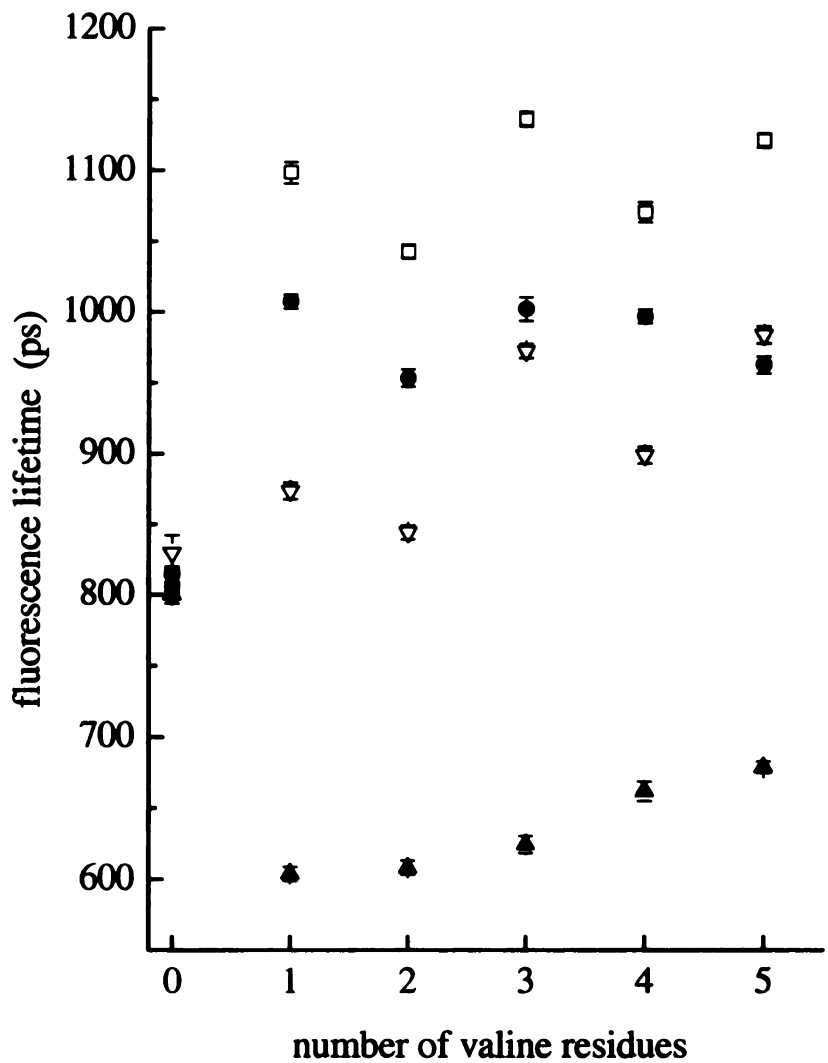


**Figure 3.5** Fluorescence lifetimes of 7AT and 7AT-Valn (n = 1-5) oligomers in water(□), Thesit (•), CTAB (▽), and SDS (▲). For points where error bars are not obvious, the uncertainty lies within the vertical dimension of the symbol.

constants are shown in Figure 3.5. Goodness of fit was determined by $\chi^2$ criterion and visual inspection of residuals of the fit. Single exponential lifetimes indicate that one fluorescent species is present in a single environment. Upon inspection of the lifetime data, it is obvious that the lifetime of zwitterionic 7AT (0 valine residues) depends little on the presence of or proximity to micelles. This finding would seem to indicate that 7AT experiences a similar environment in water and micellar solutions and that it does not interact appreciably with surfactant molecules or micelles. When comparing lifetimes of the peptide oligomers in surfactant solutions to those in water, large changes are evident. The largest differences are noted in solutions of SDS. The 7AT peptide oligomer lifetimes decrease significantly in SDS solution.

To illustrate this sensitivity, lifetimes were measured for 7AT-$Val_1$ in solutions of varying SDS concentration (Figure 3.6). The observed decreases in lifetime with increasing SDS concentration are not the result of simple quenching, nor does the decrease set in only above the CMC. These data show a ~30% decrease in lifetime to ~760 ps at a surfactant concentration of 0.5 mM SDS, followed by a constant lifetime until the CMC is exceeded. Above the CMC, the fluorescence lifetime of 7AT-$Val_1$ decreases again in a stepwise manner to ~600 ps. For other micellar solutions, slight oscillations in observed lifetimes were recovered that are analogous to steady-state shifts in emission.

To better understand the nature of interactions between the probe and micelles, we have investigated the rotational diffusion dynamics of our probes in aqueous solutions of cationic, anionic and neutral micelle-forming surfactants. Rotational diffusion measurements can provide information about intermolecular interactions over the length

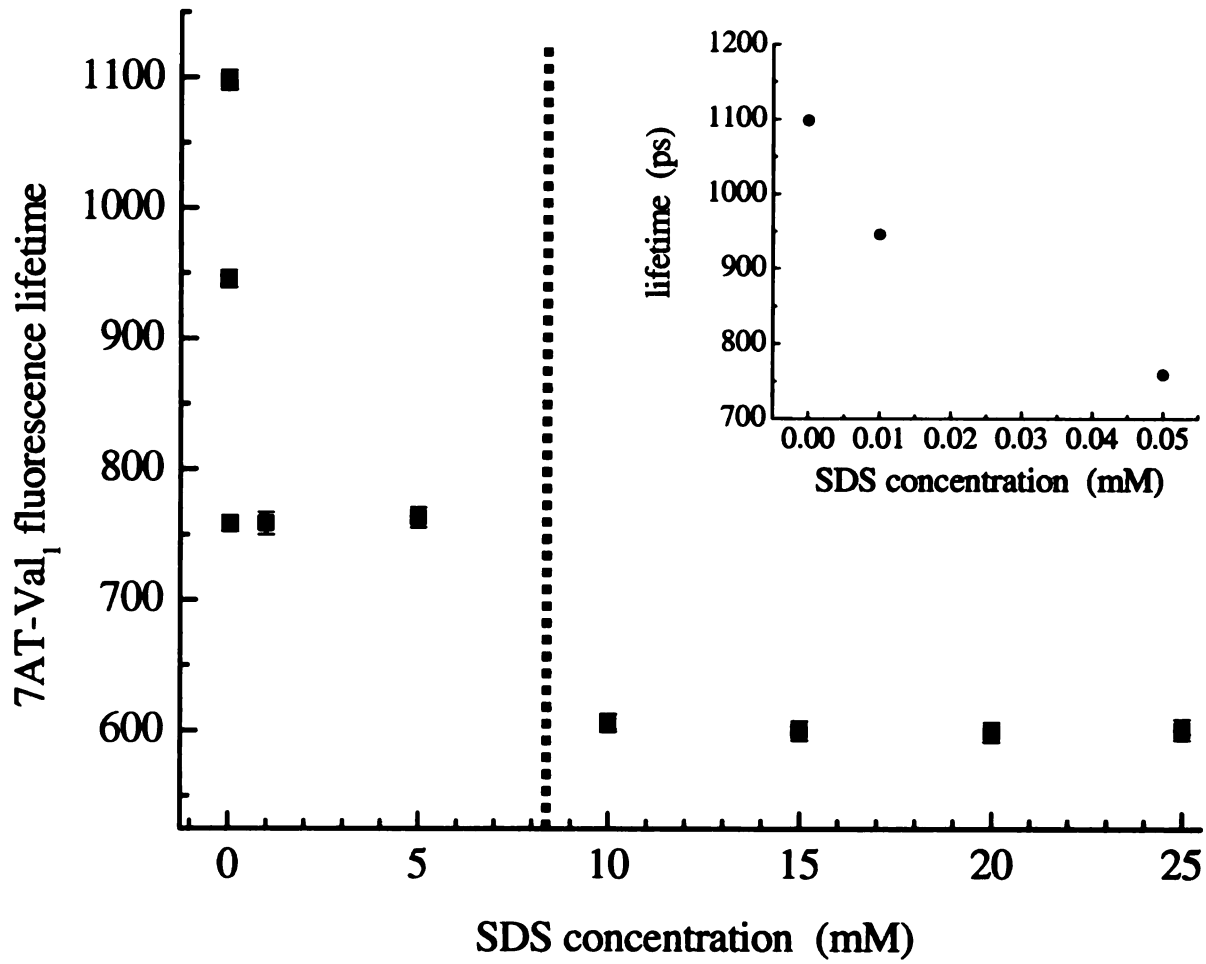


**Figure 3.6.** Dependence of 7AT-$Val_1$ fluorescence lifetime on SDS concentration. The vertical bar indicates the cmc for this system (8.3 mM). Inset: Dependence of lifetime on low SDS concentration (first three points in the figure).

scale of the probe molecule. [29,30] Reorientation data can distinguish in an unambiguous manner whether or not probes are experiencing interactions with micelles. Comparing the dynamical response of 7AT and the peptide oligomers in pure water and surfactant solutions will provide direct information on probe-surfactant association.

There is a large body of literature on the rotational diffusion of organic chromophores in single solvent and binary systems. [30,31] Micellar systems represent a

special subset of binary systems and the issue of reorientation in a micellar environment has been examined before. [32-34] Rotational diffusion has found wide use as a means of probing intermolecular interactions and transient solution-phase organization because the theory is relatively well established and the relevant molecular interactions proceed on a time scale that can be accessed experimentally. The interactions responsible for determining the reorientation dynamics of a chromophore in solution occur rapidly and, over the course of the chromophore's reorientation, many such intermolecular interactions contribute to the overall experimental observation. A common conclusion of these measurements made in binary solutions is that the molecular-scale interactions responsible for the dynamical behavior of the probes are not dictated by the bulk properties of the solvent. For polar systems the relevant intermolecular interactions may include dielectric friction, [35] dipolar interactions, and under certain circumstances, formation of solvent-solute complexes. We consider our data on the reorientation of 7AT-Val oligomers in micellar environments. Our measurements point to the strong interaction between the oligopeptide(s) and the micelles and we interpret our reorientation data in the context of a hindered rotor.

We excite the ensemble of 7AT chromophores in solution with a (vertically) polarized light pulse and monitor the time evolution of emission intensity polarized parallel and perpendicular to the excitation polarization. We combine these data to generate the induced orientational anisotropy function, R(t),

$$R(t) = \frac{I_{\parallel}(t) - I_{\perp}(t)}{I_{\parallel}(t) + 2I_{\perp}(t)} \qquad (3.1)$$

where $I_{\parallel}(t)$ and $I_{\perp}(t)$ are the time-dependent emission intensities. The function R(t) represents the re-randomization of the ensemble of excited molecules and the central

issue in such measurements is the application of models and theories to relate the functionality of the R(t) decay to the immediate environment of the chromophore. In principle, R(t) can contain up to five exponential decays, depending on the angle between the transition moments and the shape of the volume swept out by the rotating chromophore. [36] In homogeneous environments, it is unusual to observe more than two decays and the most common case is a single exponential decay. R(t) decays as a single exponential for 7AT and the 7AT-$Val_{1-5}$ methyl ester peptide series in water. The experimental anisotropy functions for the same chromophore containing peptides in micellar solutions decay with two exponential components,

$$R(t) = R_1(0)\exp\left(-t/\tau_1\right) + R_2(0)\exp\left(-t/\tau_2\right) \tag{3.2}$$

It is significant that we observe different functionalities for the anisotropy decay in neat solvent (water) and in micellar solutions. This finding points to the incorporation of the probe(s) in micellar environments and we thus need to consider two different models to account for our experimental findings.

For the case of reorientation in water, a one component decay is consistent with our earlier findings[22] and we can interpret these data in the context of the modified Debye-Stokes-Einstein (DSE) model.

$$\begin{aligned} \mathrm{R}(t) &= \mathrm{R}(0)\exp(-t/\tau_{OR}) \\ \tau_{OR} &= \frac{\eta V f}{k_B T S} \end{aligned} \tag{3.3}$$

where $\tau_{OR}$ is the reorientation time constant, $\eta$ is the solution bulk viscosity, $V$ is the hydrodynamic volume[37] of the reorienting moiety, $f$ is a friction coefficient to account for the solvent-solute boundary condition and $S$ accounts for the non-spherical shape of the

volume swept out by the reorienting molecule. The experimental data show a linear dependence of the reorientation time on the number of valine residues (Figure 3.7), consistent with incremental increases in the hydrodynamic volume of the reorienting moiety. A linear fit of the reorientation times of the positively charged 7AT-$(Val)_{1-5}$ methyl ester series yields a slope of 32.5 ± 1.2 ps/valine. This result is consistent with the predictions of Eq. 3.3 in the stick limit, where the volume of a valine methyl ester moiety is taken to be 123 $Å^3$ ($S$ = 1), yielding a predicted slope of 30 ps/valine.[37] Although these results follow the DSE model, this is not necessarily an expected result. Proteins are known to display segmental motion caused by fast local reorientation of a fluorescent residue and a longer-time component associated with the motion of the peptide as a whole. [38-40] For the short oligomers we use in this work, segmental motion is not necessarily expected, but it is interesting to note that the data fit well to a single exponential decay.

We now consider the reorientation of the peptide oligomers in micellar solutions. The first issue to address is whether or not the chromophore is incorporating in some fashion into the micelle. We assert that the change in functionality of R(t) upon micelle formation indicates incorporation. In cases where a single exponential anisotropy decay is seen in micellar solution, the location of the chromophore can be open to question. With the assumption that the oligomers incorporate into micelles, there is an issue of how to model the reorientation of these species. The fluorescence depolarization of a probe molecule in a micelle can be described by up to three independent motions. These motions may include movement of the probe in a restricted region within the micelle, translational motion of the probe as it is adsorbed to the surface of the micelle, and

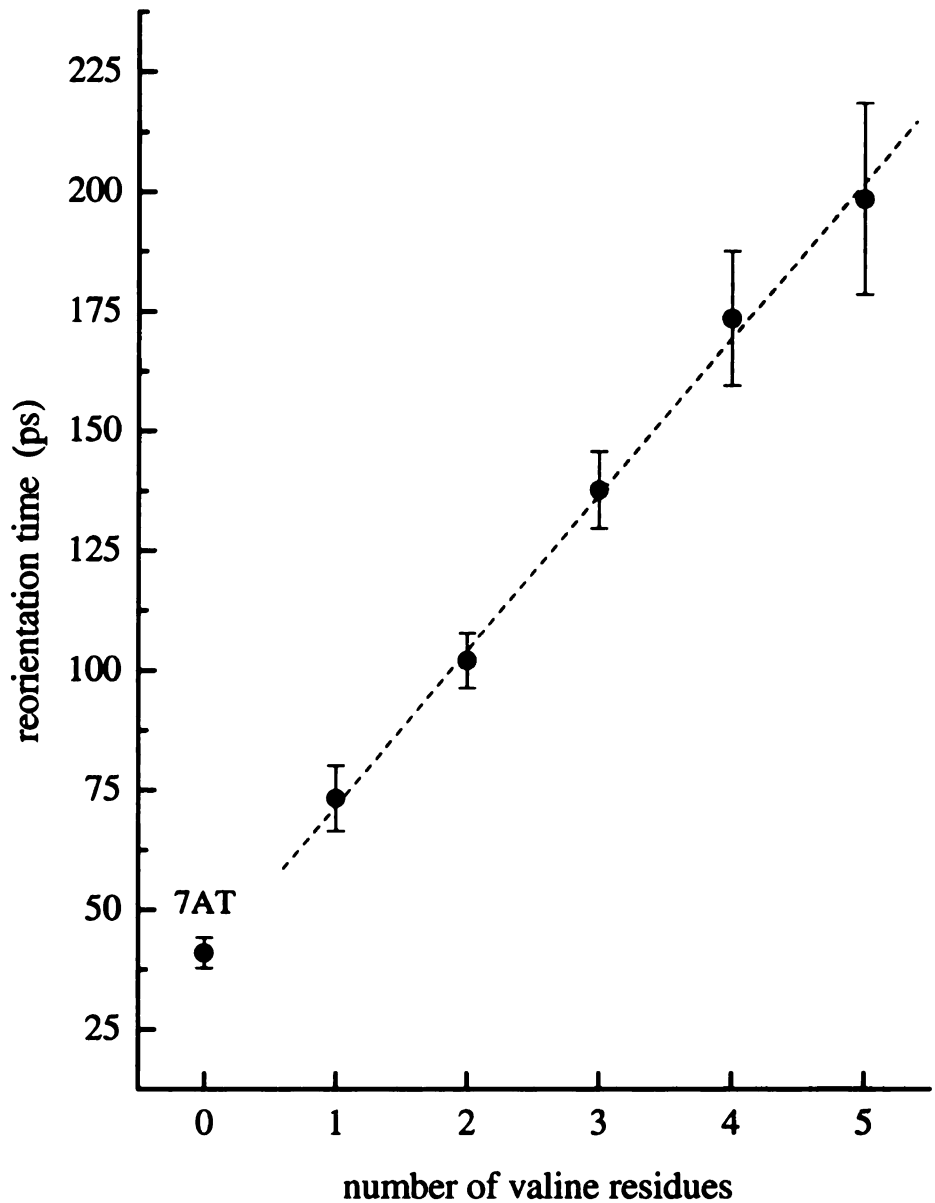


**Figure 3.7** Rotational diffusion time constants of 7AT and 7AT-$Val_n$ as a function of *n* in water at 20° C. The slope of the best-fit line for these data is 32.5 ps/valine unit.

rotation of the micelle as a whole. There are several models that may be applicable to the interpretation of R(t) decays in an environment where rotation of a species is hindered. [41-44] Two models predict R(t) to decay as a single exponential. In one of these models, the chromophore is attached to the micelle as a rigid entity, with the anisotropy

decay time constant representing the motion of the (spherical) micelle as a whole, and we designate this time constant $\tau_M$. The second model that predicts a single exponential decay of R(t) models the chromophore as being located in the core of a micelle and free to rotate within that confined volume. In this model, the anisotropy is expected to decay as a single exponential with a rate constant of $(\tau_M^{-1} + \tau_R^{-1})^{-1}$ where $\tau_R$ is the decay time constant corresponding to chromophore motion in the (homogeneous) core of the micelle. The experimental data suggest that neither of these models are appropriate for the systems we report on here.

There are more complex models that predict anisotropy decays with two or three exponential components, depending on the details of the model. For the case where the chromophore is bound near the surface of the micelle, a biexponential decay is expected, with time constants of $\tau_w$ arising from restricted motion analogous to that of a hindered rotor and $\tau_M$ for overall reorientation of the cone equal to micellar motion. [42] If translational motion of the chromophore about the surface of the micelle is considered, a third decay component, $\tau_d$, is expected. [32] The anisotropy function for this model is shown in Eq. 3.4,

$$R(t) = R(0)[S'^2 + (1 - S'^2)\exp(-t/\tau_w)]\exp(-t(1/\tau_d + 1/\tau_M)) \qquad (3.4)$$

where R(0) is the zero time anisotropy, $S'$ is an order parameter which is a measure of the equilibrium orientational distribution of the chromophore transition moment. It is clear from the above discussion that, depending on the complexity of the model used in the interpretation of the experimental data, there is the potential for over-interpretation. We apply Ockham's razor to our treatment of the data.

The experimental data for reorientation of (zwitterionic) 7AT in anionic SDS micellar solution (25 mM, 3x CMC) shows that R(t) decays to be single exponential to within our ability to resolve. The time constant of $\tau_{OR}$ of 54 ± 5 ps is measurably longer than that of 7AT in water ($\tau_{OR}$ = 41 ± 4 ps) in water, despite the fact that the bulk viscosity of the SDS solution is essentially the same as that of water. This finding suggests that there is indeed some interaction of the 7AT with the micelle, but the nature of the interaction and its persistence time cannot be addressed directly by these data alone. The reorientation dynamics of the 7AT-$(Val)_n$ oligopeptides in SDS are qualitatively different. For all of the (cationic) oligopeptides in SDS, the experimental R(t) function decays with two exponential components (Figure 3.8). The average time constants of the two decays are 73 ps and 491 ps and there is no clear dependence of these time constants on oligomer length. It is tempting to assume that the interactions of the cationic peptides are mediated by ionic interactions with the anionic SDS micelle head groups based on a comparison of these data with that for zwitterionic 7AT. Based on these findings, it is tempting to presume that the two time constants correspond to fast, possibly restricted motion within the micelle and slower global motion of the micelle as a whole. The difficulty with that interpretation, however, is that neither of the time constants correspond to the expected values for these motions. The most glaring mismatch between experimental data and model prediction is for the longer time constant. The overall motion of SDS micelles is predicted by Eq. 3.3 to occur on the several nanosecond timescale. The ~500 ps decay time constant we recover appears to be too fast to account for global micelle motion. The peptides do not display single exponential dynamics or time constants that would be consistent with the probe being

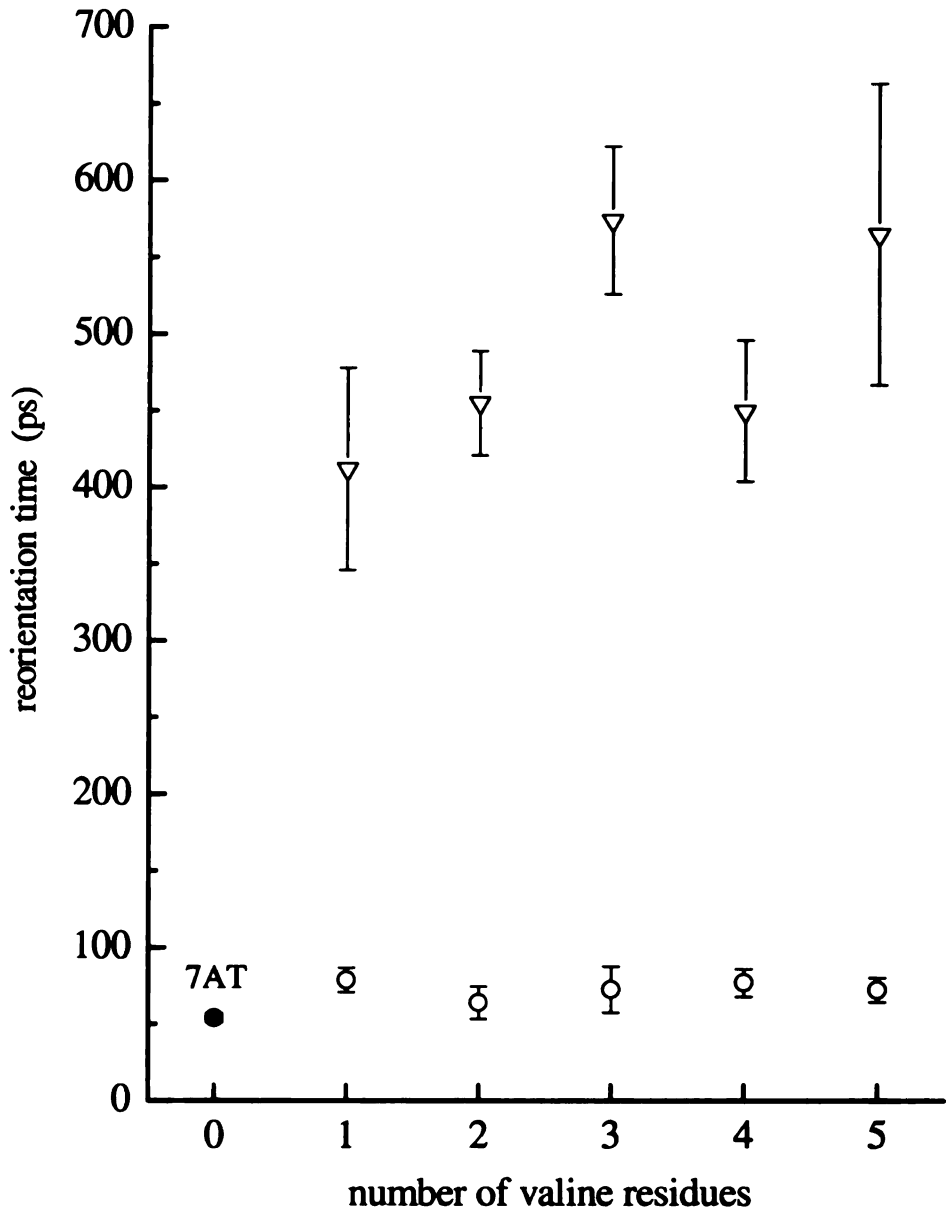


**Figure 3.8** Rotational diffusion time constants of 7AT and 7AT-$Val_n$ in SDS (25 mM, 3 x cmc). The anisotropy functions of the oligomers decay as a two component exponential and 7AT decays as a single exponential.

bound rigidly in the micelle or free to rotate within the core. Double exponential decay dynamics could result if the oligopeptides reside in two distinct environments, partitioned between the micelles and aqueous phase of the solution. If this were the case, the short time components should correspond to the reorientation values in water and the long

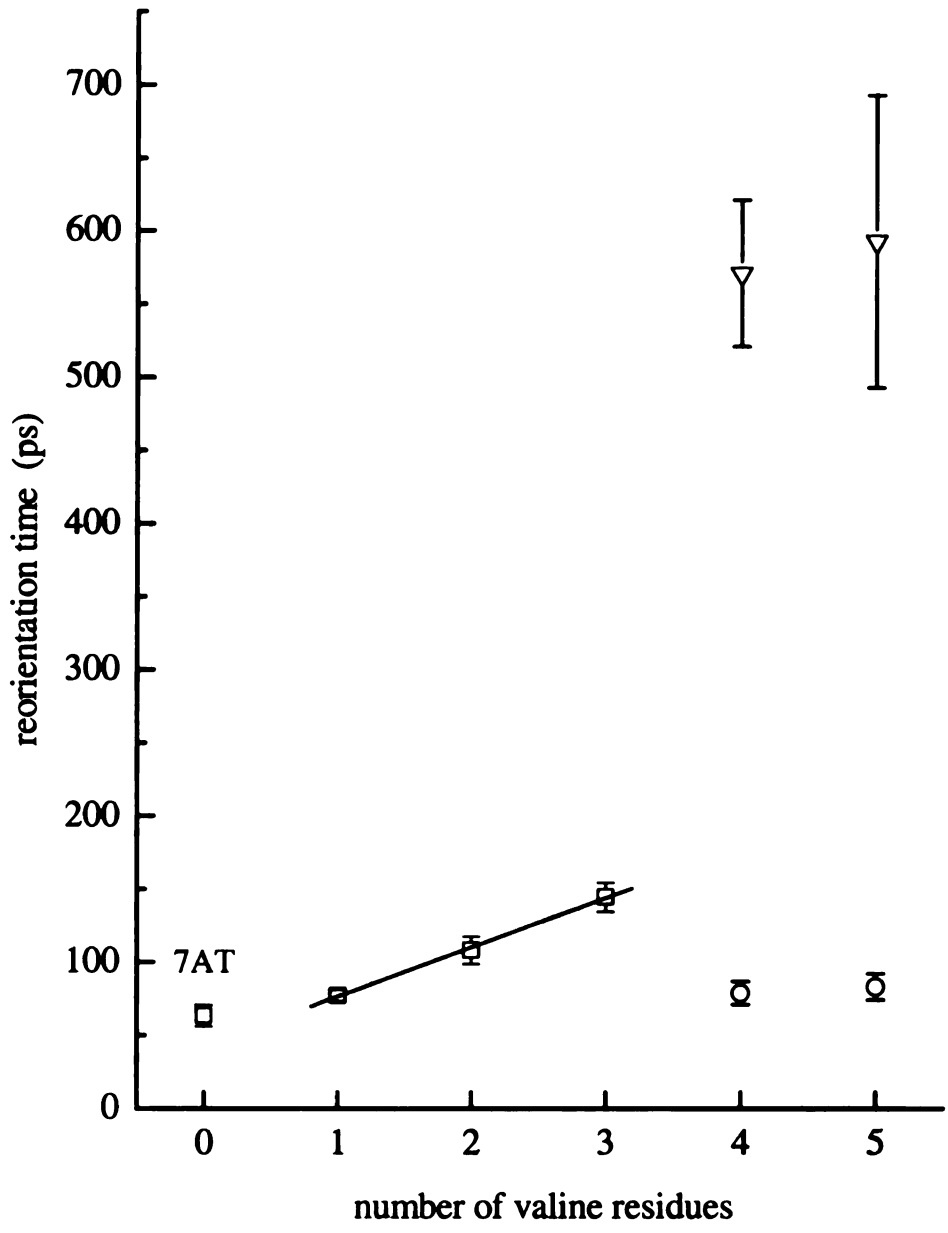


**Figure 3.9** Rotational diffusion time constants of 7AT and 7AT-$Val_n$ in CTAB (2.5 mM, 2.7 x cmc). The anisotropy functions of the oligomers $n$ = 4 and 5 decay as a two component exponential while 7AT and 7AT-$Val_1$ – 7AT-$Val_3$ decay as a single exponential with a slope of 33.6 ps/valine unit.

component should be much longer if it is attached rigidly to or contained within a micelle. The fact that single exponential fluorescence decays are recovered in some cases supports the notion that the probes are located primarily in a single environment. The

anisotropy could yield double exponential dynamics if the probes are intercalated in the micelle but the long component recovered for R(t) is much less than the expected $\tau_M$ for SDS of ~9 ns. [34] The slow time constant is not consistent with the motion of the free oligopeptide either (Fig. 3.7), leaving quasi-translational motion of the chromophore along the outer extent of the micelle as the only physical motion consistent with this time constant. We will return to a discussion of this point after considering the reorientation dynamics of the oligopeptides in cationic and neutral micelles.

The reorientation dynamics of the 7AT-Valine methyl ester series in (cationic) CTAB surfactant solution (1.0mM, 10x CMC) are shown in Figure 3.9. The most striking feature contained in these data is the change in reorientation dynamics with increasing oligopeptide length. We observe that the functionality of R(t) is a single exponential decay in 7AT-$Val_1$ – 7AT-$Val_3$ and R(t) decays as a double exponential for 7AT-$Val_4$ and 7AT-$Val_5$. This behavior is qualitatively different than the dynamics seen in SDS, where all oligopeptides produced double exponential anisotropy decays. For the oligopeptides 7AT-$Val_1$ – 7AT-$Val_3$, the slope of the volume-dependence for reorientation is 33.6 ± 1.6 ps/valine residue, the same to within the experimental uncertainty as that recovered from the reorientation dynamics for the 7AT-$Val_1$ – 7AT-$Val_5$ oligomers in water. In addition, the reorientation time constants for 7AT-$Val_1$ – 7AT-$Val_3$ peptides in CTAB match those measured in water. These data indicate that the 7AT-$Val_1$ – 7AT-$Val_3$ peptides do not associate with CTAB micelles to a significant extent; they are essentially free in solution. The longer peptides 7AT-$Val_4$ and 7AT-$Val_5$ exhibit a two component anisotropy decay CTAB micellar solution, with the average time constants for the two components being 76 ps and 533 ps. It is important to note

that the two components are characterized by the same time constants for both 7AT-$Val_4$ and 7AT-$Val_5$.

It is clear that there is a substantial interaction between the longer oligopeptides and the CTAB micelles and the dynamics recovered suggest that the interaction is quite similar to that seen for these probes in SDS micelles. We attribute this peptide length-dependent behavior to the balance between electrostatic and van der Waals interactions in these systems. The cationic oligopeptides will experience ionic (electrostatic) repulsion by the CTAB cationic head groups and the strength of this interaction is such that it requires the van der Waals interactions between four or more valine residues and the micelle lipophilic region to overcome electrostatic repulsion. While it is not possible to quantitate the strength of this interaction, we can speculate that the van der Waals interactions will be similar in magnitude to those seen in alkanethiol monolayers on gold, where the interchain interaction energy is taken to be ~ 300 cal/mol-$CH_2$. Clearly, the valine structure is more complicated and the nature of the micellar structure is more fluxional than that of SAMs. For the valine units, there are two CH groups and two $CH_3$ groups per monomer. If we assume the interaction strength to be the same for these groups, on average, as for $CH_2$ groups, then four valine residues would produce a strength of interaction roughly equivalent to a $C_{16}$ aliphatic chain, or ~ 4.8 kcal/mol. The corresponding disorder-to-order transition in alkanethiols occurs between 9 and 10 carbons, or 2.7 – 3 kcal/mol, but these systems are capable of a much greater degree of organization than valine oligomers in micelles. This crude calculation suggests, however, that the electrostatic repulsion term for CTAB – 7AT-$Val_n$ interactions is on the order of a few kcal/mol at most.

For the neutral surfactant Thesit®, the valine oligomer length dependence of the reorientation dynamics is presented in Figure 3.10. Not surprisingly, these data present a case that appears to be intermediate between the anionic SDS and cationic CTAB micelle systems. These data show a change in reorientation behavior from single to double exponential anisotropy decays for the oligomers, with the onset of a two-component decay beginning at 7AT-$Val_2$. For Thesit®, the dipeptide 7AT-$Val_1$ displays a single exponential anisotropy decay with a time constant the same as that measured in water. By analogy to the data for CTAB, the absence of electrostatic contributions to Thesit® interactions with the probes reduces the barrier to valine-micelle interactions. Because of the different structures of CTAB and Thesit®, the strength of valine-micelle interactions will clearly not be the same for the two systems. For the longer oligopeptides, where a two-component anisotropy decay is seen, the time constants are independent of peptide length and the slow time constant is slightly smaller than the corresponding data for CTAB and SDS micelles.

We assert that the systems that exhibit two-component anisotropy decays with decay time constants in the ~75 ps and ~500 – 600 ps time windows can be explained using a single formalism. The fundamental physics responsible for the data we observe is essentially the same for all of the micellar systems, with differences in the details being associated with the specific identities of the micellar constituents. We summarize our findings as follows: (1) 7AT exhibits only small changes in $\tau_{OR}$ for each surfactant solution compared to its behavior water, indicating that the probe molecule itself does not associate with micelles to a significant extent. This finding is consistent with the lifetime data. (2) Peptides either interact strongly with micelles and manifest a two-component

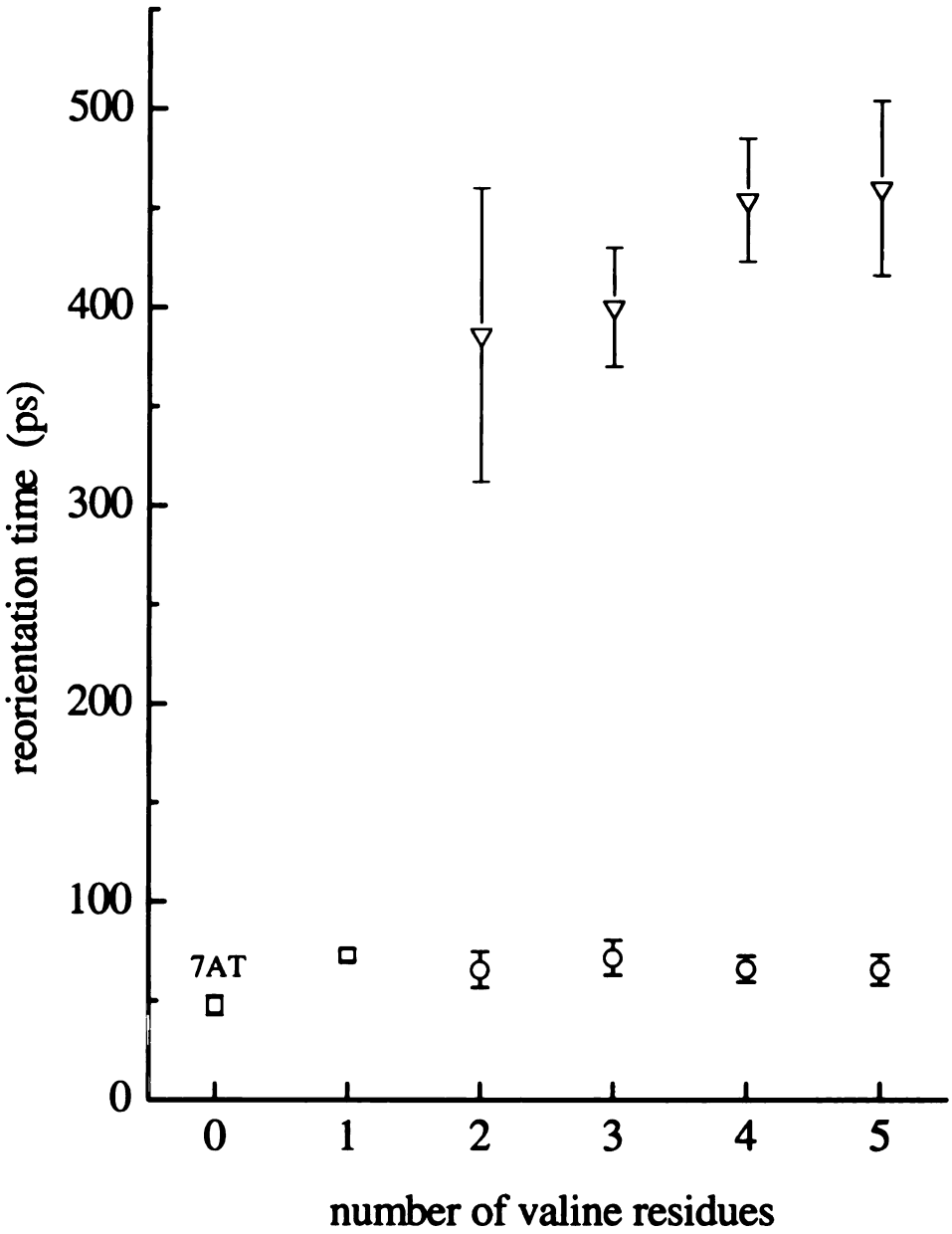


**Figure 3.10** Rotational diffusion time constants of 7AT and 7AT-$Val_n$ in Thesit® (1.0 mM, 10 x cmc). The anisotropy functions of the oligomers $n$ = 2-5 decay as a two component exponential while 7AT and 7AT-$Val_1$ decays as a single exponential.

anisotropy decay, or they do not interact with the micelles to a measurable extent. (3) For systems manifesting a two component decay, the decay time constants are independent of oligopeptide length in a given micellar system and similar for all three micelles studied

here. For this reason, we use the average of fitted decay time constants for a given micelle in the modeling we discuss below.

*Wobbling-in-a-cone with translational diffusion and micelle rotation.* As discussed above, the expected reorientation time constant for a micelle is several nanoseconds and we do not observe any such long time anisotropy decay in our data. The possible reasons for this absence are either that we are not sensitive to such a long-time component, which is not the case, or that the persistence time of the micelle-oligopeptide association is substantially shorter than the reorientation time of the micelle. This explanation is consistent with relatively weak interactions between the probe and micelle, in keeping with our estimate of the interaction energies of several kcal/mol for these systems. We consider that the interaction between the oligopeptide and the micelle structure is characterized by interactions between the lipophilic portion of the micelle and the valine peptide tails, and that the 7AT head group is in closest proximity to the micelle head groups, where it is characterized by some freedom to translate or move about on the surface of the micelle. The translational diffusion of a chromophore on a spherical surface will manifest itself as a reorientation of emission dipoles. Eq. 3.4 describes the general case of the anisotropy decay for three independent motions and we apply the appropriate simplifications to bring this model into consistency with the experimental data,

$$1/\tau_d = 1/\tau_{slow} - 1/\tau_M \tag{3.5}$$

$$1/\tau_w = 1/\tau_{fast} - 1/\tau_d - 1/\tau_M = 1/\tau_{fast} - 1/\tau_{slow} \tag{3.6}$$

We determine values for $\tau_M$ from the DSE equation at 20 °C or we assume it to be infinitely long, but in either case we are insensitive to this quantity experimentally. The

translational diffusion coefficient may be related to $\tau_d$ using the value for $r_h$ (Table 3.1) the radius of the surface of the micelle over which the probe diffuses by Eq. 3.7. [34]

$$D_t = r_h^2 / 6\tau_d \tag{3.7}$$

This diffusion constant is related to the slower of the two motions we sense. The wobbling-in-a-cone model[42,44] is characterized by a molecule constrained within a cone of semi-angle $\theta_0$ with the motion of the molecule in the confined environment being described by a wobbling diffusion coefficient ($D_w$). We can extract the value of $D_w$ from the experimental data using the quantities $\tau_w$ and $S'$,

$$\begin{aligned} D_w = &\{\tau_w (1 - S'^2)\}^{-1}[-\cos^2\theta_0(1+\cos\theta_0)^2\{\ln[(1+\cos\theta_0)/2] \\ &+(1-\cos\theta_0)/2\}\{2(1-\cos\theta_0)\}^{-1} + (1-\cos\theta_0) \\ &\times(6+8\cos\theta_0 - \cos^2\theta_0 - 12\cos^3\theta_0 - 7\cos^4\theta_0)/24] \end{aligned} \tag{3.8}$$

In this model, the quantity $\theta_0$ is related to the order parameter through Eq. 3.9.

$$S' = 0.5\cos\theta_0(1+\cos\theta_0) \tag{3.9}$$

The values for $S'$, $\tau_{slow}$ and $\tau_{fast}$ were extracted from the experimental data using Eq. 3.4 and from this information, the quantities $\theta_0$, $D_w$, and $D_t$ were calculated for each surfactant system (Table 3.2). The values $D_w$ for all the peptides in water are given for comparison in Table 3.3. In water, $D_w$ is calculated using $D_w = (6\tau_{OR})^{-1}$ based on the assumption that in water the order parameter is zero and the equilibrium orientational distribution is random because the probe rotates freely.

The values of the order parameter, $S'$, vary from 0.50-0.73 for reorientation of the 7AT-$Val_n$ oligopeptides in the micelles. The order parameter is a measure of the time-averaged orientational distribution of the peptides and can take on values from zero for a fully random orientational distribution, to one for completely ordered systems. The

**Table 3.2** Values of quantities extracted from the "Wobbling-in-a-Cone" model.

| Surfactant | $S'$ | $\theta^0$ (degrees)[a] | $D$w x 109 ($s^{-1}$) | $D$t x 10-9 ($m^2/s$) |
|---|---|---|---|---|
| SDS | 0.73 | 36 ± 3 | 1.2 | 0.86 |
| CTAB | 0.58 | 46 ± 2 | 1.7 | 0.91 |
| Thesit® | 0.50 | 52 ± 2 | 2.3 | 1.1 |

[a]$\theta_0$ calculated according to Eq. 9. $\theta_0 = \cos^{-1}\left(0.5\left(\sqrt{1+8S'}-1\right)\right)$. Uncertainty in the determination of S' is taken to be ± 5%.

values recovered for the order parameter indicate that the peptide oligomers do indeed have a preferential orientation with the micelle surface. In SDS ($\theta_0$ = 36°) they are considerably more confined than in CTAB ($\theta_0$ = 46°) and Thesit® ($\theta_0$ = 50°). In SDS there is clear evidence for order, but the proximity of the cone angle observed in Thesit® to the magic angle suggests substantial disorder.

The diffusion coefficients for the peptides in water decrease with peptide size, according to the increase in correlation times, (Table 3.3), and this is an expected result. The recovered parameter $D_w$ for the 7AT-$Val_n$ oligomers demonstrates that the 7AT chromophore is free to reorient about its tethering bond to the valine chain. The wobbling diffusion constant, $D_w$, reveals substantial confinement of the 7AT chromophore in micellar environments. The value of $D_w$ in micelles is two to three times slower than that for 7AT in bulk water. It is important to keep in mind that the free volume accessible to the 7AT chromophore in the micelle is substantially less than that of 7AT in water. We calculate from the cone angles $\theta_0$ that the volume accessible to the

**Table 3.3** Experimental diffusion constants for oligopeptides in water.

| | $D_W$ x $10^9$ ($s^{-1}$) |
|---|---|
| 7AT | 4.1 |
| 7AT-$Val_1$ | 2.3 |
| 7AT-$Val_2$ | 1.6 |
| 7AT-$Val_3$ | 1.2 |
| 7AT-$Val_4$ | 0.96 |
| 7AT-$Val_5$ | 0.83 |

7AT chromophore in SDS is 7% of a full sphere, for CTAB, 9% and for Thesit® 9.4%. When the $D_w$ data are corrected for accessible volume, we recover an effective viscosity of 47 cP for the SDS micelle, 26 cP for the CTAB micelle and 18 cP for the Thesit® micelle. While these viscosities may seem high, they are not substantially different than that of bulk 1-dodecanol or ethylene glycol (~20 cP). In the glycols, hydrogen bonding is thought to dominate the viscous flow properties while in the *n*-alcohols, van der Waals interactions are thought to be responsible.

It is also useful to consider the magnitude of $D_t$. The oligopeptides exhibit moderately fast translational diffusion on the surface of the micelles. The self-diffusion of the ionic surfactants in this study has been investigated previously and are reported to be on the order of (0.2-1.5) x $10^{-10}$ $m^2$ $s^{-1}$. [45,46] The translational diffusion constants we recover for the oligopeptides used in this study are ~ $10^{-9}$ $m^2$ $s^{-1}$, a factor of ~10 faster than surfactant self-diffusion. This is not necessarily a surprising result because of the inability of the oligopeptides to incorporate into the micellar structure with the same efficiency as a constituent surfactant molecule. The largest translational diffusion

constant we measure is for the neutral Thesit® micelles. We note that Thesit® is the least ordered micelle used in this study and the intrinsic disorder of the micelle may be related to efficient translational diffusion. The loosely organized hydrophilic ethylene glycol chains create the surface and outer layer of Thesit® micelles.

## 3.4 Conclusions

We have studied the steady-state and time-resolved optical response of 7AT and 7AT-$Val_n$ peptide oligomers in water and aqueous micelle solutions. The charge and chain length of the peptides dictate interactions with micelles. The reorientation dynamics of the peptides were consistent with the model of wobbling-in-cone dynamics with translational diffusion of the dye along the surface of the micelle with rotation of the micelle as a whole. Our experimental data reveal a balance between electrostatic or ionic interactions and van der Waals interactions for polyvaline oligopeptides and selected micellar structures. For the case of anionic micelle headgroups and cationic oligopeptides, we see the strongest interactions because ionic and van der Waals forces are both attractive. For the cationic micelle CTAB, we observe the balance between ionic and van der Waals interactions because of the opposing nature of these forces. This balance allows us to estimate the strength of ionic interactions between the probe and the micelle to be on the order of several kcal/mol. Using a neutral surfactant Thesit® provides an intermediate case, as expected. Our experimental reorientation data indicate transient interactions between the micelle and the probe oligopeptides, with limited structural freedom for the probe molecules in the apparently viscous micellar environment.

## 3.5 Literature Cited


1. Tulock, J. J.; Blanchard, G. J. *J. Phys. Chem. A* **2000**, *104*, 8340-8345.
2. Rasimas, J. P.; Blanchard, G. J. *J. Phys. Chem.* **1995**, *99*, 11333-11338.
3. Rasimas, J. P.; Berglund, K. A.; Blanchard, G. J. *J. Phys. Chem.* **1996**, *100*, 17034-17040.
4. Rasimas, J. P.; Berglund, K. A.; Blanchard, G. J. *J. Phys. Chem.* **1996**, *100*, 7220-7229.
5. Tulock, J. J.; Blanchard, G. J. *J. of Phys. Chem. B* **1998**, *102*, 7148-7155.
6. Lakowicz, J. R. *Principles of Fluorescence Spectroscopy*, Second Edition ed.; Plenum Publishers: New York, 1999.
7. Cockle, S. A.; Szabo, A. G. *Photochem. Photobiol.* **1981**, *34*, 23-27.
8. Ross, J. B.; Rousslang, K. W.; Brand, L. *Biochemistry* **1981**, *20*, 4361-4369.
9. Steward, L. E.; Collins, C. S.; Gilmore, M. A.; Carlson, J. E.; Ross, J. B. A.; Chamberlin, A. R. *J. Am. Chem. Soc.* **1997**, *119*, 6-11.
10. Negrerie, M.; Bellefeuille, S. M.; Whitham, S.; Petrich, J. W.; Thornburg, R. W. *J. Am. Chem. Soc.* **1990**, *112*, 7419-7421.
11. Rich, R. L.; Negrerie, M.; Li, J.; Elliott, S.; Thronburg, R. W.; Petrich, J. W. *Photochem. Photobiol.* **1993**, *58*, 28-30.
12. Rich, R. L.; Chen, Y.; Neven, D.; Negrerie, M.; Gai, F.; Petrich, J. W. *J. Phys. Chem.* **1993**, *97*, 1781-1788.
13. Rich, R. L.; Smirnov, A. V.; Schwabacher, A. W.; Petrich, J. W. *J. Am. Chem. Soc.* **1995**, *117*, 11850-11853.

14. Brennan, J. D.; Clark, I. D.; Hogue, C. W. V.; Ito, A. S.; Juliano, L.; Paiva, A. C. M.; Rajendran, B.; Szabo, A. G. *Appl. Spectrosc.* **1995**, *49*, 51-59.

15. Broos, J.; Ter Veld, F.; Robillard, G. T. *Biochem.* **1999**, *38*, 9798-9803.

16. Hogue, C. W.; Szabo, A. G. *Biophys. Chem.* **1993**, *48*, 159-169.

17. Sheehan, J. C.; Cruickshank, P. A.; Boshart, G. L. *J. Org. Chem.* **1961**, *26*, 2525.

18. Nozaki, S. *Chem. Lett.*, **1997**; *1*, 1-2.

19. Kocienski, P. J. *Protecting Groups*; Thieme: New York, 1994.

20. Robson, R. J.; Dennis, E. A. *J. Phys. Chem.* **1977**, *81*, 1075.

21. Tanford, C. *J. Phys. Chem.* **1972**, *76*, 3020.

22. Kelepouris, L.; Blanchard, G. J. *J. Phys. Chem. A* **2000**, *104*, 7261-7267.

23. Hu, C.-M.; Zwanzig, R. *J. Chem. Phys.* **1974**, *60*, 4354-4357.

24. Debye, P. *Polar Molecules*; New York, 1929.

25. Perrin, F. *J. Phys. Radium* **1934**, *4*, 497.

26. Dewitt, L.; Blanchard, G. J.; Legoff, E.; Benz, M. E.; Liao, J. H.; Kanatzidis, M. G. *J. Am. Chem. Soc.* **1993**, *115*, 12158-12164.

27. Ashby, K. D.; Das, K.; Petrich, J. W. *Anal. Chem.* **1997**, *69*, 1925-1930.

28. English, D. S.; Rich, R. L.; Petrich, J. W. *Photochem. Photobiol.* **1998**, *67*, 76-83.

29. Jiang, Y.; Blanchard, G. J. *J. Phys. Chem.* **1994**, *98*, 9411-9416.

30. Jiang, Y.; Blanchard, G. J. *J. Phys. Chem.* **1995**, *99*, 7904-7912.

31. Gudgin-Templeton, E. F.; Kenny-Wallace, G. A. *J. Phys. Chem.* **1986**, *90*, 2896.

32. Chou, S. H.; Wirth, M. J. *J. Phys. Chem.* **1989**, *93*, 7694-7698.

33. Quitevis, E. L.; Marcus, A. H.; Fayer, M. D. *J. Phys. Chem.*, **1993**; *97*; 5762-5769.

34. Maiti, N. C.; Krishna, M. M. G.; Britto, P. J.; Periasamy, N. *J. Phys. Chem. B* **1997**, *101*, 11051-11060.

35. Kivelson, D.; Spears, K. G. *J. Phys. Chem.* **1985**, *89*, 1999-2001.

36. Chuang, T. J.; Eisenthal, K. B. *J. Chem. Phys.* **1972**, *57*, 5094-5097.

37. Edward, J. T. *J. Chem. Ed.* **1970**, *47*, 261.

38. Hanson, D. C.; Yguerabide, J.; Schumaker, V. N. *Biochem.*, **1981**; *20*; 6842-52.

39. Kroes, S. J.; Canters, G. W.; Gilardi, G.; van Hoek, A.; Visser, A. J. *Biophys J.*, **1998**; *75*; 2441-2450.

40. Lakshmikanth, G. S.; Krishnamoorthy, G. *Biophys. J.*, **1999**; *77*; 1100-1106.

41. Lakowicz, J. R.; Cherek, H.; Maliwal, B. P.; Gratton, E. *Biochem.* **1985**, *24*, 376.

42. Lipari, G.; Szabo, A. *Biophys. J.* **1980**, *30*, 489-506.

43. Szabo, A. *J. of Chem. Phys.* **1984**, *81*, 150.

44. Kinosita, K., Jr.; Kawato, S.; Ikegami, A. *Biophys. J.* **1977**, *20*, 289-305.

45. Ahlnas, T.; Soderman, O.; Hjelm, C.; Lindman, B. *J. Phys. Chem.* **1983**, *87*, 822.

46. Nery, H.; Soderman, O.; Canet, D.; Walderhaug, H.; Lindman, B. *J. Phys. Chem.* **1986**, *90*, 5802.

# Chapter 4

## Dynamics of 7-Azatryptophan and Tryptophan Derivatives in Micellar Media. The Role of Ionic Charge and Substituent Structure

## Summary

We have investigated the motional and population relaxation dynamics of several derivatives of 7-azatryptophan (7AT) and tryptophan (TRP), and N-acetyl-tryptophanamide (NATA) in anionic, cationic, and neutral surfactant solutions above the surfactant critical micelle concentrations. The specific derivatives of 7AT and TRP used, and NATA were chosen to elucidate the roles of chromophore charge and side group structure in mediating interactions with micelles. Fluorescence lifetime data are sensitive to local environment, revealing significant differences in the ability of different chromophores to interact with the micelles. Reorientation dynamics of these chromophores indicate persistent probe-micelle interactions that are determined by a balance between ionic charge(s) and dispersion interactions.

## 4.1 Introduction

The dynamics of peptides and proteins in solution is of fundamental importance to many essential biological processes and fluorescence spectroscopy has proven to be a versatile tool for examining such phenomena. The characteristic time scale of fluorescence population decays is matched well to the speed of many important dynamical phenomena in protein and peptide systems.[1] One of the key issues in the study of biological systems is the choice of a fluorescent probe that will not itself serve to perturb the structure of the molecular system under investigation. Tryptophan (TRP) is a widely used chromophore for investigations of peptide and protein behavior because it is one of a limited number of fluorescent amino acids; tyrosine and phenylalanine have been studied less extensively owing to their lower absorbance cross sections, fluorescence quantum yields and absorption and emission band positions. The indole chromophore present in tryptophan is sensitive to its local environment, and is characterized by an emission maximum between 308 nm and 355 nm, depending on its immediate environment.

While TRP is found naturally in many biologically active peptides and proteins, it is not an ideal probe because its fluorescence population decay is non-exponential, and this anomalous behavior is thought to arise from efficient charge transfer behavior between multiple stable conformations of the indole chromophore to the side chain. [2] Within the framework of this interpretation, the lifetime of the chromophore is conformation-dependent, making the interpretation of fluorescence lifetime data difficult. In addition, the presence of multiple tryptophan residues in a protein can preclude the extraction of site-specific information from TRP probes.

In recent years, several non-natural amino acids have been investigated as alternatives to TRP as biological probes, including 7-azatryptophan (7AT). [3-6] The spectral response of 7AT is red-shifted relative to that of TRP, allowing its use in the study of protein structure and dynamics. [7-9] 7AT is characterized by a single exponential population decay of its $S_1$ state over a wide pH range, and the time constant of the decay is sensitive to the immediate environment of the chromophore. [6,9] The single exponential population relaxation dynamics of 7AT is an expected result for organic chromophores and its behavior stands in contrast to that of the structurally similar TRP. This difference in relaxation dynamics has been attributed to a relatively low barrier to the formation of a charge transfer excited-state in 7AT. [10]

We use steady-state and time-resolved fluorescence spectroscopy to obtain information on molecules containing the 7-azaindole and indole chromophores in micellar solutions. We are interested determining the effects of chromophore and micelle head group charge, and probe molecule structure on their interactions. We use three substituted forms of each chromophore in this comparative study (Figure 4.1). At neutral pH, they are the zwitterionic amino acids 7-azatryptophan (7AT) and tryptophan (TRP), anionic species formed by the addition of a *tert*-butoxy group at the N-terminus of each amino acid, named boc-7AT and boc-TRP, and cationic species produced though a peptide bond with dodecylamine at the C-terminus of the amino acid residues, designated DD-7AT and DD-TRP. The latter chromophores possess an aliphatic moiety that will allow significant dispersion interactions with micelles. Tryptophan octyl ester has attracted considerable interest as a suitable model for TRP in the case of membrane proteins, [11-15] and the fluorophores DD-7AT and DD-TRP may also serve this purpose.

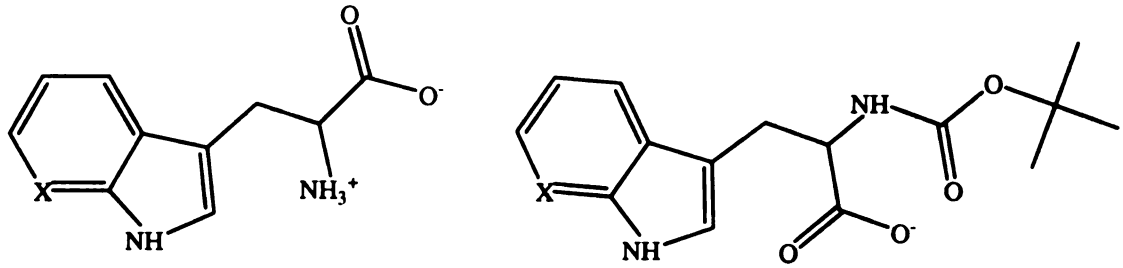

7AT, TRP



Boc-AT, Boc-TRP

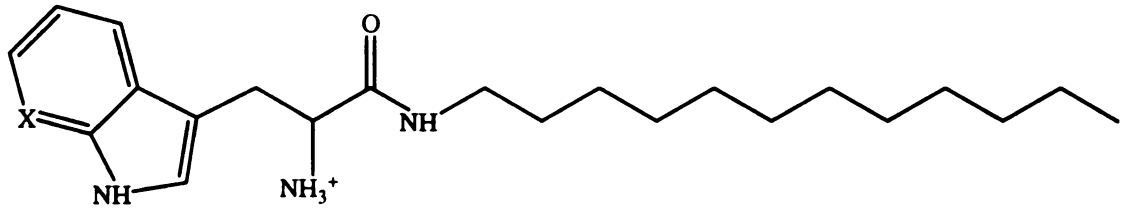

DD-AT, DD-TRP

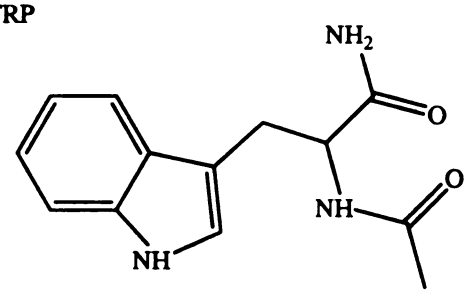

N-acetyltryptophanamide
(NATA)

**Figure 4.1** Structures of the chromophores in this study. For 7AT X=N and X=C for TRP.

We have also examined *n*-acetyl-tryptophanamide (NATA) in the same micelles. NATA is a neutral species and is of interest because it is an indole-containing molecule that has been used before as a mimic of TRP contained in a peptide backbone. It is characterized by a single exponential $S_1$ population decay. [16,17] We are interested in micelles because they are a reasonably well understood class of heterogeneous systems that can function as simplistic models for biomembrane structures. Surfactants and micelles have been investigated extensively due to their many uses, ranging from acting as media in which chemical reactions and excitation transport studies can be performed, to systems for enhancing protein solubility and effecting chemical separations.

We report here on our study of the dynamics natural and non-natural amino acid derivatives in aqueous micelles formed by anionic, cationic and neutral surfactants. Our experimental data suggest that probe interactions with the surface or interior of the micelles can dominate, depending on the charge of the chromophore used and the identity of its pendant moiety.

## 4.2 Experimental

*Materials.* The surfactants sodium dodecyl sulfate (SDS), cetyltrimethylammonium bromide (CTAB) and polyethylene glycol 400 dodecyl ether (Thesit®) were obtained from Sigma-Aldrich, Inc., checked for fluorescent impurities, and used as received. All chromophores and reagents needed for derivatization were also obtained from Sigma-Aldrich, Inc. The molecules D,L-7-azatryptophan hydrate, D,L-tryptophan hydrate, N-acetyl-tryptophanamide, and N-*t*-boc-tryptophan were used as received. N-*t*-boc-7-azatryptophan was prepared by the procedure described by Petrich[6] using D,L-7-azatryptophan hydrate, 2-(*tert*-butoxycarbonyloxyimino)-2-phenylacetonitrile (BOC-ON), and triethylamine in water/dioxane solvent.

DD-7AT and DD-TRP were prepared by condensations of the *N-t*-boc-amino acid with dodecylamine followed by removal of the boc group. The coupling of amino acids to dodecylamine was performed using the water soluble carbodiimide, 1-[3-(dimethylamino)propyl]-3-ethylcarbodiimide, hydrochloride (EDCI) [18,19] along with the coupling catalyst hydroxybenzotriazole (HOBt). A description of the coupling and deprotection procedure has been described before. The deprotection procedure was modified slightly. The DD-boc-X compounds (X = 7AT, TRP) were stirred into 9:1 trifluoroacetic acid:dimethyl sulfide and the progress of the reaction was followed by thin layer chromatography and worked up as indicated previously. [20]

All aqueous solutions were prepared with water from a Milli-Q water filtration system. All solutions used were $\leq 5$ $\mu$M in chromophore concentration and spectroscopic measurements were performed within 24 hours of solution preparation. The sample

temperature was controlled using a brass block cuvette holder maintained at 20.0 ± 0.1 °C (Neslab).

*Steady-State Absorption and Emission Spectra.* Absorption spectra were acquired using a Cary Model 300 double beam UV-visible absorption spectrometer set at 2 nm resolution. Emission spectra were recorded with a Spex Fluorolog 3 spectrometer using a 5 nm bandpass for excitation and a 2 nm bandpass for emission collection.

*Time-Correlated Single Photon Counting (TCSPC) Spectrometer.* The spectrometer we used for the lifetime and dynamical measurements has been described in detail before. [21] The light pulses used to excite the sample are produced by a synchronously pumped, cavity-dumped dye laser (Coherent 702-2, 5 ps pulses, 4 MHz repetition rate). The dye laser is excited by the second harmonic of the output of a continuous wave (cw) mode-locked Nd:YAG laser (Quantronix 416, 100 ps pulses, 80 MHz repetition rate). Samples were excited at their absorption maxima (Pyromethene 567 dye, Exciton, KDP Type I SHG). Emission was monitored at the chromophore florescence maximum in the solution of interest using a 20 nm bandpass for collection. Fluorescence was collected at polarizations of 0°, 54.7°, and 90° with respect to the vertically polarized excitation pulse. The instrument response function for this system is typically 35 ps FWHM and lifetimes measured range from ~600 ps to ~8.5 ns.

## 4.3 Results and Discussion

The objectives of this work are to understand the similarities and differences in the optical response of related chromophores that arise from structural modifications, and to elucidate how these modifications influence probe interactions with their immediate environment. In this study, micelles serve as a heterogeneous solution environment in which to examine these issues. The interactions of these probes with solvent, surfactant, and micelles will be mediated by their charge, substituent structure and functionality, and specific chromophore characteristics. We consider the steady-state and time-resolved spectroscopic data separately, following a brief discussion of solution and chromophore properties important to both groups of measurements.

The surfactant concentrations used were several times their critical micelle concentration (CMC) to ensure micelle formation. In order to interpret the data and be certain that changes in the optical responses of the probes are not due to changes in bulk solution properties, several physical parameters and solution properties of the surfactants and micelle solutions must be known. The relevant physical parameters of the surfactant solutions used are listed in Table 4.1. The micelle hydrodynamic radius, $r_h$, is among the quantities needed to interpret the data. For ionic surfactants, this value is estimated by summing the micelle core radius, the head group radius, and two layers of water. [22,23] This method of determining $r_h$ for ionic surfactants has been found to be in agreement with values obtained from light scattering experiments. The micelles formed by the neutral surfactant Thesit® are not as well ordered as those made using ionic CTAB and SDS amphiphiles. The hydrophilic portion of these two classes of micelles differ significantly. The hydrophilic portion of SDS and CTAB are bulky sulfate and

**Table 4.1** Solution and physical parameters of micelles of micelles used in this work.

| Surfactant[a] | Charge | Viscosity (cP) | pH | Concentration (mM)/number of CMC | $r_h$ (Å) | $\tau_M$ (ns) |
|---|---|---|---|---|---|---|
| CTAB | + | 1.00 ± .01 | 6.2 | 2.5 / 0.92 | 25.7 | 17.6 |
| SDS | - | 1.03 ± .01 | 6.6 | 25.0 / 8.3 | 20.7 | 9.2 |
| Thesit | neutral | 0.99 ± .01 | 7.1 | 1.0 / 0.1 | 35 | 44.4 |

[a] CTAB = Cetyltrimethylammonium bromide; SDS = sodium dodecyl sulfate; Thesit = poly(ethylene glycol) 400 dodecyl ether.

ammonium groups, respectively, while Thesit® is comprised of a poly(ethylene glycol) chain. This latter structural condition results in a hydrated mantle with a less well defined surface aqueous region, and $r_h$ is estimated at 35 Å. [20]

The dominant forms of the free amino acids TRP and 7AT depend on solution pH due to the presence of carboxylic acid and amine functionalities. Amino acids can take on a positive or negative charge or be zwitterionic, depending on the solution pH. In addition, 7AT can be protonated at the $N_7$ position, resulting in a significant emission red shift and decreased excited state lifetime below pH ~5. [24] TRP does not possess a labile proton on its indole moiety, but has been reported to exhibit an additional fluorescence decay component above pH 9. The existence of multiple different protonated states and low energy excited electronic states in TRP and 7AT accounts for the sensitivity of their emission spectra to local environment.

Viscosity affects rotational diffusion time constant(s) according to the modified Debye-Stokes-Einstein equation. [25-27] The bulk surfactant solution properties of viscosity

and pH were measured at 20 °C with a Canon-Fenske viscometer and a pH meter, respectively. The addition of surfactants at concentrations above their CMC in this study has a negligible effect on bulk solution viscosity. We measure changes in pH in the solutions but these pH changes do not occur in a region that affects the state of protonation of the chromophore or the overall charge of probe molecules. The changes in bulk solution properties associated with the formation of the micelles are small and will not influence the optical response of the chromophores substantially.

*Steady-state spectroscopy.* The experimental absorbance and emission maxima of the chromophores studied here are given in Table 4.2. Representative emission spectra are shown in Figure 4.2 for the TRP derivatives in SDS and Figure 4.3 for boc-AT in water and aqueous micelle solutions. Inspection of the absorbance maxima indicate the ground states of the chromophores are not perturbed to a great extent by covalent modification of the chromophore side groups or by the presence of micelles in solution. The structure- and environment-dependent changes in emission maxima for these chromophores are more pronounced. Both 7AT and TRP are known to exhibit emission spectral shifts when incorporated into peptides and proteins, with the spectral shifts seen for TRP being larger than those for 7AT. The first comparison we make is between the free residues, the N-boc modified chromophores, and C terminus modified dodecylamine forms, all in water. Compared to the free residues, emission of the boc-modified forms are red shifted by 5 nm (7AT) and 4 nm (TRP), and the dodecylamine-modified chromophores are blue-shifted by 2 nm (7AT) and 8 nm (TRP). The spectral shifts we observe for these chromophores are not due to changes in bulk solution properties, but

**Table 4.2** Absorbance, emission, and fluorescence decay parameters for probes in water and micelles. The α-ratio (last column) is the ratio of the prefactors for the two decay components.

| | | $\lambda_{abs\ max}$ | $\lambda_{em\ max}$ | $\tau_{fl1}$ (ps) | $\tau_{fl2}$ (ps) | $\alpha_1/\alpha_2$ |
|---|---|---|---|---|---|---|
| AT | Aqueous | 290 | 399 | 800±9 | | |
| | CTAB | 290 | 399 | 815± | | |
| | SDS | 290 | 399 | 829± | | |
| | Thesit® | 290 | 399 | 770± | | |
| boc-7AT | Aqueous | 290 | 404 | 637±9 | | |
| | CTAB | 290 | 397 | 1505±13 | | |
| | SDS | 289 | 404 | 642±11 | | |
| | Thesit® | 289 | 404 | 660±12 | | |
| DD-7AT | Aqueous | 290 | 397 | 901±10 | | |
| | CTAB | 290 | 397 | 1467±11 | | |
| | SDS | 290 | 384 | 578±9 | | |
| | Thesit® | 290 | 387 | 924±11 | 2407±70 | 9.4 |
| TRP | Aqueous | 279 | 359 | 872±100 | 3470±50 | 0.11 |
| | CTAB | 279 | 359 | 634±47 | 3384±80 | 0.13 |
| | SDS | 279 | 359 | 885±150 | 3100±70 | 0.15 |
| | Thesit | 279 | 359 | 689±68 | 3473±80 | 0.11 |
| boc-TRP | Aqueous | 279 | 363 | 1033±39 | 8450±26 | 0.14 |
| | CTAB | 282 | 352 | 1858±33 | 5923±33 | 0.45 |
| | SDS | 279 | 363 | 792±36 | 8361±18 | 0.25 |
| | Thesit® | 279 | 363 | 1000±27 | 8383±20 | 0.27 |
| DD-TRP | Aqueous | 279 | 351 | 1849±109 | 3049±102 | 0.49 |
| | CTAB | 281 | 351 | 1253±32 | 3634±56 | 0.59 |
| | SDS | 279 | 339 | 948±35 | 2827±25 | 0.52 |
| | Thesit® | 281 | 345 | 2849±113 | 6783±192 | 1.67 |
| NATA | Aqueous | 279 | 360 | 3153±18 | | |
| | CTAB | 279 | 358 | 3067±22 | | |
| | SDS | 279 | 358 | 1035±90 | 2746±40 | 0.2 |
| | Thesit® | 279 | 360 | 3168±60 | | |

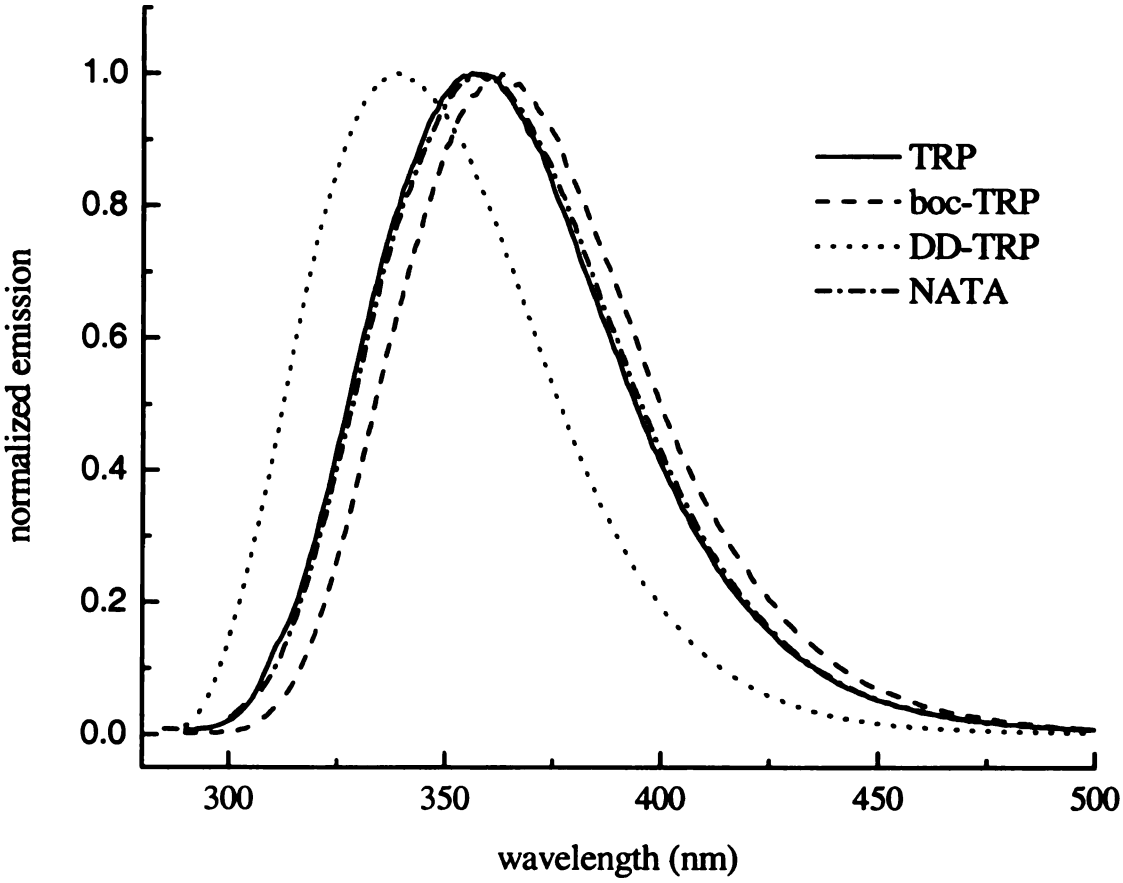


**Figure 4.2** Normalized emission spectra of tryptophan derivatives in 25 mM SDS solution. TRP = solid line, boc-TRP = dashed line, DD-TRP = dotted line, NATA = alternating dot/dash line.

arise from substituent effects on the excited states of the chromophores. It is known that the charged groups of zwitterionic TRP influence its excited state(s) and the emission shifts we observe are related to the stabilization of different charge distributions on the substituted molecules.

In micellar solutions, the behavior of 7AT and TRP are similar to that seen in aqueous solutions. The steady state responses of the amino acids show no change in

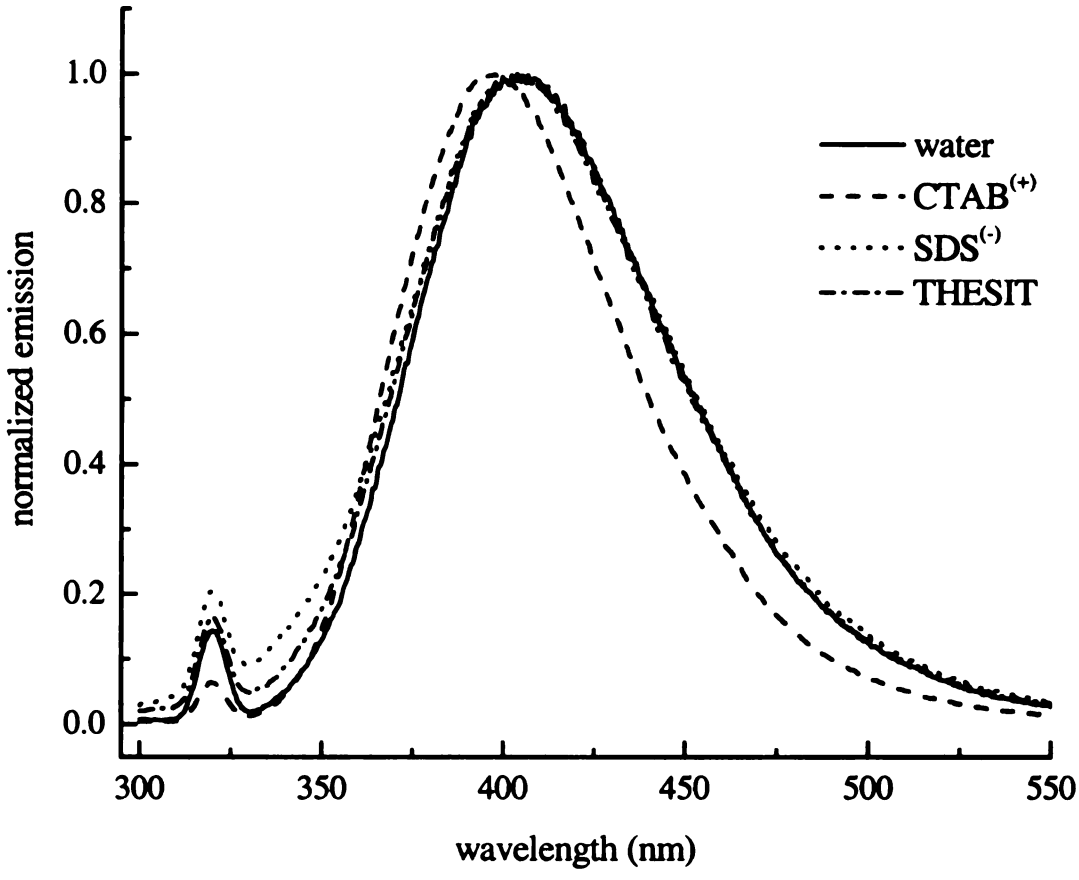


**Figure 4.3** Normalized emission spectra of boc-7AT in aqueous micelle solutions and water. boc-7AT in water = solid line, CTAB solution = dashed line, SDS solution = dotted line, Thesit® solution = alternating dot and dashed line.

emission maxima in micellar solution, indicating that the presence of the micelles is not altering their local environment to a significant extent. The boc-modified derivatives are anionic above ~pH 3 by virtue of the presence of a free carboxylate functionality, and exhibit emission blue shifts relative to water in solutions containing the cationic micelle CTAB. The chromophores modified at their C terminus with dodecylamine are cationic below pH 9 and these chromophores also exhibit a significant blue shift in solutions

containing anionic SDS micelles. Emission spectral shifts of organic dye molecules in surfactant solutions are common and are typically attributed to partitioning of the chromophore into the micelles. The spectral blue shifts seen for various indoles in micellar environments has been attributed to incorporation of the chromophores into the micellar core of Brij-35 but at concentrations far above the CMC, [28] similar blue shifts for indole are reported to occur only at high concentrations of SDS, while the negatively charged tryptophan derivative N-acetyltryptophan (NATA) is reported to blue shift with decrease in quantum yield around the CMC of CTAB. [29] Large blue shifts have been reported for TRP residues that reside in hydrophobic protein pockets. The steady state emission data of the chromophores we report on here are thus useful for gauging interactions between the chromophores and micellar structures in solution.

*Fluorescence lifetimes of 7AT, TRP and NATA.* Excited state lifetime measurements can provide information on solution composition and may also contain information on the interactions between the probe and the micelle. For the same reason that the emission spectra of the chromophores are sensitive to local environment, their fluorescence lifetimes reflect intermolecular interactions. 7AT is zwitterionic at pH 7 and its emission intensity decays as a single exponential with a time constant of ~800 ps. As noted above, 7AT has been incorporated into peptide fragments and oligomers, and its excited state population decays as a single exponential in uniform environments, with the exception of the octapeptide, as reported by Petrich. [30] The excited state population decay of TRP is more complex. TRP typically displays a biexponential fluorescence intensity decay in its zwitterionic form and when incorporated into peptides and proteins. NATA has been used as a simple model for tryptophan incorporated into a peptide

backbone. This is not necessarily a good model since NATA is anomalous among indole-containing molecules; it is known to exhibit a single exponential fluorescence intensity decay. [16,17] We consider the population relaxation dynamics of these three chromophores separately.

The fitted parameters for the emission intensity decays of the probes used in this study are listed in Table 4.2. All fluorescence lifetimes fit well to either a single or a double exponential decay. Goodness of fit was evaluated by $\chi^2$ criterion and visual inspection of the residuals of the fitted function to the data. A single exponential intensity decay indicates that the fluorescent species exists in a single environment or that there is rapid exchange between multiple environments over the time scale of the measurement. Deviations from single exponential decay behavior indicate the fluorescent species exists in multiple stable environments where exchange is slow, or simultaneous relaxation from multiple excited electronic states. Probe molecules containing the 7-azaindole chromophore exhibit a time-domain response fitted best to a single exponential decay, except for DD-7AT in Thesit®. Inspection of the lifetime data reveals that the lifetime of zwitterionic 7AT depends little on the presence of or proximity to micelles, suggesting that 7AT experiences a similar environment in water and micellar solutions and that it does not interact appreciably with surfactant molecules or micelles. Modifying the amino and carboxylic acid functionalities of 7AT affects the steady state emission properties of the chromophore and has a pronounced effect on the fluorescence lifetime. In water, the fluorescence lifetimes range from ~640 ps for boc-7AT to ~800 ps for 7AT and ~900 ps for DD-7AT.

The fluorescence decays for boc-7AT in water, SDS, and Thesit® are similar but, in CTAB, the lifetime more than doubles to 1.5 ns. It is unusual to recover lifetimes this long for the 7AT chromophore in aqueous media. Lifetimes for 7-azaindole of 1.4 ns are seen in heptane, [31] and ~1.7 ns in cyclohexane. [32] As mentioned previously, boc-7AT exhibits an emission spectral blue shift in CTAB relative to water, consistent with the chromophore residing in a nonpolar environment. The interior of a CTAB micelle is less polar than bulk water and, in heptane, the boc-7AT emission blue shift is greater than in micellar media. For the 7-azaindole chromophore, two emission bands are seen in nonpolar, aprotic solvents. In heptane a dominant band (~326 nm) is associated with the "normal" species and secondary Stokes shifted tautomer emission (~480 nm) arising from excited state double proton transfer of the dimer. [31] The presence of small amounts of water disrupts the dual emission behavior. For boc-7AT in CTAB there is no evidence of dual emission and it would not be expected unless the chromophore were sequestered in the center of the micelle, since water is known to penetrate significantly into the mantle of ionic micelles.

The lifetime of DD-7AT depends sensitively on its local environment. In SDS micelles, DD-7AT has a lifetime of ~580 ps. Its lifetime increases to ~1.5 ns in CTAB, nearly the same as for boc-7AT in CTAB, with which DD-7AT shares an essentially identical steady state emission response. This finding suggests that the substituted chromophores may reside in similar environments and states of solvation despite their opposite charge and different pendant structures. DD-7AT displays a second slow fluorescence decay component in the neutral micelle Thesit® that contributes approximately 10% to the total decay as given by the prefactors of the fitted exponential

function, with the time constants being 924 ps (90%) and 2.4 ns (10%). There are several possible explanations for these data. The first is that we are measuring partitioning between free and micelle-bound probes. This explanation is consistent with the fast decay component being similar to that of DD-7AT in water but the steady state emission is shifted 10 nm with respect to water. The second possibility is that the probe is predominantly bound to the micelles, with the micelle presenting two distinct environments to the chromophore. This explanation would require slow exchange between the two environments during the lifetime of the excited chromophore, and we believe this situation to be physically unrealistic. A third possibility is that the solvation state induced by the Thesit® micelles causes dual exponential decay due to a small fraction of probes in a proper state of solvation to undergo interactions with the terminal alcohol groups of Thesit®.

The fluorescence intensity decay of TRP is known to be biexponential, with time constants of ~0.8 ns and ~3.5 ns in water. When TRP is placed in micellar solutions, only small changes in the time constants are observed. This finding suggests that the presence of micelles has a limited effect on the chromophore excited state, consistent with our findings for 7AT. The fluorescence intensity decay of boc-TRP in water is also biexponential, with time constants of ~1 ns and ~8.5 ns (Table 4.2). The slow decay time constant is significantly longer for boc-TRP than for TRP and one explanation for this finding is that the TRP long lifetime is shortened due to self-quenching by the charged amino group at neutral pH. The lifetime of boc-TRP is similar in water, SDS, and Thesit® but with time constants of ~2 ns and ~ 6 ns in CTAB. For boc-TRP, the short lifetime component shows a significant increase in lifetime in CTAB, like the 7AT

derivatives, while the long component decreases with respect to its value in water. While the interactions of boc-TRP are likely mediated by electrostatic forces, interpretation of its lifetimes is complicated by the complex and opposing manner in which the two components are manifested. It is interesting to note at this point that bromide ions of CTAB are a reported to quench the fluorescent probes HANS and DANS. [33] In contrast, we have noted significant increases in lifetimes for the AT probes in CTAB with respect to water and a less well defined effect on the lifetimes of the TRP probes in CTAB. This means that either the probes reside within the micelles where bromide counterions do not have access or that the chromophores are not highly susceptible to bromide quenching. We believe that for the AT probes, the latter explanation is more likely; their emission maxima indicate a highly polar environment because the probes reside near the headgroup region of the micelles, an area rich in bromide counterions.

DD-TRP displays the most environmentally sensitive fluorescence response, with unique fluorescence decay time constants for each system measured. The decay times of boc-TRP and DD-TRP do not appear to be correlated to one another, in contrast to the data for boc-7AT and DD-7AT. In comparison to the other indole containing species, the fluorescence response of DD-TRP in Thesit® is the most unusual as was DD-7AT for the azaindole probes. The short and long time components of DD-TRP in Thesit® are about twice their value(s) in water (Table 4.2). In CTAB, the short time constant decay comprises the majority of the fluorescence decay, in contrast to the behavior seen for 7-azaindole-based probes. We note that this anomalous behavior is not seen for the reorientation data (*vide infra*) and further investigation will be required to identify the basis for these findings.

The fluorescence of the neutral chromophore NATA exhibits single exponential decay kinetics with a decay time constant of ~3.1 ns in water, CTAB and Thesit® (Table 4.2). In SDS-containing solutions, NATA exhibits a two-component population decay. The lifetimes recovered for NATA and DD-TRP in SDS are similar. We believe this situation to be coincidental; the indole chromophores are not experiencing the same environment, as seen by the large difference in the steady state emission (19 nm) and the relative contributions of each lifetime component for these two probes.

To better understand the interactions between the probes and micelles, we have investigated the rotational diffusion dynamics of the chromophores in aqueous solutions of micelle-forming surfactants. Time resolved fluorescence depolarization experiments provide information on the rotational diffusion of the probe molecules. These measurements are sensitive to and can provide information about intermolecular interactions over the length scale of the probe molecule. [34,35] Reorientation data provides direct information on probe-surfactant association. We can distinguish whether or not probes are interacting significantly with micelles by comparing the dynamical response of the probes in water and micellar solutions.

There are many studies in the literature of the rotational diffusion of organic chromophores in neat and selected binary solvent systems. [35,36] Micellar environments have been examined before[37-41] and are a special subset of binary systems. The theory of rotational diffusion is well established and, because the relevant molecular processes proceed on a time scale that can be accessed experimentally, it has found wide use as a means of probing intermolecular interactions and transient solution-phase organization. The time scale of the events determining reorientation dynamics are short and, as a result,

many interactions occur over the course of the chromophore's reorientation resulting in the overall experimental observation being a representation of the average molecular environment experienced by the probe. For reorientation measurements in binary solutions it is often found that the molecular-scale interactions responsible for the dynamical behavior of the probes are not dictated by the bulk properties of the solvent. In polar systems, the relevant intermolecular interactions may include dipolar interactions, dielectric friction, [42] and under certain circumstances, formation of solvent-solute complexes. We consider our data on the reorientation of NATA, and 7AT and TRP derivatives in micellar environments. Our measurements point to the existence of strong interactions between certain of the probes and the micelles and we interpret our reorientation data in the context of a hindered rotor model shown previously to be appropriate for such systems.

We use a pulse of vertically polarized light to excite an ensemble of chromophores in solution and monitor the time-dependent decays of the polarized components of emission. We combine the emission intensity data polarized parallel and perpendicular to the excitation polarization and generate the induced orientational anisotropy function, R(t),

$$R(t) = \frac{I_{\parallel}(t) - I_{\perp}(t)}{I_{\parallel}(t) + 2I_{\perp}(t)} \tag{4.1}$$

where $I_{\parallel}(t)$ and $I_{\perp}(t)$ are the time-dependent emission intensities. The function R(t) represents the re-randomization of the ensemble of excited molecules. In these measurements the data is compared to various models and theories in an effort to relate the functionality of the R(t) decay to the immediate environment of the chromophore. Theoretically, R(t) can contain up to five exponential decays and its form depends on the

shape, size, flexibility of the labeled molecule, and the angle between the transition moments of the chromophore. [43] In simple homogeneous environments a single exponential decay is commonly recovered and it is unusual to observe more than two decays. The anisotropy of all the chromophores we examine in this study decay by a single exponential in water and the anisotropy decay of DD-AT in water is shown in Figure 4.4. These same probes displayed marked changes in their anisotropy decay in at least one type of micelle solution with exception of the free amino acids that remain single exponential. The experimental anisotropy functions are seen to change from single to decays with two exponential components (see Figure 4.5) in micellar solutions,

$$R(t) = R_1(0)\exp\left(-t/\tau_1\right) + R_2(0)\exp\left(-t/\tau_2\right) \tag{4.2}$$

and a central issue is the assignment of origin of the biexponential behavior. It is significant that we observe different functionalities for the anisotropy decay in water and in micellar solutions. This finding points to the incorporation of the probe(s) into micellar environments and we thus need to consider two different models to account for our experimental findings.

In water, a one-component reorientation decay is consistent with our earlier findings for AT derivatives[20,24] as well as one-component decays reported for tryptophan and NATA. [44] These simple decay data may be interpreted in the context of the modified Debye-Stokes-Einstein (DSE) model, [25-27]

$$\mathrm{R}(t) = \mathrm{R}(0)\exp(-t/\tau_{OR}) \tag{4.3}$$

$$\tau_{OR} = \frac{\eta V f}{k_B T S}$$

where $\tau_{OR}$ is the reorientation time constant, $\eta$ is the solution bulk viscosity, $V$ is the solute hydrodynamic volume, [45] $f$ is a friction coefficient to account for the solvent-solute boundary condition and $S$ accounts for the non-spherical shape of the volume swept out by the reorienting molecule.

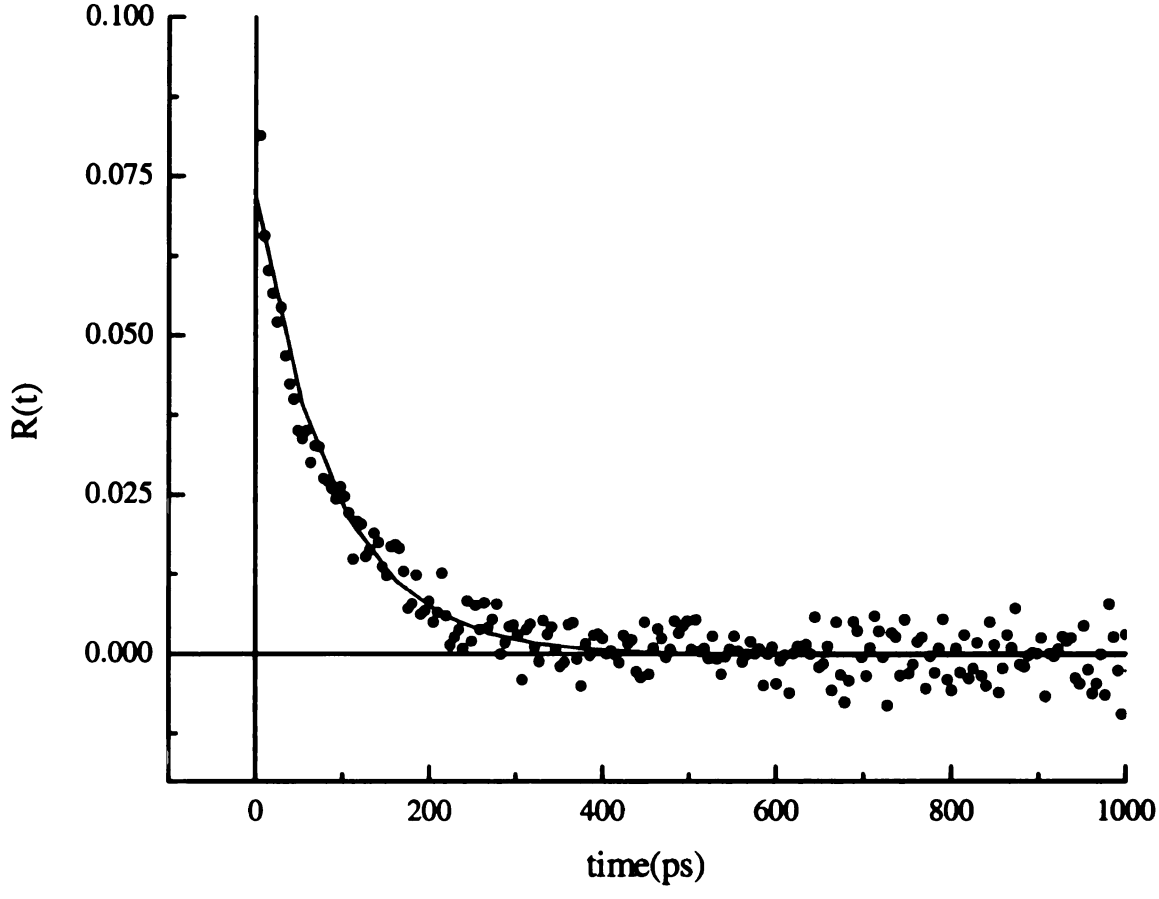


**Figure 4.4** Experimental anisotropy decay of DD-AT in water (data points) and best-fit line to a single exponential decay function.

We now consider the reorientation of the probes in micellar solutions. Comparing the reorientation data gathered in water to the data for the micellar solutions allows us to determine whether or not the chromophores are associating or incorporating in some

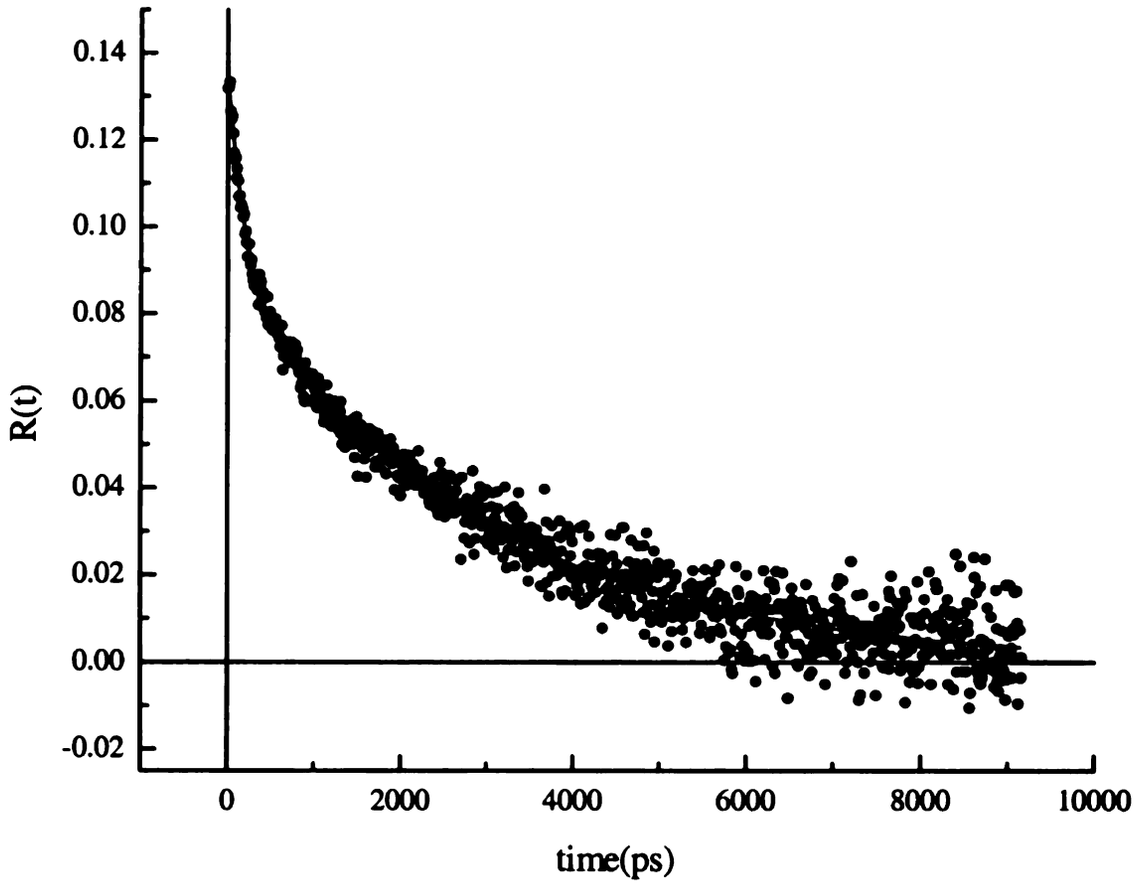


**Figure 4.5** Experimental anisotropy decay of DD-AT in Thesit® solution (data points) and best fit line to a biexponential decay function.

manner into micelles. In cases where a single exponential anisotropy decay is seen in micellar solution, the location of the chromophore can be open to question. We assert a change in the functionality of anisotropy in micellar solutions indicates incorporation into micelles. We observed that certain probes display biexponential anisotropy decays signaling incorporation into micelles, and we need to choose an appropriate model to aid interpretation of the observed dynamics.

The fluorescence depolarization of a probe molecule in a micelle results from both the rotation of the micelle and the molecular dynamics of the probe within the micelle. The rotation of the micelle in solution is independent of the dynamics of the associated probe molecule. The probe dynamics in the micelle may include movement of the probe in a restricted region of the micelle and translational motion of the adsorbed or tethered probe in or across the surface of the micelle. These dynamics depend sensitively on probe and micelle molecular structure.

There are several models that may be applicable to the interpretation of R(t) decays in an environment where rotational motion is hindered. [46-49] R(t) can be predicted to decay as a single exponential in the following two cases. The anisotropy decay time constant represents the motion of the (spherical) micelle in the case where the chromophore is attached to the micelle as a rigid entity and this motion is characterized by a time constant, $\tau_M$. In the second case, the chromophore is located in the core of a micelle and is free to rotate within that confined volume. In this model, the anisotropy decays with a time constant of $(\tau_M^{-1} + \tau_R^{-1})^{-1}$ , a single exponential, where $\tau_R$ is the decay time constant associated with chromophore motion in the core of the micelle. The experimental time constants we recover and their magnitudes suggest that neither model is appropriate for the systems we report on here.

The time constants and zero-time anisotropies for reorientation of the probes in water and the micelles SDS, CTAB and Thesit® are given in Table 4.3. The zwitterionic species 7AT and TRP exhibit single exponential anisotropy decays in all solutions. There are measurable differences in the reorientation time constants for these probes in surfactant solutions, and these differences cannot be accounted for simply by changes in

**Table 4.3** Fitted decay time constants and zero-time anisotropies for the systems indicated in the left column The experimental data were fitted to the function: $R(t) = R_1(0)\exp(-t/\tau_1)+R_2(0)\exp(-t/\tau_2)$. For probe/solution systems with one decay constant indicated, $R_2(0) = 0$.

| | | $R_1(0)$ | $\tau_{OR}$ (ps) | $R_2(0)$(ps) | $\tau_{OR2}$ (ps) |
|---|---|---|---|---|---|
| AT | Aqueous | .063 ±.01 | 41±5 | | |
| | CTAB | .065 ±.005 | 63±8 | | |
| | SDS | 0.07 ±.005 | 54±5 | | |
| | Thesit® | 0.064 | 50±4 | | |
| boc-7AT | Aqueous | 0.061±.005 | 63±8 | | |
| | CTAB | 0.041±.003 | 256±18 | 0.05±.002 | 2122±120 |
| | SDS | 0.064±.003 | 66±6 | | |
| | Thesit® | 0.06±.005 | 73±7 | | |
| DD-7AT | Aqueous | 0.066±.002 | 98±5 | | |
| | CTAB | 0.033±.002 | 196±17 | 0.031±.002 | 1337±97 |
| | SDS | 0.032±.004 | 85±19 | 0.046±.004 | 498±47 |
| | Thesit® | 0.047±.002 | 196±10 | 0.088±.002 | 2975±81 |
| TRP | Aqueous | 0.09±.01 | 51±5 | | |
| | CTAB | 0.1±.01 | 70±7 | | |
| | SDS | 0.08±.01 | 67±7 | | |
| | Thesit® | 0.08±.01 | 47±6 | | |
| boc-TRP | Aqueous | 0.11±.02 | 80±8 | | |
| | CTAB | 0.05±.01 | 146±21 | 0.07±.01 | 1341±166 |
| | SDS | 0.14±.02 | 124±10 | | |
| | Thesit® | 0.082±.02 | 101±15 | 0.068±.02 | 529±.04 |
| DD-TRP | Aqueous | 0.09±.01 | 118±15 | | |
| | CTAB | 0.051±.005 | 205±17 | 0.052±.005 | 1213±56 |
| | SDS | 0.06±.008 | 223±25 | 0.05±.005 | 1557±66 |
| | Thesit® | 0.035±.004 | 207±43 | 0.09±.003 | 1204±57 |
| NATA | Aqueous | 0.1±.01 | 72±7 | | |
| | CTAB | 0.11±.01 | 71±7 | | |
| | SDS | 0.09±.01 | 76±12 | 0.04±.006 | 630±86 |
| | Thesit® | 0.09±.01 | 73±10 | | |

bulk solution properties; the bulk viscosities of the micelle solutions are essentially the same as that of water. There must be some interaction of 7AT and TRP with the micelles, but the nature of the interaction and its persistence time cannot be addressed directly by these data alone. The single exponential anisotropy decays seen for these chromophores suggest that the persistence time of any probe-micelle interaction is short relative to the reorientation time of the micelle.

The reorientation dynamics of substituted 7AT and TRP, and with NATA in several of the micelles are fundamentally different than those seen for TRP and 7AT. For the oppositely charged probe/micelle systems (boc-$X^-$/$CTAB^+$ or X-$DD^+$/$SDS^-$), the experimental R(t) function is a biexponential decay. It is tempting to interpret this functionality as representing the interactions between probe and micelle being facilitated by ionic interactions. While such interactions are likely important, we see evidence in the data that (neutral) NATA also interacts significantly with ionic micelles. Thus ionic interactions alone cannot account for the probe/micelle interactions. Additionally, when the chromophores have structural features in common with the surfactants, such as $C_{12}$ aliphatic chain, ionic interactions appear not to dominate the probe/micelle interactions. This finding is consistent with the existence of a double layer structure at the interface between amphiphile head groups and the bulk medium. Screening from such a double layer structure can serve to mediate the importance of ionic interactions.

The anisotropy functions of the cationic probes DD-7AT and DD-TRP exhibit two-component exponential decays in all micellar solutions. The existence of two reorientation time constants could result either from the probe partitioning into two distinct environments or from the probe residing in a single environment and the two-

component reorientation dynamics resulting from the effective rotor shape of the probe. An examination of the fluorescence lifetime data in conjunction with the reorientation data allows these possibilities to be distinguished. The azaindole-containing probes exhibit single exponential emission intensity decays in water. The fluorescence intensity decay of DD-7AT in Thesit® displays a major component (90%) with a time constant of 924 ± 11 ps and a minor component (10%) with a time constant of 2407 ± 70 ps. The short component for this system is the same as that recovered in pure water, 901 ± 10 ps. The lifetime data suggest a small fraction of probe being incorporated into micelles, with the majority of the probe in water. Thus the reorientation data are indicative of the probe partitioning into two environments; one on or within the micelle and the other dominated by bulk water. The fact that the fast reorientation time of DD-7AT in the micellar system (~200 ps) is twice that measured in water (~100 ps) indicates that the probe resides in an aqueous environment that is influenced substantially by the presence of the micelles. It is possible that the fast reorientation time constant for this system is the result of rapid association/dissociation kinetics for probe/micelle interactions. DD-7AT exhibits a two-component anisotropy decay in CTAB and SDS micellar solutions, as does boc-7AT in CTAB. The variations in anisotropy decay time constants for these systems point toward there being significant and relatively short-lived probe interactions with the micelles.

The analogous indole probes display double exponential anisotropy decays in micellar solutions. The recovered time constants for the indole and azaindole probes show similar trends but considerably different time constants in their reorientation dynamics. Intuition suggests that these chromophores would exhibit similar reorientation behavior. The structural similarity of TRP and 7AT derivatives is central to the use of

7AT as an alternative to TRP as a probe in biological systems. While 7AT has been used effectively in situations where biological activity is retained, the rates of activity changed significantly upon substitution. Another indication of the significant differences 7AT-substitution introduces into biological environments is the experimental finding that certain 7AT-substituted proteins can be crystallized, where the corresponding non-mutant tryptophan-containing proteins have not been crystallized. [50] It appears that the presence of the ring-bound N at the 7-position in 7AT plays an important structural as well as spectroscopic role in determining the properties of this molecule.

When two decays are seen in a micellar system, it is reasonable to assume that the decays correspond to fast, restricted motion within the micelle or at its surface, and slower global motion of the micelle. The recovered short time constants span a range from 85 to 260 ps and the long components vary from 0.5 to 3 ns. The probes are not bound rigidly in the micelle or free to rotate within the core because they do not display single exponential dynamics or possess time constants consistent with these scenarios. The short component depends on the specific probe/micelle system and the time constants recovered are not inconsistent with those expected for restricted motion in or on a micelle. For all of the systems we report here, the long decay time constant never approaches that expected for global micelle motion if the probes are attached rigidly to or contained within a micelle. The correlation times expected for the micelles, $\tau_M$, are listed in Table 4.1. These correlation times were calculated using Eq. 4.3 in the stick-limit ($f$=1, $S$=1) using $r_h$ for the radius of the micelles to determine volume. These predicted correlation times range from several ns to tens of ns, depending on the size of the micelle. The slow time constants we measure experimentally are not consistent with the motion of

the free probes. These findings leave quasi-translational motion of the chromophore along the outer extent of the micelle as the only physical motion consistent with this time constant. [20]

Owing to the structures of the probes and micelles used here, there are two significant types of interactions that can occur. These are ionic and dispersion interactions, and they can act either in concert with one another or in an opposing manner, depending on the specific system. It is evident from the experimental data that there is substantial interaction between the oppositely charged probes and micelles and when the probes share common structure with micellar constituents. For the cationic probes DD-7AT and DD-TRP, we observe qualitatively similar behavior in cationic, anionic and neutral micelles, with the differences in the time constants between systems likely being related to the characteristic persistence times for the dominant interactions. We take these findings to indicate that for $C_{12}$ aliphatic chains interacting with micelles of similar length, the dispersion forces compete effectively with ionic forces and dominate the observed dynamics. This finding can be reconciled if we consider that the nominally charged probe and micelle moieties are likely screened efficiently by spectator ions, leaving dispersion interactions as the dominant forces in these systems. For the anionic boc-7AT and boc-TRP derivatives, we recover two-component anisotropy decays in cationic CTAB micelles, single component decays in anionic SDS micelles and in water, and probe-dependent behavior in the neutral Thesit® micelle. We understand the behavior of these probes in CTAB and SDS as being mediated primarily by ionic interactions, and the different behavior of the two probes in Thesit® results from the subtle structural difference between the chromophores. We have discussed this issue

above. The neutral probe NATA appears to remain predominantly in the aqueous phase of all micellar systems, with measurable contributions from micelle-incorporated chromophore being seen only for SDS.

We apply a single formalism to the systems that exhibit two-component anisotropy decays to explain their physical behavior. The fundamental physics responsible for the data we observe is essentially the same for all of the micellar systems, with differences in the details being associated with the specific identities of the micellar constituents. We summarize our findings as follows: (1) 7AT and TRP exhibit only small changes in $\tau_{OR}$ for each surfactant solution compared to their behavior in water, indicating that the probe molecule itself does not associate substantially with the micellar structures. This finding is corroborated by the lifetime and steady state emission data. (2) The number of anisotropy decays seen for any of the probes studied here is an indicator of the extent of probe/micelle interactions for that system. Two-component anisotropy decays indicate strong probe/micelle interactions and one-component anisotropy decays suggest that the probe resides primarily in the aqueous environment. (3) The details of the probe/micelle interactions are determined by the balance between ionic and dispersion interactions, where the double layer serves to attenuate ionic interactions.

We consider next the time constants we obtain experimentally and how to reconcile these data with the structural features of the systems we have investigated. For the case where the chromophore is bound near the surface of the micelle, a biexponential decay is expected, with time constants $\tau_w$ arising from restricted motion analogous to that of a hindered rotor, and $\tau_M$ for overall reorientation of the micelle. [48] If translational

motion of the chromophore about the surface of the micelle is considered, a third decay component, $\tau_d$, is expected. [38] The anisotropy function derived from this model is given by Eq. 4.4,

$$R(t) = R(0)[S'^2 + (1 - S'^2)\exp(-t/\tau_W)]\exp(-t(1/\tau_d + 1/\tau_M)) \quad (4.4)$$

where R(0) is the zero time anisotropy, $S'$ is an order parameter which is a measure of the equilibrium orientational distribution of the chromophore transition moment. Because the micelles are relatively large the additional orientational relaxation imposed on the probe only affects the slow decay component due to translational diffusion. These motions take place independently and their decay rates can be added thus Eq. 4.4 does not include these motions explicitly. Depending on the complexity of the model used in the interpretation of the experimental data, it is possible to over-interpret the information present. We are cognizant of this possibility and we choose to use the simplest model that accounts for the features of the data.

The expected reorientation time constant for a micelle is several nanoseconds and we do not observe any such long time anisotropy decay in our data. The possible reasons for this finding are either that our measurements are not sensitive to such a long-time component, which is not the case, or that the persistence time of the micelle-probe association is substantially shorter than the reorientation time of the micelle. The latter explanation is consistent with interactions between the probe and the micelle that are characterized by a relatively small driving force. We consider that the interaction between the probes and the micelles is dominated by ionic interactions for the smaller charged probes and by dispersion-mediated penetration of aliphatic moieties with the lipophilic portion of the micelle for DD-7AT and DD-TRP. In all cases, the

chromophore is in closest proximity to the micelle head groups, and this portion of the probe is capable of motion at or near the surface of the micelle. We treat this motion as translational diffusion on a spherical surface. Eq. 4.4 describes the general case of the anisotropy decay for three independent motions and we can apply the following simplifications to bring this model into consistency with the experimental data,

$$1/\tau_d = 1/\tau_{slow} - 1/\tau_M \tag{4.5}$$

$$1/\tau_w = 1/\tau_{fast} - 1/\tau_d - 1/\tau_M = 1/\tau_{fast} - 1/\tau_{slow} \tag{4.6}$$

We determine values of $\tau_M$ from the DSE equation at 20 °C, or we assume $\tau_M = \infty$, but in either case we are insensitive to this quantity experimentally. The translational diffusion coefficient, $D_t$, can be related to $\tau_d$ through the radius of the micelle, $r_h$, (Table 4.1) over which the probe diffuses, by eq 4.7. [4]

$$D_t = r_h^2 / 6\tau_d \tag{4.7}$$

This diffusion constant is related to the slower of the two motions we sense. The fast time constant is related to the rotational motion of the chromophore about its tethering bond to the micelle. The wobbling-in-a-cone model[46,48] assumes the molecule is constrained within a cone of semi-angle $\theta_0$ with the rotational motion of the molecule being described by a wobbling diffusion coefficient, $D_w$. The value of $D_w$ is related to our experimental data through the quantities $\tau_w$ and $S'$,

$$\begin{aligned} D_w = \{\tau_w(1-S'^2)\}^{-1}[-\cos^2\theta_0(1+\cos\theta_0)^2\{\ln[(1+\cos\theta_0)/2] \\ +(1-\cos\theta_0)/2\}\{2(1-\cos\theta_0)\}^{-1} + (1-\cos\theta_0) \\ \times(6+8\cos\theta_0-\cos^2\theta_0-12\cos^3\theta_0-7\cos^4\theta_0)/24] \end{aligned} \tag{4.8}$$

where the cone semi-angle $\theta_0$ is related to the order parameter through

$$S' = 0.5\cos\theta_0(1+\cos\theta_0) \tag{4.9}$$

**Table 4.4** Values of quantities extracted from the hindered rotor model. S' is the order parameter, determined from fits to Eq. 4.4.

| probe | solution | S' | $\theta_0$ (degrees) | $D_w \times 10^9$ ($s^{-1}$) | $D_t \times 10^{-9}$ ($m^2/s$) |
|---|---|---|---|---|---|
| AT | Aqueous | | 90 | 4.07 | |
| | CTAB | | 90 | 2.65 | |
| | SDS | | 90 | 3.09 | |
| | Thesit® | | 90 | 3.33 | |
| boc-7AT | Aqueous | | 90 | 2.65 | |
| | CTAB | 0.741 | 35 | 0.335 | 0.456 |
| | SDS | | 90 | | |
| | Thesit® | | 90 | 2.65 | |
| DD-7AT | Aqueous | | 90 | 1.70 | |
| | CTAB | 0.696 | 39 | 0.496 | 0.761 |
| | SDS | 0.768 | 33 | 0.858 | 1.36 |
| | Thesit® | 0.807 | 30 | 0.350 | 0.640 |
| TRP | Aqueous | | 90 | 3.27 | |
| | CTAB | | 90 | 1.67 | |
| | SDS | | 90 | 1.34 | |
| | Thesit® | | 90 | 3.55 | |
| boc-TRP | Aqueous | | 90 | 2.10 | |
| | CTAB | 0.764 | 34 | 0.546 | 0.760 |
| | SDS | | 90 | 1.34 | |
| | Thesit® | 0.673 | 40 | 0.976 | 3.81 |
| DD-TRP | Aqueous | | 90 | 1.41 | |
| | CTAB | 0.711 | 38 | 0.440 | 0.845 |
| | SDS | 0.674 | 40 | 0.467 | 0.381 |
| | Thesit® | 0.849 | 26 | 0.232 | 1.65 |
| NATA | Aqueous | | 90 | 2.31 | |
| | CTAB | | 90 | 2.35 | |
| | SDS | 0.555 | 48 | 1.97 | 1.15 |
| | Thesit® | | 90 | 2.28 | |

$\theta_0$ calculated according to Eq. 4.9. $\theta_0 = \cos^{-1}\left(0.5\left(\sqrt{1+8S'}-1\right)\right)$. Uncertainty in the determination of S' is taken to be ± 5%.

The values for $S'$, $\tau_{slow}$ and $\tau_{fast}$ were extracted from the experimental data using Eq. 4.4 and from this information, the quantities $\theta_0$, $D_w$, and $D_t$ were calculated for each surfactant system (Table 4.4). The values of $D_w$ for probes yielding single exponential decay were calculated using $D_w = (6\tau_{OR})^{-1}$. The order parameters in these solutions are zero and the equilibrium orientational distribution is random because the probes are assumed to reorient freely.

The values of the order parameter, $S'$, vary from 0.56 to 0.85 for reorientation of the probes in the micelles. The order parameter is a measure of the time averaged orientational distribution of the chromophores and can take on values from zero for a fully random orientational distribution, to one for rigid, highly ordered systems such as crystals. The values recovered for the order parameter indicate the probes do have preferential orientation with respect to the micelle surface. On the basis of the $S'$ values we extract from our data, the most motionally restrictive environment is formed by Thesit® for the probes DD-TRP and DD-7AT. These probe/micelle systems displayed among the largest changes in reorientation times compared to their behavior in water. These probes likely interact significantly with the polyethylene glycol mantle of the Thesit® micelles. The lowest value of S' is seen with the NATA/SDS system. NATA/SDS also yields the largest wobbling diffusion coefficient, approaching that of NATA in water. These complementary pieces of information point to NATA being only weakly associated with the micelle, with the most likely interaction occurring at the micelle/water interface.

The recovered diffusion coefficients for the probes in water vary inversely with probe size as expected. It is also useful to consider the magnitude of $D_t$, the translational

diffusion coefficient along the micelle/water interface. The probes exhibit moderately fast translational diffusion at the micelle/water interfaces. The self-diffusion behavior of the ionic surfactants used in this study has been investigated previously, with values for $D_t$ the lateral diffusion of surfactant molecule in micelles reported on the order of (0.2-1.5) x $10^{-10}$ $m^2$ $s^{-1}$. [51,52] The translational diffusion constants we recover for the probes used in this study range from ~ $10^{-9}$ -$10^{-10}$ $m^2$ $s^{-1}$, with the smallest value for the oppositely charged probe/micelle systems. The smallest value of $D_t$ we recover is for DD-TRP in SDS. This probe can interact significantly with the nonpolar interior regions of micelles, with the strength of interaction being similar to that of a constituent surfactant molecule. The combination of strong dispersion interactions with favorable ionic interactions leads to a probe/micelle system that are relatively tightly bound. We note also the relatively slow translational diffusion constants seen for the boc-derivatized probe/CTAB systems, which we attribute to the existence of attractive ionic interactions. The largest translational diffusion constants we measure are for probes in (neutral) Thesit® micelles. The order parameter data in Thesit® vary considerably depending on probe. For boc-AT a low order parameter and large $D_t$ value both point to the absence of extensive order in the micelle a result consistent with the physical picture of Thesit® micelles. DD-Trp has the highest order parameter indicating a restrictive environment immediately surrounding the probe but also the second fastest translational diffusion in the study. We explain this apparent contradiction by suggesting that the chromophore is indeed in a highly ordered environment, drawn relatively deeply into the Thesit® micelle by its aliphatic moiety and with little opposing force due to the probe's overall hydrophobic nature and absence of ionic interactions competing near the surface mantle

region of this neutral micelle. As a result, the experimental reorientation time is higher than expected since, in this calculation, it is assumed that the probe is at or near the surface of the micelle. The DD-AT probe yields differing results from that of its TRP analog. It too has a high order parameter but with much lower translational diffusion constant than DD-TRP. This is a manifestation of the differing physical interactions of these probes induced by the $N_7$ in the ring of 7AT. While structurally very similar, this subtle difference in the chromophore results in its association with the hydrophilic alcohol terminated, polyethylene glycol portion of the Thesit® micelle. The Azaindole chromophore is well known to hydrogen bond in alcohols and differences in $D_t$ of a factor of two have been attributed to its propensity for hydrogen bonding between the chromophore DPP with TX-100 micelles as compared to the structurally similar non hydrogen bonding DMDPP.[53] The experimental data, in conjunction with the model we use, allow the interpretation of our findings based on a balance between ionic and dispersion interactions.

## 4.4 Conclusions

We have studied the steady-state and time-resolved optical response of several indole and azaindole derived probes in water and aqueous micelle solutions. The charge and structure of the probes dictate interactions with micelles. The reorientation dynamics of the probes were consistent with the model of wobbling-in-cone dynamics with translational diffusion of the probe along the micelle/water interface for SDS and CTAB, and within the mantle of Thesit® micelles, along with slower rotation of the micelle in all cases. Our experimental data reveal the ability of ionic interactions to mediate probe/micelle interactions and that van der Waals interactions can overcome these forces. For the case of oppositely charged probe/micelle systems we see the strongest interactions because ionic and van der Waals forces are acting in concert. Probes with structure in common (aliphatic chain) interact with micelles, regardless of probe charge. Our experimental reorientation data indicate transient interactions between the micelle and the probe oligopeptides, with limited structural freedom for the probe molecules in the apparently viscous micellar environment. Taken as a whole, this work demonstrates that there is a clear balance between ionic and dispersion interactions in amphiphilic systems, and that these interactions can be controlled in a straightforward and intuitive manner through the structure of the probe and surfactant.

## 4.5 Literature Cited


1. Lakowicz, J. R. *Principles of Fluorescence Spectroscopy*; second ed.; Plenum Publishers: New York, 1999.
2. Petrich, J. W.; Chang, M. C.; McDonald, D. B.; Fleming, G. R. *J. Am. Chem. Soc.* **1983**, *105*, 3824-3832.
3. Rich, R. L.; Chen, Y.; Neven, D.; Negrerie, M.; Gai, F.; Petrich, J. W. *J. Phys. Chem.* **1993**, *97*, 1781-1788.
4. Rich, R. L.; Negrerie, M.; Li, J.; Elliott, S.; Thronburg, R. W.; Petrich, J. W. *Photochem. Photobiol.* **1993**, *58*, 28-30.
5. Rich, R. L.; Smirnov, A. V.; Schwabacher, A. W.; Petrich, J. W. *J. Am. Chem. Soc.* **1995**, *117*, 11850-11853.
6. Negrerie, M.; Bellefeuille, S. M.; Whitham, S.; Petrich, J. W.; Thornburg, R. W. *J. Am. Chem. Soc.* **1990**, *112*, 7419-7421.
7. Brennan, J. D.; Clark, I. D.; Hogue, C. W. V.; Ito, A. S.; Juliano, L.; Paiva, A. C. M.; Rajendran, B.; Szablo, A. G. *Appl. Spectrosc.* **1995**, *49*, 51-59.
8. Broos, J.; Ter Veld, F.; Robillard, G. T. *Biochem.* **1999**, *38*, 9798-9803.
9. Hogue, C. W.; Szabo, A. G. *Biophys. Chem.* **1993**, *48*, 159-169.
10. Chen, Y.; Gai, F.; Petrich, J. W. *J. Phys. Chem.* **1994**, *98*, 2203-2209.
11. de Foresta, B.; Gallay, J.; Sopkova, J.; Champeil, P.; Vincent, M. *Biophys. J.* **1999**, *77*, 3071-3084.
12. Chattopadhyay, A.; Mukherjee, S.; Rukmini, R.; Rawat, S. S.; Sudha, S. *Biophys. J.* **1997**, *73*, 839-849.
13. Ladokhin, A. S.; Holloway, P. W. *Biophys. J.* **1995**, *69*, 506-517.

14. Sengupta, B.; Sengupta, P. K. *Biochem. Biophys. Res. Commun.* **2000**, *277*, 13-19.

15. Tortech, L.; Jaxel, C.; Vincent, M.; Gallay, J.; de Foresta, B. *Biochim. Biophys. Acta-Biomembr.* **2001**, *1514*, 76-86.

16. Borkman, R. F.; Douhal, A.; Yoshihara, K. *Biophys. Chem.* **1993**, 203-211.

17. Beechem, J. M.; Brand, L. M. *Ann. Rev. Biochem.* **1985**, 43.

18. Nozaki, S. *Chem. Lett.* **1997**, 1-2.

19. Sheehan, J. C.; Cruickshank, P. A.; Boshart, G. L. *J. Org. Chem.* **1961**, *26*, 2525.

20. Kelepouris, L.; Blanchard, G. J. *J. Phys. Chem. B* **2002**, *106*, 6600-6608.

21. DeWitt, L.; Blanchard, G. J.; LeGoff, E.; Benz, M. E.; Liao, J. H.; Kanatzidis, M. G. *J. Am. Chem. Soc.* **1993**, *115*, 12158-12164.

22. Tanford, C. *J. Phys. Chem.* **1972**, *76*, 3020.

23. Robson, R. J.; Dennis, E. A. *J. Phys. Chem.* **1977**, *81*, 1075.

24. Kelepouris, L.; Blanchard, G. J. *J. Phys. Chem. A* **2000**, *104*, 7261-7267.

25. Hu, C.-M.; Zwanzig, R. *J. Chem. Phys.* **1974**, *60*, 4354-4357.

26. Perrin, F. J. *J. Phys. Radium* **1934**, 497.

27. Debye, P. *Polar Molecules* New York, 1929.

28. Ashby, K. D.; Das, K.; Petrich, J. W. *Anal. Chem.* **1997**, *69*, 1925-1930.

29. Eftink, M. R.; A., G. C. .*J. Phys. Chem.* **1975**, *80*, 486-493.

30. English, D. S.; Rich, R. L.; Petrich, J. W. *Photochem. Photobiol.* **1998**, *67*, 76-83.

31. Guha Ray, J.; Sengupta, P. K. *Chem. Phys. Lett.* **1994**, *230*, 75-81.

32. Chapman, C., F.; Maroncelli, M. *J. Phys. Chem. A* **1992**, *96*, 8430.

33. Matzinger, S.; Hussey, D. M.; Fayer, M. D. *J. Phys. Chem. B* **1998**, *102*, 7216-7224.

34. Jiang, Y.; Blanchard, G. J. *J. Phys. Chem.* **1994**, *98*, 9411-9416.

35. Jiang, Y.; Blanchard, G. J. **1995**, *99*, 7904-7912.

36. Gudgin-Templeton, E. F.; Kenny-Wallace, G. A. *J. Phys. Chem.* **1986**, 2896.

37. Chou, S. H.; Wirth, M. J. *J. Phys. Chem.* **1989**, *93*, 7694-7698.

38. Quitevis, E. L.; Marcus, A. H.; Fayer, M. D. *J. Phys. Chem.* **1993**, *97*, 5762-5769.

39. Maiti, N. C.; Krishna, M. M. G.; Britto, P. J.; Periasamy, N. *J. Phys. Chem. B* **1997**, *101*, 11051-11060.

40. Klein, U. K. A.; Haar, H. P. *Chem. Phys. Lett.* **1978**, 531.

41. Blatt, E.; Ghiggino, K. P.; Sawyer, W. H. *Chem. Phys. Lett.* **1985**, 47.

42. Kivelson, D.; Spears, K. G. *J. Phys. Chem.* **1985**, *89*, 1999-2001.

43. Chuang, T. J.; Eisenthal, K. B. *J. Chem. Phys.* **1972**, *57*, 5094-5097.

44. Davis, D. M.; McLoskey, D.; Birch, D. J. S.; Gellert, P. R.; Kittlety, R. S.; Swart, R. M. *Biophys. Chem.* **1996**, 63-77.

45. Edward, J. T. *J. Chem. Ed.* **1970**, *47*, 261.

46. Kinosita, K., Jr.; Kawato, S.; Ikegami, A. *Biophys. J.* **1977**, *20*, 289-305.

47. Lakowicz, J. R.; Cherek, H.; Maliwal, B. P.; Gratton, E. *Biochem.* **1985**, *24*, 376.

48. Lipari, G.; Szabo, A. *Biophys. J.* **1980**, *30*, 489-506.

49. Szabo, A. *J. Chem. Phys.* **1984**, *81*, 150.

50. Evrard, C.; Fastrez, J.; Declercq, J.-P. *Acta Crystal., Section D: Biological Crystallography* **1999**, *D55*, 430-435.

51. Ahlnas, T.; Soderman, O.; Hjelm, C.; Lindman, B. *J. Phys. Chem.* **1983**, *87*, 822.

52. Nery, H.; Soderman, O.; Canet, D.; Walderhaug, H.; Lindman, B. *J. Phys. Chem.* **1986**, 5802.

53. Dutt,G. B., *J. Phys. Chem. B.* **2002**, *106*, 7398-7404.

# Chapter 5

# Conclusions and Future Work

## 5.1 Conclusions

This body of work has demonstrated the application of fluorescence probes to interrogate solution phase interactions. We chose to use the biological probes 7-azatryptophan and 7-azaindole because of their well-behaved photophysics, and biological compatibility amenability. These molecules were used to investigate solutions of aqueous adipic acid and their steady state and fluorescence emission decays were both found to be sensitive to solute concentration. The time domain emission decays of the two probes were fundamentally different and through comparison of lifetime measurements in adipic acid solution and buffered solutions, it was evident that 7AI forms a short-lived complex with adipic acid. The buffered solution measurements also lead to the finding that both molecules are sensitive to collisional quenching in citric acid/dipotassium hydrogen phosphate buffer.

Reorientation measurements showed that these molecules reorient in the stick limit, in accordance with the DSE equation, and revealed the ability of 7AT to interact with adipic acid, presumably through the carboxylic acid moieties. An increase in the reorientation time of 7AT was observed near and above adipic acid saturation concentration. 7AT was determined to form complexes with adipic acid though its common functionality but the persistence time of these complexes is short relative to the reorientation of the molecule.

The information gathered for 7AT and 7AI in the adipic acid solutions demonstrates the utility of these probes for sensing and reporting on their environment. The importance of probe structure in determining the ability to sense spontaneous solute self-assembly was evident in the orientational relaxation response of these probes. These data, along with previous knowledge from this group on the adipic acid system, demonstrates the ability of the lock-and-key approach and criteria necessary to choose appropriate probes for successful interrogation of carboxylic acid systems.

The steady-state optical response of 7AT incorporated into peptide oligomers was investigated in water and aqueous micelles. The sensitivity of 7AT to the peptide environment was evident in the steady state and fluorescence decays. This sensitivity in water was indicated by slight changes in emission maxima and fluorescence lifetime with increasing length of the 7AT-Val oligomer. Fluorescence lifetimes were sensitive to surfactant species and a clear discontinuity in lifetime was observed in SDS above the CMC, indicating peptide association with micelles.

The rotational diffusion time constants of 7AT-$(Val)_n$ peptide series were found to depend linearly on the number of valine residues in the peptide oligomers. This result agreed well with predicted values from the modified DSE model in the stick limit for the theoretical volume of these peptides, when the oligomers are modeled as a sphere. This result and the apparent lack of segmental motion agrees with the notion that the hydrophobic valine residues fold back over the chromophore, restricting its independent motion and affecting its molecular environment in water. This is supported by the shifts noted in the steady state response and the time-resolved emission decays of 7AT contained within the oligomers chain. The dynamics revealed a balance between ionic and van der Waals forces that serve to mediate interactions between peptides and micelle

structures. The strong interactions were between the anionic SDS headgroups and the cationic 7AT-$Val_{1-5}$ probes. Conversely, only the longest cationic 7AT-$Val_{4,5}$ oligomers interact with the cationic CTAB, owing to their greater lipophilic valine structure overcoming repulsive forces.

Investigating the balance between ionic and dispersion forces in probe-micelle interactions led to further investigations where chromophore charge and structure were varied systematically. Derivatives of tryptophan and 7AT were produced to yield probes with net positive or negative charge and varying physical structure. The emission characteristics of these probes varied greatly in micellar solutions compared to water. Substantial blue shifts were seen for all oppositely charged micelle-probe combinations. The rotational dynamics revealed that the indole and azaindole probes, although very similar in structure, yield significantly different responses in certain micelles and are likely due to the ability of 7AT to hydrogen bond with surfactant molecules.

The probes examined in this thesis, when interacting with micelles, were found to exhibit motion consistent with hindered rotor dynamics and translational diffusion along the surface of the micelle.[1-4] The application of this theory to the experimental data helps to elucidate the location and environment of the probes within or at the surface of the micelles. These results demonstrate the utility this class of biological probes possess for investigation of a variety of systems if fictionalized prudently or incorporated into peptides and proteins.

## 5.2 Future Work

Chapters 3 and 4 of this thesis have described the optical response of various indole and azaindole containing peptides and analogs in micellar media. Through the lifetime and reorientation data, along with application of theory related to guest probes in micelles, we have gained insight into the factors effecting location and environment of these probes in various micelles. Certain probe and micelle combinations displayed significant interactions, although the reorientation times of the probes never approach that of the expected reorientation times for the micelles as a whole. We attribute this mainly to lateral diffusion of the probes and significant local rotational freedom of the chromophore when contained in or at the micelle surface. This is a physically reasonable picture of probe micelle interactions and although micelles serve as a convenient medium in which to study peptide and probe interactions, they also introduce some ambiguity. The micelles used in this study have been well characterized and are dynamic entities resulting in micelle fragments, free surfactant, and an overall average size distribution of whole micelles.

In order to understand the contribution of micelle dynamics and better understand translational diffusion, molecular micelles (polymerized micelles) could be used. Molecular micelles have been of utility as a psuedostatioary phase for both achiral and chiral separations in capillary electrophoresis (CE).[5-8] Polymerized micelles are widely applicable to many separations as a great array of molecular micelles may be synthesized to promote specific separations by tailoring of the head groups. They are produced in solution by polymerization of micelle forming surfactants like *N*-undecylenyl-L-glycinate (SUG) that have vinylic groups at their hydrophobic end as illustrated in Figure 5.1.[5]

Polymerized micelles have enhanced stability and rigidity and are controllable in size due to covalent bonding between surfactants eliminating the normal dynamic equilibrium between surfactant monomers and micelles. These properties are of great utility in that unambiguous placement of probe molecules by covalent incorporation into the micelles could be accomplished. Polymerizing probes into micelles characterized by varying lengths of aliphatic chains could result in depth profiling of the micelles. Comparison of probes covalently attached to those unattached would give a great deal of information on the location of free probes and a more direct measure of translational diffusion in these systems.

Continued systematic investigation of nonnatural amino acids in peptides is also of significant interest. Specifically the effects of intramolecular environment on the optical response of chromophores. Useful experiments would include probe species situated centrally within an oligopeptide as well as at the N and C termini with varying charge on the peptide.

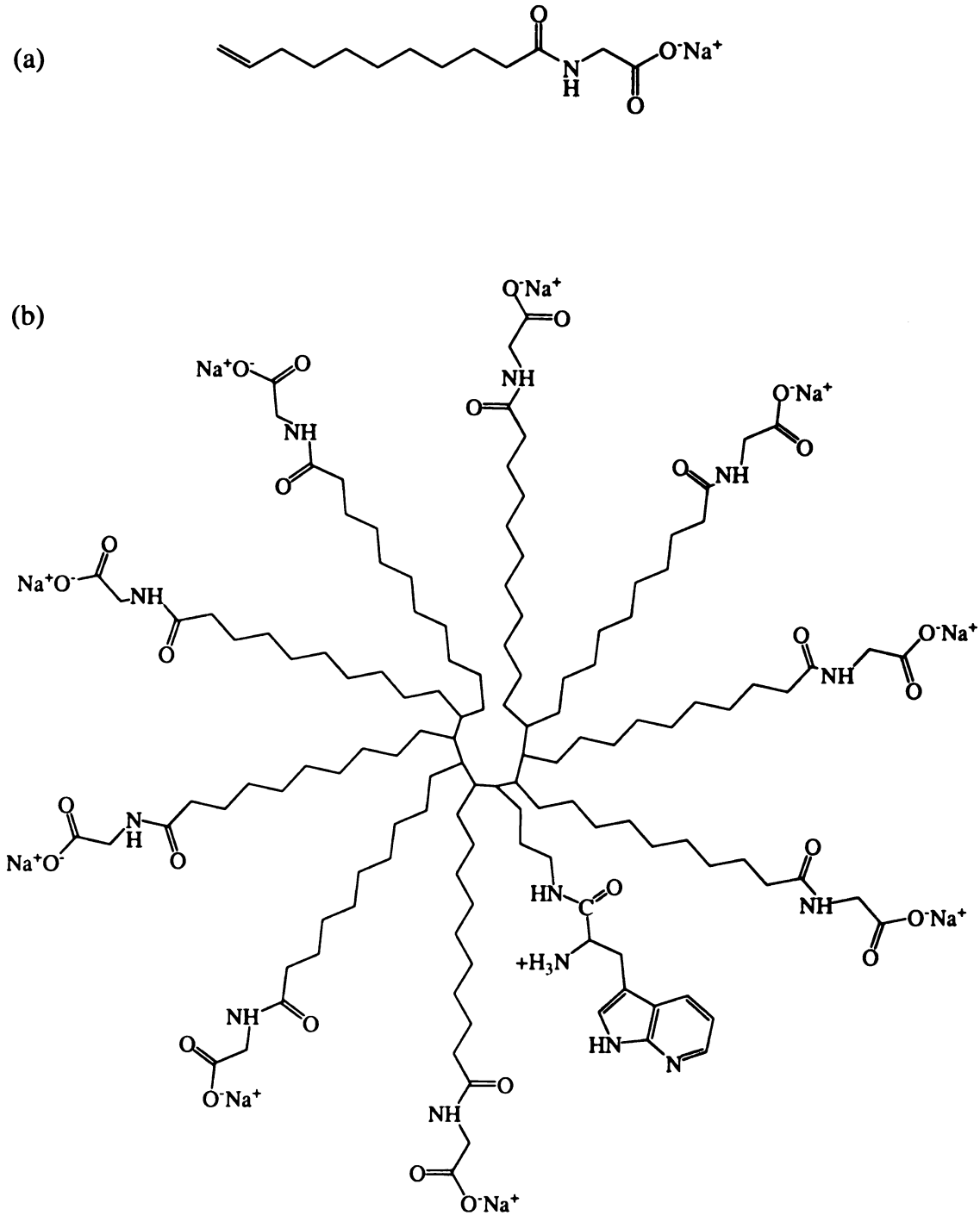


**Figure 5.1** Structures of (a) monomeric SUG and (b) polymeric SUG with probe molecule incorporated.

## 5.3 Literature Cited


1. Periasamy, N. *J. of Fluores.* **2001**, *11*, 161-166.
2. Maiti, N. C.; Krishna, M. M. G.; Britto, P. J.; Periasamy, N. *J. Phys. Chem. B* **1997**, *101*, 11051-11060.
3. Kelepouris, L.; Blanchard, G. J. *J. Phys. Chem. B* **2002**, *106*, 6600-6608.
4. Krishna, M. M. G.; Das, R.; Periasamy, N.; Nityananda, R. *J. Chem. Phys.* **2000**, *112*, 8502.
5. Wang, J.; Warner, I. M. *Anal. Chem* **1994**, *66*, 3773-3776.
6. Palmer, C., P.; Terabe, S. *J. Microcolumn Sep.* **1996**, *8*, 115-121.
7. Shamsi, S. A. *Anal. Chem.* **2001**, *73*, 5103-5108.
8. Tabor, D., G.; Underwood, A. L. *J. Chromatogr.* **1989**, *463*, 73.